EFFECT OF AMPLIFIER NON-LINEARITY ON THE PERFORMANCE OF CDMA COMMUNICATION SYSTEMS IN A RAYLEIGH FADING ENVIRONMENT

JAMEEL SYED

Submitted in fulfillment of the requirements for the Degree of Master of Science in Engineering in the School of Electrical, Electronic and Computer Engineering at the University of KwaZulu-Natal, Durban.

July 2009

Supervisor: Prof. F. Takawira

Co-Supervisor: Prof. A.D. Broadhurst

As supervisor, I approve the dissertation as ready for submission.

…….. .....

Supervisor: Prof. F. Takawira Date

Preface

The research work presented in this dissertation was performed by Jameel Syed under supervision of Prof. F. Takawira and co-supervision of Prof. A.D. Broadhurst in the School of Electrical, Electronic and Computer Engineering at the University of KwaZulu-Natal, Durban, South Africa.

The entire dissertation, unless otherwise stated, is the Author's work and has not been submitted in part, or in whole, to any other university.

…….. .....

Author: Jameel Syed Date

Acknowledgements

I gratefully acknowledge the advice and encouragement received from my current supervisor, Professor F. Takawira and my previous supervisor Professor A. D. Broadhurst, from the School of Electrical, Electronic and Computer Engineering at the University of KwaZulu-Natal.

I extend my appreciation to the Management of RDI Communications (Pty) Ltd for their support and encouragement and thank Mr. D. van Renen for his interest, encouragement and critique.

This work is dedicated to Shaista, Aadil, extended family and friends for their patience and understanding over the period of this research.

Abstract

The effect of amplifier non-linearity on the performance of a CDMA communications system is investigated in the presence of Additive White Gaussian and Rayleigh fading channels. Amplifier models and characteristics are presented to facilitate expansion of the system performance models to other types of amplifiers. Linearisation techniques are investigated as a mechanism to improve performance and the results of a practical investigation of the pre-distortion method are presented.

It is shown that the bit error rate performance of a CDMA downlink may be analytically evaluated in terms of a scale factor that depends on the amplifier type and back-off level. A systematic methodology is presented and verified by simulation. Simulation results show that the downlink system performance depends on the amplifier back-off level and the number of users.

The previously published work is then extended to apply to a Rayleigh fading channel. The bit error rate is initially expressed in terms of a probability conditioned to a particular fading factor. This expression is then integrated over the Rayleigh probability density function to yield an analytical model for the bit error rate of a CDMA system in the presence of Additive White Gaussian noise and Rayleigh fading. A mathematical proof is presented and verified by simulation. Results illustrate and compare the effect of the fading channel to the non-fading channel for the power limited and unlimited downlink systems.

Additionally, the CDMA satellite uplink is considered where each terrestrial user makes use of a non-linear amplifier and a Rayleigh fading channel. Simulation results show that the uplink system performance does not depend on the amplifier back-off level and is only dependent on the number of users.

List of Figures

List of Tables

List of Abbreviations

Symbol	Description
ΔMAI	Additional Multiple Access Interference
ACPR	Adjacent Channel Power Ratio
ADSL	Asymmetric Digital Subscriber Line
AM/AM	Amplitude Modulated/Amplitude Modulation
AM/PM	Amplitude Modulated/Phase Modulation
ASK	Amplitude Shift Keying
AWGN	Additive White Gaussian Noise
BER	Bit Error Rate
BJT	Bipolar Junction Transistor
BPSK	Binary Phase Shift Keying
CDMA	Code Division Multiple Access
CDMA2000	3G Wireless Technology
CNR	Carrier-to-noise ratio
DAB	Digital Audio Broadcast
DC	Direct Current
Demod	Demodulator
DFT	Discrete Fourier Transform
DPCCH	Dedicated Physical Control Channel
$DPDCH_i$	Dedicated Physical Data Channel i
DSP	Digital Signal Processor
DSSS	Direct Sequence Spread Spectrum
DUT	Device Under Test
DVB	Digital Video Broadcast
E-UTRA	Enhanced UMTS Terrestrial Radio Access
EVM	Error Vector Magnitude
FDD	Frequency Division Duplex
FFT	Fast Fourier Transform
FSK	Frequency Shift Keying
GRV	Gaussian Random Variable
HPA	High Power Amplifier
HPSK	Hybrid Phase Shift Keying

Symbol	Description
Hz	Hertz
I	In-phase
I/Q	In-phase/Quadrature
IBO	Input Back-off
IDFT	Inverse Discrete Fourier Transform
IFFT	Inverse Fast Fourier Transform
Im	Imaginary Operator
IMD	Intermodulation Distortion
IMT-2000	International Mobile Telecommunication System 2000
IPA	Ideal Pre-distortion Amplifier
LINC	Linear Amplification using Non-linear Components
LPF	Low Pass Filter
MAI_0	Undistorted Multiple Access Interference
MC-CDMA	Multi-Carrier CDMA
MESFET	Metal Semiconductor Field Effect Transistor
MFSK	Multi-Frequency Shift Keying
M-IMR	Multi-tone Intermodulation Ratio
MOSFET	Metal Oxide Silicon Field Effect Transistor
MPSK	M-ary Phase Shift Keying
MSK	Minimum Shift Keying
NLA	Non-linear Amplifier
NLD	Non-linear Distortion
OBO	Output Back-off
OFDM	Offset Frequency Division Multiplexing
OVSF	Orthogonal Variable Spreading Factor
PAR	Peak-average-ratio
PDF	Probability Density Function
PRBS	Pseudo Random Bit Sequence
PSK	Phase Shift Keying
Q	Quadrature Phase
QAM	Quadrature Amplitude Modulation
QPSK	Quadrature Phase Shift Keying
Re	Real Operator

Symbol	Description
RF	Radio Frequency
RFPA	Radio Frequency Power Amplifier
SNR	Signal to Noise Ratio
SSPA	Solid State Power Amplifier
SVE	Signal Vector Error
TD	Total Degradation
TWT	Travelling Wave Tube
TWTA	Travelling Wave Tube Amplifier
UMTS	Universal Mobile Telecommunications System
UTRA	UMTS Terrestrial Radio Access
W-CDMA	Wideband CDMA
WiMAX	802.16 protocol

List of Symbols

Symbol	Description
$1/C_{C1}$	Coupling factor of directional coupler C1
A	Amplifier gain
a_i	Complex Taylor series coefficients
$a_m^{(k)}$	Symbol m of k^{th} user
A_o	Amplifier output saturation voltage
A_{sat}	Amplifier input saturation voltage
B	Bandwidth
b_i	Real Taylor series coefficients
c(t)	Spreading waveform
c^k	Spreading code
c_n, d_n	Taylor series constants
D(t)	Distortion term
$D_n(t)$	n^{th} order Volterra response
$\phi(k)$	Phase change
E_b	Energy per bit
f(x(t))	Pre-distortion function
$F_A(\rho)$	AM/AM conversion
F_b	Feedback constant
f_c	Channel center frequency
f_o	Frequency offset from the channel center frequency
$F_P(\rho)$	AM/PM conversion
$f_R(r)$	Rayleigh PDF
G(t)	Chip waveform
G_{rx}	Receiver antenna gain
G_{tx}	Transmitter antenna gain
$g_r(t)$	Receiver response to g(t)
$h_n(\tau_1 .. .\tau_n)$	n^{th} order Volterra kernel
I	Integer index i
k_{Bolt}	1.38×10^{-23}
K	User k
k_p	Phase modulator gain

Symbol	Description
K	Number of users
K_o	NLA scale factor
L_{fs}	Free space path loss
M	Modulation order
N	Spreading factor
N_o	One-sided power spectral density
OBO	Output back-off
p	Integer, such that $1 \leq p < \infty$
P	Number of bits per symbol
$P_{average}$	Average power
P_b	Probability of bit error
P_{B1}	Power in frequency band 1
P_{B2}	Power in frequency band 2
P_d	Average non-linear distortion power
P_i	Average power of input signal
P_o	Average power of output signal
P_{peak}	Peak power
P_{psu}	Average power drawn from power supply
P_{rx}	Receiver sensitivity
q	Integer, such that $1 \leq q < \infty$
Q_i	Code word
r	Instantaneous fading term
r(t)	Channel fading waveform
R_b	Bit rate
s(t)	RF signal
S(ρ)	Amplifier transfer function
t	Sample time
T_{Noise}	Noise Temperature
T_c	Chip time
u(t)	NLA output signal
v(t)	Filtered signal at receiver
$V_d(t)$	Non-linear distortion
$V_{env}(t)$	Signal envelope

Symbol	Description
$V_{err}(t)$	Error signal
W_j	Walsh sequence
w_{max}	Ratio of maximum carrier power to noise power
x	Complex signal at amplifier input
X(f)	Fourier transform of x(t)
y(t)	Signal at component output
$y_m^{(k)}$	Decision variable for m^{th} symbol of k^{th} user
$\alpha_a(f)$, $\beta_a(f)$	Saleh frequency dependent parameters
$\alpha_\theta(f)$, $\beta_\theta(f)$	Saleh frequency dependent parameters
β	Input back-off
η	SNR before receive filter
Θ	SNR after receive filter
M	Chip factor
μ_1, μ_2	Mean of GRV
$\nu(t)$	Low-pass equivalent noise
$\nu_{m,n}$	Sampled $\nu(t)$
P	Magnitude of input signal
σ_1	Standard deviation of GRV
σ_D^2	Variance of NLD noise
σ_o^2	Variance of input signal
σ_w^2	Variance of AWGN
$\sigma_{MAI_o}^2$	Variance of MAI_o
σ_r^2	Variance of Rayleigh fading random variable
T	Time constant
Φ	Phase of signal
$\bar{\gamma}_b$	Average SNR for Rayleigh fading
Ω	Angular frequency
$\Gamma(z,a,b)$	Generalised Gamma function

Contents

1 Introduction

"Spread spectrum has been widely used in the military communication environment to resist intentional jamming and to achieve a low-probability of detection. Code division multiple access (CDMA) is used in numerous commercial cellular and personal communication systems, including the 3rd generation cellular systems. Intermodulation distortion in the RF stages of these networks results in unwanted frequency components in the frequency band used for the transmission of these signals. This is known to affect the bit error rate (BER) of the system. Complex systems of power control are used to limit the transmitted power to minimize these effects[1]."

Linear modulation schemes are widely used in systems currently deployed in many countries. The Digital Audio Broadcast (DAB) and Digital Video Broadcast (DVB) schemes use Orthogonal Frequency Division Multiplexing (OFDM) [20], the Universal Terrestrial Radio Access Mobile Telecommunication System (UMTS) uses QPSK in the Frequency Division Duplex (FDD) mode [22] and CDMA2000 uses BPSK and QPSK in the radio configuration modes 3 to 7 [23]. An analytical approach for the performance analysis of such systems has been proposed in the literature [1], [3], [4]. Prior to this research, simulation and hardware evaluation were the only options available to predict the system performance in the presence of amplifier non-linearity.

Modulation techniques like QPSK and 64-QAM produce non-constant envelope signals that generate intermodulation distortion (IMD) products at the power amplifier. This produces undesirable interference in the adjacent channels. To reduce these IMD products linear amplifiers are usually used. However it has been suggested that non-linear amplifiers with pre-distortion may be used to compensate for these distortions instead of simply backing off a Class A amplifier [31], [32]. Amplifier back-off has the undesirable effect of decreasing the power efficiency in applications where battery life needs to be maximized.

Herrmann [57] compared the QPSK, O-QPSK and MSK receivers with integrators to the discrete and continuous ML receivers. The Maximum-Likelihood Receiver in a non-linear satellite channel was shown to improve the system performance. It was found that almost all the degradation due to the intersymbol and non-linear distortion could be mitigated by appropriate receiver design.

[1] Adapted from Dissertation Proposal written by Prof. A. D. Broadhurst in consultation with J. Syed

Herrmann [58] used a power series to describe the non-linear channel. It was shown that equalization techniques used at the receiver did not correct for the effect of non-linear channels even when MLSE was used.

Satellite link availability was determined using a combination of theoretical and empirical methods. The pdf of the SNR of a satellite link could be determined from the pdf's of the signal attenuation due to atmospheric absorption, rainfall attenuation, scintillation, antenna pointing error and wind velocity [59].

Gaudenzi [62] compared the performance of turbo-coded Amplitude Phase Shift Keying (APSK) to trellis-coded Quadrature Amplitude Modulation (QAM) that was concatenated with Reed Solomon codes. It was shown that turbo-code APSK produced a significant improvement in power and spectral efficiency over a non-linear channel.

Weinberg [60] studied the effect of pulsed radio frequency interference (RFI) on the performance of a satellite repeater with a non-linear power amplifier. The non-linear amplifier was modeled as a limiter with a specified AM/PM characteristic. Results were presented showing how the BER was affected by the RFI duty cycle and various coding/decoding choices.

Huang [61] considered spread spectrum signalling over a non-linear satellite channel. A mathematical model of a band-limited non-linear satellite repeater subjected to continuous wave (CW) intereference was formulated. Numerical results were presented showing the relationship between BER and SNR for various CW power levels.

A non-linear channel can be modeled as an Inter-symbol Interference (ISI) channel with memory. Ghrayeb [54] proposed that this ISI can be equalized using a scheme that grew exponentially with the length of the channel memory. Wu [55] considered an interference cancellation scheme that grew linearly with the channel memory length. Burnet [56] showed that a 16QAM Turbo equalization scheme, using a maximum likelihood sequence estimation technique, can mitigate the ISI without the exponential growth in memory length.

Springer [9] considered the effect of a NLA on the UMTS system. More specifically, simulations were performed on the UTRA FDD mode using BPSK modulation. The AM/AM conversion characteristic of the NLA was fitted to a 5^{th} order polynomial. Using the concept of Error Vector Magnitude (EVM) and Adjacent Channel Power Ratio (ACPR) it was found that the NLA under investigation needed to be operated with an input back-off level of

approximately 7 dB to meet the ACPR of -33 dB specified by the UMTS specification. It was also noted that the NLA contribution to the EVM was 3%.

In the uplink CDMA system each transmitted signal might undergo distortion at the HPA. Kashyap [29] noted that if such a signal was modulated using BPSK or QPSK modulation then the BER performance was not significantly affected by the NLA at each transmitter when the amplifier was operated near its saturation region (i.e. hard limiter). The reason for this was attributed to the constant envelope of the signal presented to each of the amplifiers.

In a communication system, a signal is subjected to amplification, attenuation, noise and other disturbances on it's path from the transmitter to the receiver. The goal of the system designer is to ensure that the signal quality degradation, as measured by the signal-to-noise ratio for analog signals and by the BER for digital signals, is minimized so that the signal may be successfully recovered at the receiver.

A form of the Link Budget equation for a communication system may be used to determine the required receiver sensitivity according to

$$P_{rx} = P_o + G_{tx} + G_{rx} + \text{Coding Gain} + \text{Processing Gain} - L_{fs} - \text{Fade Margin} - \text{OBO}. \quad 1.1$$

It incorporates parameters for the amplifier output power P_o, transmitter antenna gain G_{tx}, receiver antenna gain G_{rx}, coding gain, processing gain, free space path loss L_{fs}, fade margin and amplifier output-back-off (OBO). It can be used to determine whether information can be transmitted from a source to a destination with an acceptable BER.

If the receiver sensitivity, receiver and transmitter antenna gains, path loss, fade margin and OBO is specified then the required transmitter power can be calculated using equation 1.1.

The receiver sensitivity can be calculated from

$$P_{rx} = k_{Bolt} T_{Noise} B + SNR, \quad 1.2$$

and the signal-to-noise ratio can be expressed as

$$SNR = 10*\log_{10}(E_b/N_o) * (R/B) \quad 1.3$$

where E_b/N_o is the bit energy to noise ratio, R is the bit rate and B is the system bandwidth [27], [53].

Since the BER vs E_b/N_o relationships for various modulation formats and channel conditions are readily obtainable from published texts, the required E_b/N_o for a BER may be chosen and the required transmitter power can be analytically determined.

The purpose of this submission is to show how the BER vs E_b/N_o relationship may be analytically evaluated for a CDMA system that uses a non-linear transmitter and BPSK or QPSK modulation in a non-fading or Rayleigh fading environment. Hence, the Link Budget equation can be analytically evaluated even for CDMA systems that make use of non-linear amplifiers in a non-fading or Rayleigh fading environment.

Thesis Organisation

Chapter 2 discusses commonly used amplifier models, characteristics and linearisation methods. The results of a practical investigation into the pre-distortion method are presented.

Chapter 3 presents a literature survey on the effect of non-linear amplifiers on CDMA, Multi-code CDMA and MC-CDMA systems. It introduces prior research done on the CDMA downlink and proposes a systematic methodology to apply the work. A CDMA simulator is implemented and used to verify the analytical results. The CDMA uplink performance is investigated by means of simulation.

Chapter 4 extends the work of Chapter 3 to include the effects of Rayleigh fading on the CDMA downlink. An analytic model is derived and verified against simulation results. The CDMA uplink performance is assessed by means of simulation.

Finally, Chapter 5 provides a summary and proposes further extensions to the research.

Original Contributions to Body of Knowledge

a) Analytical model for the CDMA downlink with a non-linear amplifier and Rayleigh fading channel.

b) Simulation results for the CDMA uplink with a non-linear amplifier in a non-fading and Rayleigh fading environment showing the BER dependence on the number of users. It is also shown that the BER does not depend on the NLA output back-off level.

2 Non-linear Amplifiers

2.1 Introduction

The purpose of a communication system is to transfer voice or data information from a source to a destination via a transmission channel. As the signal propagates through the channel it undergoes attenuation and interference. An amplifier is used to increase the signal power in order to compensate for the effect of attenuation. Unfortunately, all amplifiers possess a degree of non-linearity that will distort the signal.

The type of modulation scheme used in a communication system has an influence on whether a non-linear amplifier can be used. Systems with constant envelope modulation schemes allow the use of highly non-linear amplifiers, albeit with the use of filters to remove the unwanted harmonic distortion products; whereas those that employ varying envelope modulation schemes require amplifiers with transfer characteristics that approach the ideal linear case.

This chapter presents a survey on amplifier models in preparation for further discussion in chapters 3 and 4. A discussion on amplifier power spectral density, output power, intermodulation distortion, adjacent channel power rejection, noise power ratio, carrier-to-peak ratio, peak-to-average ratio, multi-tone intermodulation, error vector magnitude efficiency and output-backoff is included. The Feedforward, Feedback, Pre-distortion, LINC and Envelope Elimination and Restoration methods of linearization are studied. Finally, measurement results are presented for a laboratory investigation that was conducted into the feasibility of pre-distortion.

2.2 Models

The fundamental purpose of an RF Power Amplifier (RFPA) is to increase the power level of a signal in order to drive a load (e.g. antenna) of a specified impedance (i.e. usually 50 ohms). The power gain has to be sufficient to overcome losses in the cables and connectors between the RFPA and antenna as well as attenuation losses in the transmission medium.

Amplifiers are commonly classified into two broad categories viz., vacuum tube and solid state. The Klystron, Gyrotron, Travelling Wave Tube (TWT) and Cross-field amplifier are examples of vacuum tube devices used in microwave amplifiers. The term "solid state amplifier" refers to amplifiers designed with semiconductor devices e.g. BJT, MOSFET and MESFET.

The transfer characteristic of an ideal amplifier is linear. Such an amplifier will amplify any instantaneous power value within its' dynamic range by the same gain factor. In general, an amplifier may be described as a device that modifies the amplitude and/or phase of an input signal.

Consider the signal

$$x(t) = \rho(t)e^{j\phi(t)} \qquad 2.1$$

where ρ is the signal magnitude and φ is the phase. The amplifier output may be represented by

$$y(t) = F_A(\rho)e^{j(\phi(t)+F_P(\rho))}, \qquad 2.2$$

where $F_A(\rho)$ is the AM/AM conversion and $F_P(\rho)$ is the AM/PM conversion characteristics of the amplifier [37].

A real amplifier will not exhibit a constant gain for any instantaneous power level; rather, the gain will tend to decrease with increasing power level, leading to distortion of the signal and interference effects. Such amplifiers are said to be non-linear.

All real amplifiers are actually non-linear to some extent. However, provided that overall transmitter properties like intermodulation distortion suppression is within acceptable limits, the RFPA will be deemed to be sufficiently linear for practical purposes. This is usually achieved by operating the RFPA far enough away from its saturation point [36].

The effect of the non-linear behavior on the system performance can be assessed through experiment, simulation or theoretical analysis. The first approach obviously requires building and testing of actual hardware; while the second and third approaches rely on a mathematical representation of the relevant transfer characteristics.

A real amplifier's transfer characteristic, whether vacuum or solid state, can be represented by appropriate models that describe the AM/AM and AM/PM relationships. Some amplifiers (e.g. TWTA) require models that describe both AM/AM and AM/PM behaviour while others are sufficiently represented by an AM/AM expression only (e.g. SSPA). More elaborate models include terms that account for memory effects like frequency. Tables 2.1 and 2.2 list typical memory and memoryless amplifier models [51], [52].

Analytical Model
Power Series Model
Frequency-independent Saleh Model
Ghorbani Model
Rapp Model
White Model

Table 2.1 Memoryless Amplifier Models

The memoryless analytical model is based on an input signal with a power spectrum centered around 0 Hz. The parameters of the Power Series, Frequency-independent Saleh, Ghorbani, Rapp and White models are determined by means of curve fitting to measurements of the AM/AM and/or the AM/PM characteristics of the amplifier [51].

Memoryless models assume that the amplifier behaviour is frequency independent. If a more accurate model is required over a wide frequency range then models that include memory (i.e. frequency dependency) should be used.

Amplifiers models with memory may be developed analytically (e.g. Volterra) or empirically (e.g. Saleh). The empirical memoryless model parameters are also determined by means of curve fitting to measurements of the AM/AM and/or the AM/PM characteristics of the amplifier [51].

The following sections examine a few commonly referenced amplifier models viz. the Ideal Pre-distortion Amplifier, Solid State Amplifier, Travelling Wave Tube Amplifier, Taylor

Series, Saleh, Blum and Jeruchim, Volterra and Generalised Power Series in preparation for inclusion in the discussions of later chapters[2].

Analytical Models	Volterra Series Model
	Polyspectral Model
Based on AM/AM and AM/PM Measurements	Poza-Sarkozy-Berger Model
	Frequency-dependent Saleh Model
	Abuelma' Atti Model
Based on Fitting to Pre-set Structures	Two-box Models (Hammerstein and Wiener)
	Three-box Models
Miscellaneous Models	Power-independent Transfer Function Model
	Non-linear Parametric Discrete-time Models
	Instantaneous Frequency Model

Table 2.2 Amplifier Models with Memory

2.2.1 Ideal Pre-distortion Amplifier

The Ideal Pre-distortion Amplifier (IPA) is usually used to describe an ideal linear amplifier with its output limited by the supply voltage.

The amplitude and phase transfer functions of the IPA are described by

$$F_A(\rho) = \begin{cases} \rho, & \rho \le A_{sat} \\ A_{sat,} & \rho > A_{sat} \end{cases}, \qquad 2.3$$

and

$$F_P(\rho) = 0, \qquad 2.4$$

respectively, where ρ is the input signal and A_{sat} is the amplifier input saturation voltage [1].

These equations are applicable to non-linear amplifiers (NLAs) that exhibit a flat or constant AM/PM transfer characteristic.

[2] The Reader is directed to references [51] and [52] for a more complete treatment of amplifier models.

2.2.2 Solid State Power Amplifier

Solid State Amplifiers (SSPAs) are based on semiconductor technology. These amplifiers demonstrate memoryless characteristics (i.e. instantaneous output depends only on instantaneous input) and are the most common type of amplifier used in communication systems. SSPAs may be designed using devices such as BJTs, MOSFETs, MESFETs etc.

The SSPA may be mathematically modeled by its AM/AM and AM/PM characteristics respectively according to the following equations.

$$F_A(\rho) = \frac{\rho}{\sqrt{1+\left(\frac{\rho}{A_0}\right)^2}} \qquad 2.5$$

$$F_P(\rho) = 0, \qquad 2.6$$

A_0 is the amplifier output saturation voltage [1].

This is one of the simpler models and has been used to investigate the effect of NLAs on a CDMA communication system.

2.2.3 Travelling Wave-tube Amplifier

The Travelling Wave Tube Amplifier (TWTA) is widely used in satellite communication applications. They typically have an efficiency of 50 to 60% [35]. These amplifiers are characterized by a non-linear AM/AM transfer function and an AM/PM that significantly influences the phase of the input signal.

The TWTA AM/AM and AM/PM characteristics are given by

$$F_A(\rho) = \frac{\rho A_{sat}^2}{\rho^2 + A_{sat}^2} \qquad 2.7$$

and

$$F_P(\rho) = \frac{\pi}{3}\frac{\rho^2}{\rho^2 + A_{sat}^2}, \qquad 2.8$$

respectively [1].

2.2.4 Taylor Series

The Taylor Series is one of the simpler techniques that may be used to model an NLA. It has the advantage that since the relative order of distortion is described by coefficients a_n, the intermodulation distortion products may be easily calculated. It is particularly suited to modeling amplifiers that contain relatively few orders of distortion like the TWTAs [20].

If the AM/PM distortion is negligible then the NLA output can be described by a Taylor series of the form,

$$y(t) = \sum_{n=1}^{\infty} a_n x^n(t), \qquad 2.9$$

where $x^n(t)$ is the result of raising the input signal to the n^{th} power and a_n are the corresponding coefficients. The Matlab function "polyfit" may be used to obtain these coefficients using a least-squares polynomial fit to the input signal x(t).

If the AM/PM distortion is significant then the NLA output needs to be expressed in terms of the complex Taylor series,

$$y(t) = \sum_{n=1}^{\infty} (c_n + jd_n) x^n(t), \qquad 2.10$$

where c_n and d_n are constants.

An alternative to using the complex Taylor series model of 2.10 is to first split the input signal into I and Q components and then use the simpler Taylor series of 2.9 for each of the I and Q branches [20].

2.2.5 Saleh

In wideband applications matching circuits are often used at the amplifier input and output. The components used will change their behaviour as a function of frequency. It follows that there will be a resulting change in the input-output relationship. The Saleh model introduces a frequency dependent term that allows modeling of a system over a wider bandwidth.

The Saleh AM/AM and AM/PM transfer function is described by

$$F_A(\rho) = \frac{\alpha_a(f)\rho}{1 + \beta_a(f)\rho^2} \qquad 2.11$$

and

$$F_P(\rho) = \frac{\alpha_\theta(f)\rho^2}{1+\beta_\theta(f)\rho^2} \qquad 2.12$$

respectively, where $\alpha_a(f), \beta_a(f)$, $\alpha_\theta(f)$ and $\beta_\theta(f)$ are frequency dependent parameters. They are obtained by curve fitting the AM/AM and AM/PM models to a series of transfer functions (obtained by measurement) over the frequency band of interest [20].

Although the above Saleh model is used to include the effects of frequency dependencies, it may be possible to apply the idea to temperature dependencies as well.

2.2.6 Blum and Jeruchim

The models described in the previous paragraphs do not include the effects of adjacent signals on the signal of interest. Their transfer functions were determined based on a frequency and power sweep of a single carrier.

Since the Blum and Jeruchim model uses a multicarrier signal to determine the transfer function of the NLA, it accounts for the adjacent signal effects [20]. The Cartesian representation of the Blum and Jeruchim model appears in Figure 2.1.

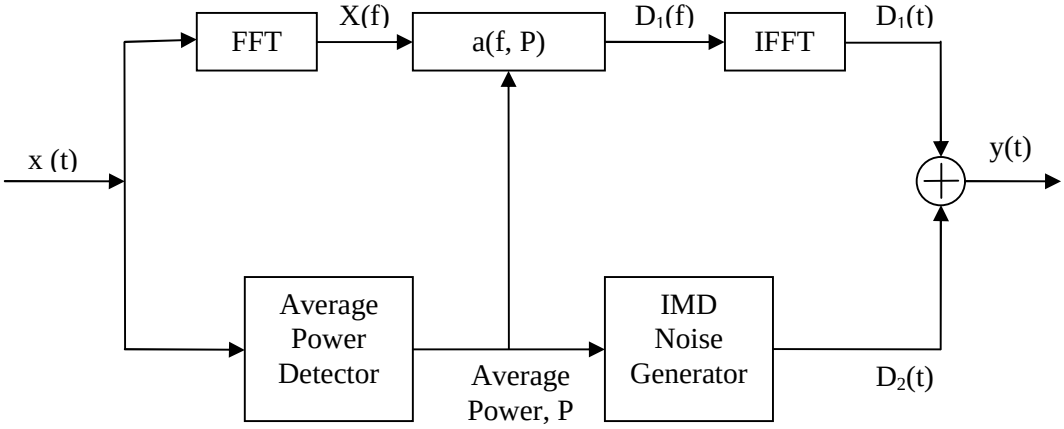

Figure 2.1 Blum and Jeruchim Model

The frequency and power dependent transfer function a(f, P) is obtained by measuring the response of the non-linear amplifier (NLA) to a Direct Sequence Spread Spectrum (DSSS) signal. One of the properties of a DSSS signal is that it is a wideband signal characterized by a number of spectral lines. The DSSS signal can therefore be regarded as a multicarrier signal. If one considers any one frequency component as the signal of interest then the

remaining signals can be considered to be the adjacent signals. This multicarrier signal applied to the input of the NLA produces a multicarrier signal at the output. A narrow bandpass filter with an adjustable center frequency is then swept across the frequency band to obtain a curve for a specified input power level. If the power level is varied across the power range of interest and the above procedure repeated, a family of curves are produced that characterize the amplifier in terms of frequency and power. [20].

The input signal x(t) is applied to the model and is converted into the frequency domain by means of the FFT to produce X(f). This signal together with information about the power level of x(t) is applied to the transfer function a(f, P) to produce $D_1(f)$. $D_1(f)$ is then converted into the time domain signal $D_1(t)$ and summed with the power dependent IMD components $D_1(t)$ to yield the output y(t) of the NLA.

2.2.7 Volterra Series

A Volterra series can be used to describe the output y(t) of a non-linear amplifier. It allows the description of an NLA output in terms of the current and previous inputs. Stated differently, the Volterra series includes the memory effect of components like capacitors and inductors. The baseband Volterra model is given by

$$y(t) = \sum_{n=0}^{\infty} y_n(t), \qquad 2.13$$

where

$$y_n(t) = \int_{-\infty}^{\infty} \ldots \int_{-\infty}^{\infty} h_n(\tau_1, \ldots, \tau_n) x(t-\tau_1) \ldots x(t-\tau_n) d\tau_1 \ldots d\tau_n \qquad 2.14$$

is the n^{th} order response of the system and $h_n(\tau_1, \ldots \tau_n)$ is the n^{th} order Volterra kernel of the NLA [20]. The kernels capture the behaviour of the system such that any applied input to the model will generate the corresponding output of the actual system. The h_0 term is the system response to a DC signal. The h_1 term is the linear unit impulse response of the system. The h_2 term is the system response to two separate unit impulses responses applied at two different time instants. The h_3 term is the system response to three separate unit impulses at three different time instants. The higher-order terms may be determined in a similar manner. It is also worth noting that the h_2 term contains one time lag constant, the h_3 term contains two time lag constants and the h_n term contains n-1 time lag constants. These time lag constants actually refer to the effect of previous responses of the system.

2.2.8 Generalised Power Series

A generalised Power series can be used to describe the output g(t) of a non-linear amplifier (NLA) by

$$y(t) = A\sum_{i=0}^{\infty} a_i \left\{ \sum_{n=1}^{N} b_n x_n (t - \tau_{n,i}) \right\}, \qquad 2.15$$

where

$$x(t) = \sum_{n=1}^{N} \left| x_n \right| \cos(\omega_n t + \phi_n) \qquad 2.16$$

is the input to the NLA, a_i are complex Taylor series coefficients, b_i are real Taylor series coefficients, τ_i are time delays and $\left|x_n\right|$ are the magnitudes of the frequency components ω_n [20].

2.3 Non-linear Amplifier Output Characteristics

Given the gain and phase transfer functions of a non-linear amplifier, the power spectral density, adjacent channel power rejection, output power and two-tone intermodulation distortion can be determined.

According to Chen et. al. [2], an RF signal can be expressed as

$$s(t) = \mathrm{Re}[\underline{s}(t)e^{j\varpi_c t}], \qquad 2.17$$

where $\underline{s}(t)$ is the complex envelope of the RF signal $s(t)$ and ω_c is the frequency of the carrier. $\underline{s}(t)$ is given by

$$\underline{s}(t) = \rho(t)e^{j\phi(t)}, \qquad 2.18$$

where $\rho(t)$ and $\phi(t)$ are the magnitude and phase of $\underline{s}(t)$, respectively. When signal $\underline{s}(t)$ is applied to a bandpass memoryless non-linear amplifier, the output complex envelope is given by

$$y(t) = F_A(\rho(t))e^{j\{\phi(t)+F_P(\rho(t))\}}, \qquad 2.19$$

where $F_A(\ .\ )$ and $F_P(\ .\ )$ are the gain and phase transfer functions of the non-linearity, respectively.

2.3.1 Power Spectral Density

The power spectral density of y(t) can be determined by evaluating

$$S_y[k] = \frac{|Y[k]|^2}{N^2} \qquad k = 0,1,...,N-1, \qquad 2.20$$

where Y[k] is the FFT of y(t) and N is the number of samples. The adjacent channel power rejection can then be determined from the frequency spectrum of $S_y[k]$ [2].

2.3.2 Output Power

The total output power of the amplifier can be calculated from

$$P_{out} = 10\log\left[\frac{1}{N}\sum_{n=0}^{N-1}\left|y(n)\right|^2\right] = 10\log\left[\frac{1}{N}\sum_{k=0}^{N-1}\left|Y(k)\right|^2\right] \quad 2.21$$

where y(n) is the sampled envelope of the RF signal and Y[k] is its frequency spectrum [2].

2.3.3 Intermodulation Distortion

A two-tone method is usually used to characterize the extent of a non-linearity by applying two equal amplitude signals at frequencies f_1 and f_2 to the amplifier. The NLA will generate additional frequencies f_{IMD} referred to as Intermodulation Distortion (IMD) products. These occur at frequencies given by

$$f_{IMD} = pf_1 \pm qf_2, \quad 2.22$$

where p and q are integers such that $1 \leq p < \infty$ and $1 \leq q < \infty$ [51].

2.3.4 Adjacent Channel Power Ratio

The Adjacent Channel Power Ratio (ACPR) attempts to quantify the extent to which the distortion products of a signal spill over into the adjacent channel as a result of the NLA. Using Figure 2.2 [20] the ACPR may be defined as

$$ACPR = \frac{P_{B1}}{P_{B2}}, \quad 2.23$$

where P_{B1} is the power in the frequency band B1 and P_{B2} is the power in the frequency band B2. B1 and B2 need not be equal. f_c is the carrier frequency and f_o is the channel spacing; so f_c-f_o is the center frequency of the adjacent channel.

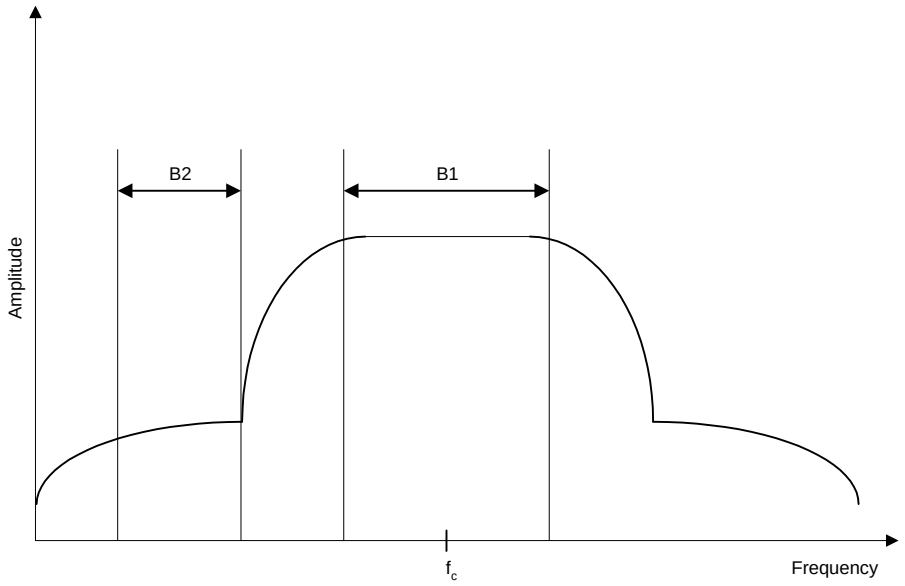

Figure 2.2 Adjacent Channel Power Ratio

2.3.5 Noise Power Ratio

The Noise Power Ratio (NPR) attempts to quantify the amount of distortion power present in the channel as a result of the NLA. A white Gaussian noise signal is used as the input signal. The NPR may then be defined as per Figure 2.3, as the ratio between the noise power spectral density measured at the notch frequency, while using a notch filter to filter out a portion of the input signal, and the noise power spectral density measured at the notch frequency without the notch filter. The NLA has to be driven with the same power level [20].

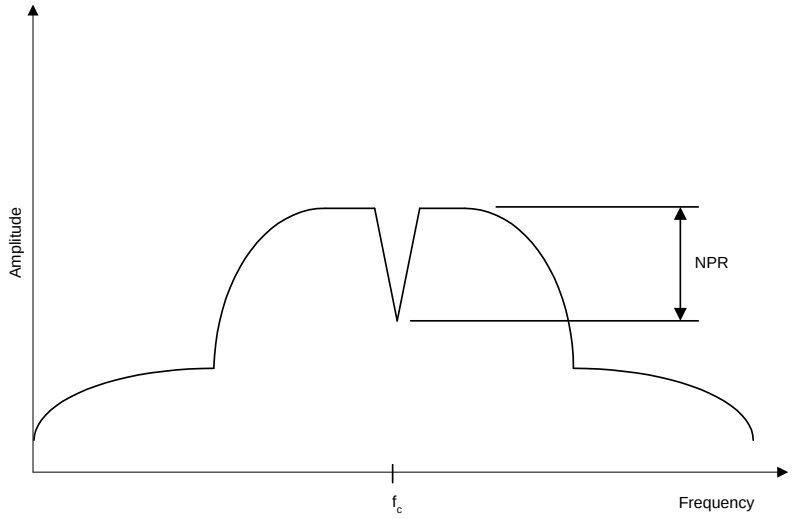

Figure 2.3 Noise Power Ratio

2.3.6 Carrier-to-Noise Ratio

The carrier-to-noise ratio (CNR) measures the relative magnitude of the carrier power $P_{carrier}$ to the noise power N_o in a bandwidth on 1 Hz, i.e.

$$\frac{C}{N_o} = \frac{P_{carrier}}{N_o}. \qquad 2.24$$

The CNR may also be written as

$$\frac{C}{N} = \frac{P_{carrier}}{N}, \qquad 2.25$$

where N is the noise power present in the signal bandwidth. The CNR is related to the E_b/N_o parameter by

$$\frac{C}{N_o} = \frac{E_b}{N_o} x R_b \qquad 2.26$$

and

$$\frac{C}{N} = \frac{E_b}{N_o} x \frac{R_b}{B} \qquad 2.27$$

where R_b is the bit rate and B is the signal bandwidth [27]

2.3.7 Peak-to-Average Ratio

The peak-to-average ratio (PAR) measures the relative magnitude of the peak power of the signal to the average power [42], i.e.

$$PAR = \frac{P_{peak}}{P_{average}}. \qquad 2.28$$

The PAR is commonly used to describe the magnitude of the signal envelope variations.

2.3.8 Multi-tone Intermodulation Ratio

The Multi-tone Intermodulation Ratio (M-IMR) attempts to quantify the effect of non-linear distortion on a multi-carrier signal (e.g. OFDM). It is defined, as per Figure 2.4, as the ratio of the wanted tone power[3] and the highest IMD tone power immediately outside the wanted frequency band [20].

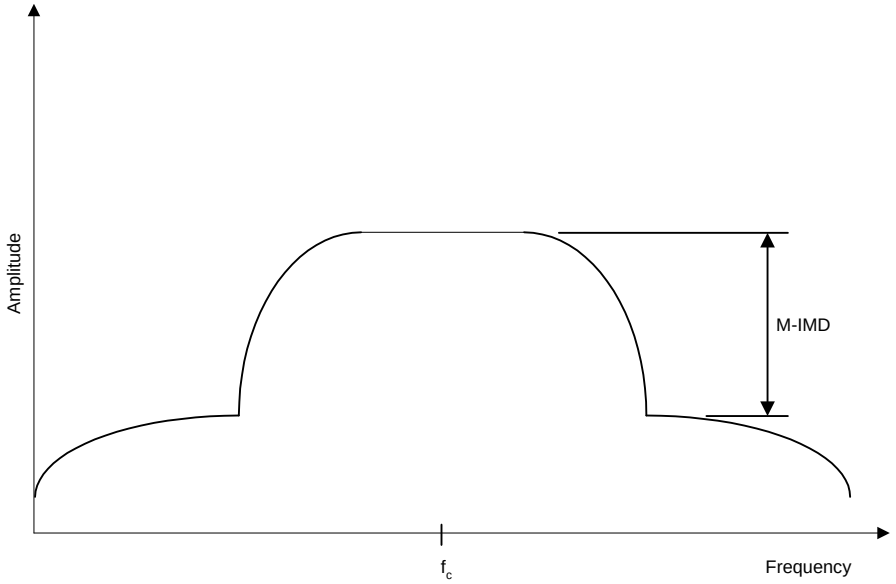

Figure 2.4 Multi-carrier Intermodulation Ratio

2.3.9 Error Vector Magnitude

The Signal Vector Error (SVE) and Error Vector Magnitude (EVM) attempt to quantify the effect of non-linear distortion. SVE may be described, as per Figure 2.5 [25], [50] as the vector difference between the measured signal vector and the ideal signal vector. The EVM is determined from

$$EVM = \sqrt{\left(R^2 + M^2\right) - 2RM\cos\phi}\,, \qquad 2.29$$

where R is the magnitude of the ideal reference signal, M is the magnitude of the measured signal and ϕ is the phase error [20].

[3] A multi-carrier signal is made up of multiple tones. For the purpose of M-IMD measurement the power of one of these tones is considered.

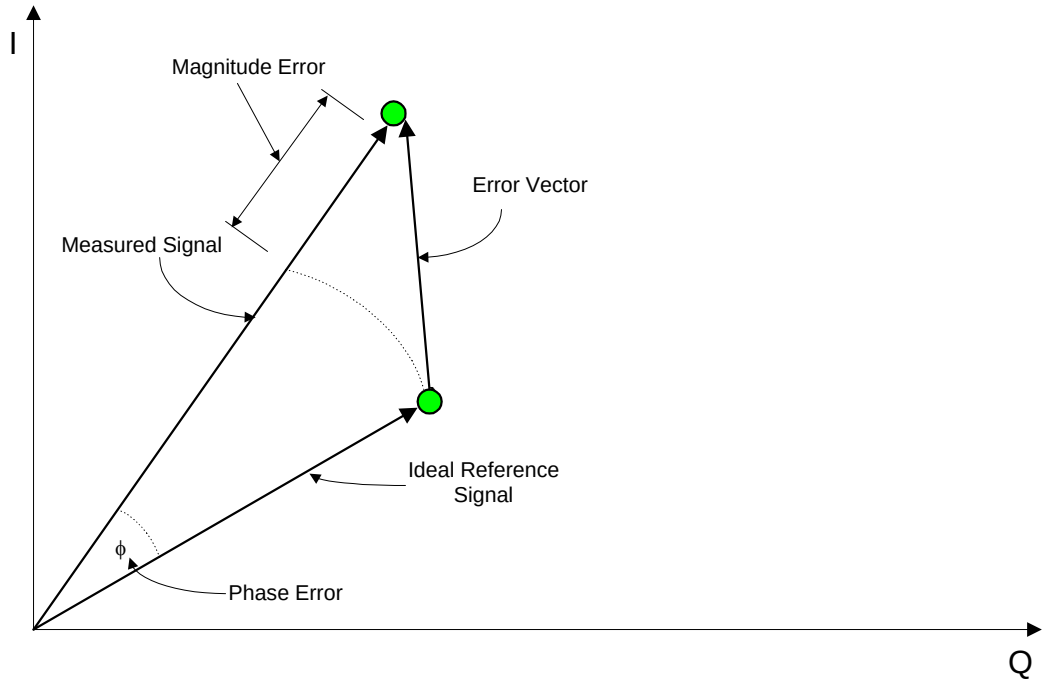

Figure 2.5 Error Vector Magnitude

2.3.10 Efficiency

Amplifier efficiency is usually defined as the ratio of amplifier output power to the power drawn from the power supply expressed as a percentage i.e.

$$\text{Efficiency} = 100x\frac{P_o}{P_{psu}}, \qquad 2.30$$

2.3.11 Output Back-off

An amplifier may be driven with an input signal with a power level set anywhere between some minimum and maximum level. The Output Back-off (OBO) attempts to describe the extent to which the average output power is lower than the maximum output sinusoidal power. It is defined as [1]

$$\text{OBO} = \frac{\text{A}_0^2}{2\text{P}_0}, \qquad 2.31$$

where $\frac{\text{A}_0^2}{2}$ is the maximum output sinusoidal power and P_0 is the mean output power. OBO

is usually expressed in decibels as

$$OBO\_dB = 10\log_{10}\left(\frac{A_0^2}{2P_0}\right), \qquad 2.32$$

2.4 Amplifier Linearisation

Amplifier linearization may be used to mitigate the effects of non-linearity. This section presents the feedforward, feedback, pre-distortion, LINC and envelope elimination and restoration techniques.

2.4.1 Feedforward

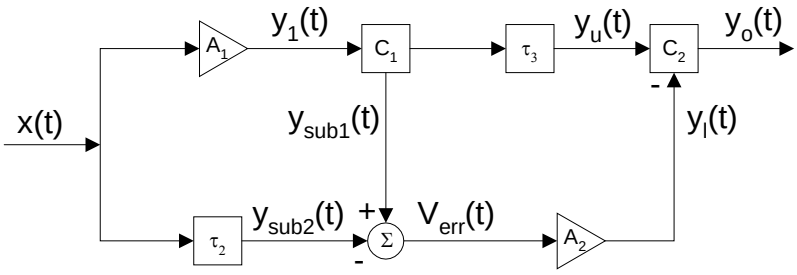

Figure 2.6 Feedforward Configuration [20] , [48]

The input signal is first split into two paths. In the first path, the signal x(t) is amplified by the NLA A1 resulting in an amplified signal

$$y_1(t) = \frac{A_1}{2} x(t) e^{j\omega_c \tau_{A1}} + V_d(t), \qquad 2.33$$

where τ_{A1} is the delay through the amplifier A_1 and $V_d(t)$ is the associated non-linear distortion. In the second path, this distorted signal is split using the directional coupler C_1 to yield

$$y_{sub1}(t) = \frac{A_1}{2C_{C1}} x(t) e^{-j\omega_c \tau_{A1}} + \frac{V_d(t)}{C_{C1}}, \qquad 2.34$$

where $1/C_{C1}$ is the coupling factor of the directional coupler C1. The output of the subtracter produces an error signal

$$V_{err}(t) = V_{sub1}(t) - V_{sub2}(t) \qquad 2.35$$

where $V_{sub2}(t)$ is the signal at the second subtracter input. This simplifies to

$$V_{err}(t) = \frac{A_1}{2C_{C1}} x(t) e^{-j\omega_c \tau_{A1}} + \frac{V_d(t)}{C_{C1}} - \frac{1}{2} x(t) e^{-j\omega_c \tau_2}. \quad 2.36$$

In order for x(t) to be completely removed from $V_{err}(t)$,

$$\tau_{A1} = \tau_2 \quad 2.37$$

and

$$C_{C1} = A_1. \quad 2.38$$

Consequently,

$$V_{err}(t) = \frac{V_d(t)}{C_{C1}}. \quad 2.39$$

The signals at the input of the directional coupler C_2 may be written as

$$y_u(t) = \frac{A_1}{2} x(t) e^{j\omega_c(\tau_{A_1} + \tau_3)} + V_d(t) e^{-j\omega_c \tau_3} \quad 2.40$$

and

$$y_l(t) = \frac{A_2 . V_d(t)}{C_{C1}} e^{-j\omega_c \tau_{A2}} \quad 2.41$$

where τ_{A2} is the time delay through amplifier A_2 and τ_3 is the delay required in the upper path to ensure the cancellation of the distortion term at the output $y_o(t)$.

The output signal $y_o(t)$ may now be written as

$$y_o(t) = y_u(t) - y_l(t) \quad 2.42$$

where the "-" sign in front of $y_l(t)$ represents the phase inversion at the lower input of directional coupler C_2. Substituting 2.40 and 2.41 into 2.42 yields

$$y_o(t) = \frac{A_1}{2} x(t) e^{j\omega_c(\tau_{A_1}+\tau_3)} + V_d(t) e^{-j\omega_c\tau_3} - \frac{A_2 . V_d(t)}{C_{C1}} e^{-j\omega_c\tau_{A2}} . \quad 2.43$$

By inspection of 2.43 it can be seen that the distortion terms will cancel perfectly if

$$\tau_{A2} = \tau_3 \quad 2.44$$

and

$$A_2 = C_{C1} \quad 2.45$$

Hence the output becomes

$$y_o(t) = \frac{A_1}{2} x(t) e^{j\omega_c(\tau_{A_1}+\tau_3)} . \quad 2.46$$

Notice that the output signal is simply an amplified version of the input signal x(t) delayed by a time constant [20] , [48].

2.4.2 Feedback

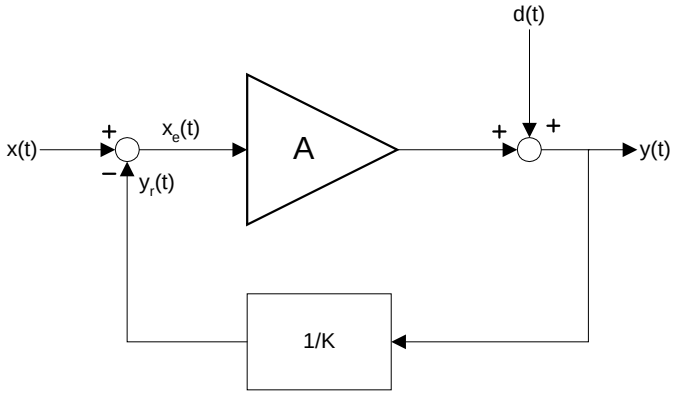

Figure 2.7 Feedback Configuration [20] , [48]

In the feedback method the distortion is modeled as an additive term after the amplifier. Negative feedback is used to generate an error signal that drives the amplifier in a direction that tends to correct for the effect of the non-linearity. To illustrate this, consider the instantaneous effect of a slightly positive d(t) term. A fraction of this slightly positive d(t) term will be subtracted from the instantaneous input signal to generate a reduced

instantaneous input signal, $x(t) - y_r(t)$. The resulting signal at the output of the amplifier will therefore be reduced. The net effect at the output will be an instantaneous voltage closer to the ideal. A similar discussion may be applied to the case of a slightly negative d(t) term.

Expressed mathematically, it can be easily shown that the output signal is given by

$$y(t) = \frac{K(Ax(t) + d(t))}{K + A} \qquad 2.47$$

where x(t) is the input signal, y(t) is the output signal, A is the amplifier gain and K is the feedback term.

If A >> K then K + A ≈ A and y(t) becomes

$$y(t) = Kx(t) + \frac{Kd(t)}{A} \qquad 2.48$$

.

It is clearly evident that the distortion term d(t) is reduced in proportion to the ratio of feedback term K and the amplifier gain A [20] , [48].

2.4.3 Pre-distortion

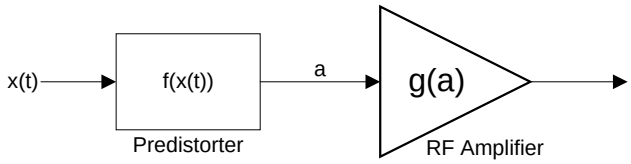

Figure 2.8 Pre-distortion Configuration [20] , [48]

Pre-distortion attempts to cancel the effect of a non-linear amplifier by distorting the signal en route to the amplifier input. This “pre-distortion” is designed to complement the amplifier transfer function such that the net effect of the pre-distorter and the NLA produces a signal that experiences linear amplification.

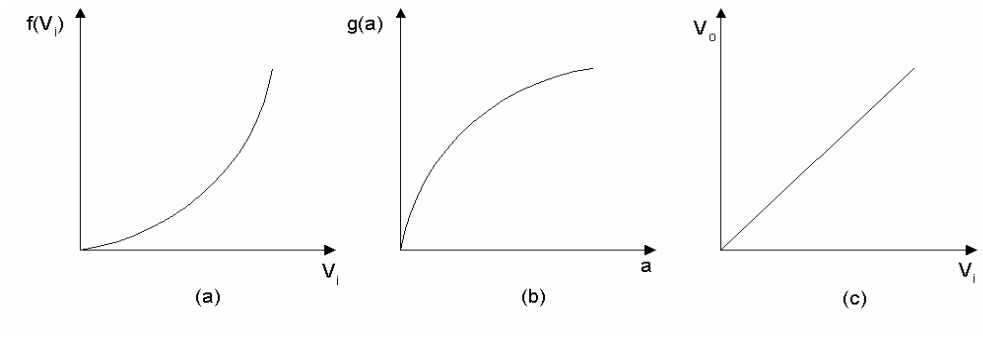

Figure 2.9 Operation of a Pre-distortion System [20] , [48]

Figure 2.9 illustrates the above discussion. Curve (a) is the transfer characteristic of a pre-distorter for the amplifier transfer characteristic of curve (b). A pre-distorter can be designed such that the input-output transfer function of the series combination of the pre-distorter and amplifier looks like the curve in (c) i.e. an ideal linear amplifier [20] , [48].

2.4.4 LINC

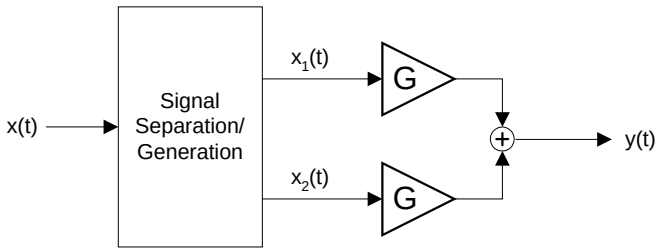

Figure 2.10 LINC System [20] , [48]

The term "LINC" is an acronym which refers to "Linear Amplification using Non-Linear Components." Linear amplification is obtained by converting the varying-envelope input signal x(t) into two constant-envelope, phase-modulated signals $x_1(t)$ and $x_2(t)$. The signals $x_1(t)$ and $x_2(t)$ are then each applied to an NLA. The signals are then summed to yield an amplified version of the input signal x(t) without the distortion contribution of the NLA's.

To understand how the signals $x_1(t)$ and $x_2(t)$ are obtained consider Figure 2.11 where the input signal is split into its envelope and phase components V(t) and $\cos(\omega_c t + \phi(t))$, respectively.

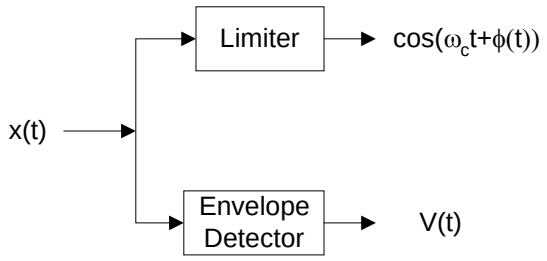

Figure 2.11 Envelope and Phase Generation

Now, consider Figure 2.12. In the upper branch V(t) phase modulates the carrier frequency to produce $x_1(t)$. In the lower branch V(t) is inverted and phase modulates the carrier frequency to produce $x_2(t)$. The phase $\alpha(t) = k_p V(t)$ where k_p is the phase modulation constant.

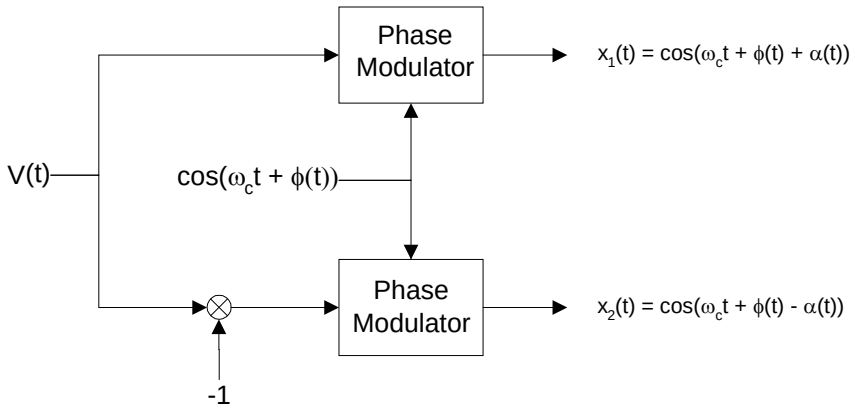

Figure 2.12 LINC Signal Generation

To understand how the sum of the signals $x_1(t)$ and $x_2(t)$ relate to the input x(t) consider the system in Figure 2.10 where an RF signal is described by

$$x(t) = V(t)\cos\left(\omega_c t + \phi(t)\right), \qquad 2.49$$

where

$$V(t) = V_{\max}\cos\left(\alpha(t)\right), \qquad 2.50$$

represents the amplitude modulation present on the signal [20], [48].

Now, 2.49 may be re-written as

$$x(t) = V_{\max} \cos(\omega_c t + \phi(t))\cos(\alpha(t)). \quad 2.51$$

Using the trigonometric identity

$$\cos A \cos B = \frac{1}{2}\cos(A+B) + \frac{1}{2}\cos(A-B), \quad 2.52$$

implies that

$$x(t) = \frac{1}{2}V_{\max} \cos(\omega_c t + \phi(t) + \alpha(t)) + \frac{1}{2}V_{\max} \cos(\omega_c t + \phi(t) - \alpha(t)). \quad 2.53$$

Defining

$$\theta(t) = \phi(t) + \alpha(t) \quad 2.54$$

and

$$\varphi(t) = \phi(t) - \alpha(t) \quad 2.55$$

implies that

$$x(t) = \frac{1}{2}V_{\max} \cos(\omega_c t + \theta(t)) + \frac{1}{2}V_{\max} \cos(\omega_c t + \varphi(t)). \quad 2.56$$

Defining

$$x_1(t) = \frac{1}{2}V_{\max} \cos(\omega_c t + \theta(t)). \quad 2.57$$

and

$$x_2(t) = \frac{1}{2}V_{\max} \cos(\omega_c t + \varphi(t)). \quad 2.58$$

implies that

$$x(t) = x_1(t) + x_2(t). \quad 2.59$$

Equation 2.59 states that the original modulated RF signal can be expressed as the sum of two constant envelope phase modulated signals $x_1(t)$ and $x_2(t)$. Each of $x_1(t)$ and $x_2(t)$ can be amplified by the non-linear SSPA without introducing distortion.

The reason why a constant-envelope phase-modulated signal minimizes distortion is that there is no information contained in the amplitude of the signal. The information is encapsulated in the phase-modulation instead. Hence, an SSPA's non-linear AM/AM characteristic will not influence the signal. Additionally, since the AM/PM curve is essentially flat (i.e. zero gradient), very little phase distortion results when this signal is amplified using an SSPA.

2.4.5 Envelope Elimination and Restoration

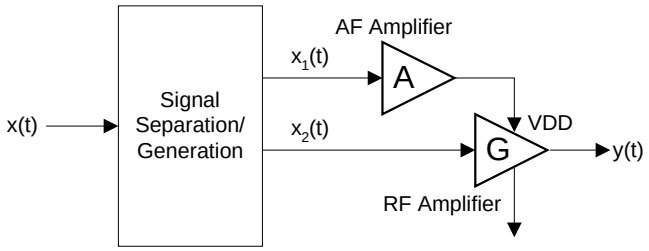

Figure 2.13 Envelope Elimination and Restoration System [20], [48]

The Envelope Elimination and Restoration System in Figure 2.13 splits the RF signal x(t) into a baseband envelope signal $x_1(t)$ and a constant envelope phase modulated carrier signal $x_2(t)$. $x_2(t)$ is then amplified by a high efficiency RF amplifier (e.g. Class C, D or E). The baseband signal $x_1(t)$ is amplified by a suitable audio amplifier and the resulting signal is used to modulate the power supply of the RF power amplifier to restore the amplitude information. This results in a high power amplified version of the signal x(t) [20] , [48] without NLA distortion.

The constant envelope phase modulated signal $x_2(t)$ may be obtained by subjecting x(t) to a limiter circuit that clips and filters x(t). The baseband signal $x_1(t)$ may be obtained by applying the signal x(t) to a diode detector circuit. This circuit follows the input signal envelope to produce $x_1(t)$ [20] , [48].

To understand how the envelope of the signal is restored consider the Class D switching amplifier in Figure 2.14 [20]. The input RF signal $x_2(t)$ is applied to a transformer which presents anti-phase signals to transistors TR1 and TR2. These transistors are switched on and off at a rate equal to the input RF signal frequency. Inductor L_1 and capacitor C_1 form a tuned circuit centered around the carrier frequency ω. The net effect of this is that y(t), is a replica of the input signal $x_2(t)$ provided V_{cc} is held constant.

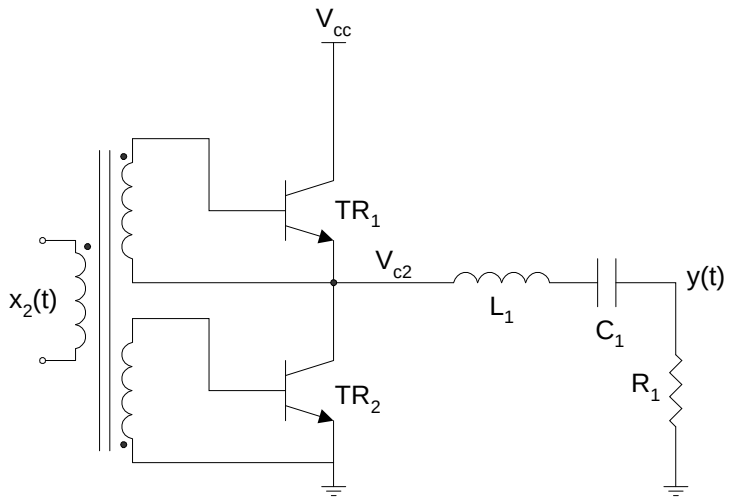

Figure 2.14 Class D Complementary Voltage Switching Amplifier [20]

Now to consider the effect of varying V_{cc} note that the voltage across the collector of transistor TR2 is

$$V_{c2} = V_{cc}\left[\frac{1}{2} + \frac{1}{2}h(\omega t)\right], \qquad 2.60$$

where

$$h(\omega t) = \begin{cases} +1 & if\ \sin(\omega t) \geq 0 \\ -1 & if\ \sin(\omega t) < 0 \end{cases}. \qquad 2.61$$

Using Fourier analysis $h(\omega t)$ may be expressed as

$$h(\omega t) = \frac{4}{\pi}\left[\sin(\omega t) + \frac{1}{3}\sin(3\omega t) + \frac{1}{5}\sin(5\omega t) + ...\right]. \qquad 2.62$$

Hence

$$V_{c2} = V_{cc}\left[\frac{1}{2} + \frac{2}{\pi}\sin(\omega t) + \frac{2}{3\pi}\sin(3\omega t) + \frac{2}{5\pi}\sin(5\omega t) + ...\right]. \qquad 2.63$$

After filtering with the tuned circuit consisting of the inductor L_1 and the capacitor C_1 the output voltage is

$$y(t) = \frac{2V_{cc}}{\pi}\sin(\omega t). \qquad 2.64$$

This result indicates that by varying the supply voltage V_{cc} to the amplifier it is possible to control the output voltage amplitude $2V_{cc}/\pi$; i.e. if the input to the amplifier is a constant envelope phase modulated signal sin(ωt) then the envelope of the signal at the amplifier output y(t) will follow the shape of the supply voltage variations as per equation 2.64.

The amplitude of the supply voltage variations depends on the amplitude of the controlling audio signal $x_1(t)$. If this audio signal is amplified linearly, which is relatively easy to do at audio frequencies, then the amplitude of the supply voltage variations will increase proportionately. The corresponding signal envelope at the amplifier output will therefore also increase by this same factor. The net effect of this is an amplified version of the original RF signal without the effect of the non-linear characteristic of the RF amplifier.

2.5 Amplifier Linearisation Experiments

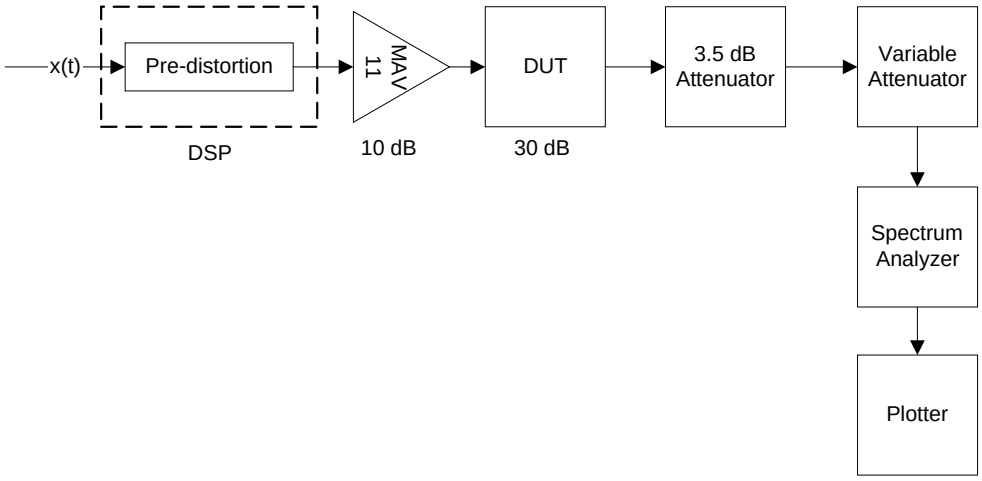

Figure 2.15 Distortion Test Setup

The system was setup according to Figure 2.15. It consisted of 10 dB of gain provided by a MAV11, followed by 30 dB of gain provided by a proprietary power amplifier module (DUT). The amplifier chain was driven by a DSP module. The amplifier output was attenuated by 40 dB before being fed into the input of a spectrum analyzer.

Software was written for the DSP module that swept the input power from a minimum to a maximum value at a specific rate. The spectrum analyzer span was set to 0Hz with a sweep time of 3 seconds. This configured the spectrum analyzer to display a plot of Output Amplitude vs Input Amplitude. Figure 2.16 displays the non-linear characteristic of the amplifier as well as the response of a DSP based pre-distortion implementation using a 3rd order polynomial fit to the pre-distorter curve[4]. The pre-distorter was designed such that the series combination of the pre-distorter and amplifier non-linearity yielded a linear response.

Figure 2.17 displays the result of a linear piece-wise linearisation method with 5-segments. This method involved selecting 6 points on the pre-distorter curve, joining consecutive points with straight lines and then using the equation of each line to approximate the curve over the corresponding domain and range. It was noted that pre-distortion (i.e. blue curve) produced an overall improvement in the IMD response to a two-tone signal as illustrated by the suppressed sidebands.

[4] The curve marked “Pre-distortion Response” in Figure 2.16 is the response of the combination of the pre-distorter and the NLA.

The piece-wise curve was replaced with a 3rd order polynomial fit to the selected points. Figure 2.18 illustrates that the improvement in IMD products (i.e. suppressed sidebands) was better than that for the piecewise linearization. The polynomial fit provided a smoother gradient transition from one "segment" to the next. Since the gradient is equal to the gain, a stepped change in gain produces a stepped change in amplifier output. This translates into a poorer IMD performance.

The effect of power supply voltage on harmonic distortion was also investigated The pre-distortion characteristic was optimized for a supply voltage of 21V. Figure 2.19 shows a 12 dB improvement in the 1st and 2nd IMD products.

Figure 2.20 and Figure 2.21 plot the response of the pre-distortion implementation for supply voltages of 18 and 24 volts, respectively. It was observed that the improvement in IMD suppression was less for the 18V (9 dB improvement in 1st and 2nd IMD product) and 24V (9 dB in 1st IMP product, 1 dB improvement in 2nd IMD product) cases. This was expected because the supply voltage affects the operating point of the amplifier leading to an altered transfer function. The pre-distorter did not match the response as well; hence the poorer IMD response. It was also noted that the pre-distorter produced an 8% improvement in RF conversion efficiency and improved the DC power consumption by 29% for an output power of 4.4. watts.

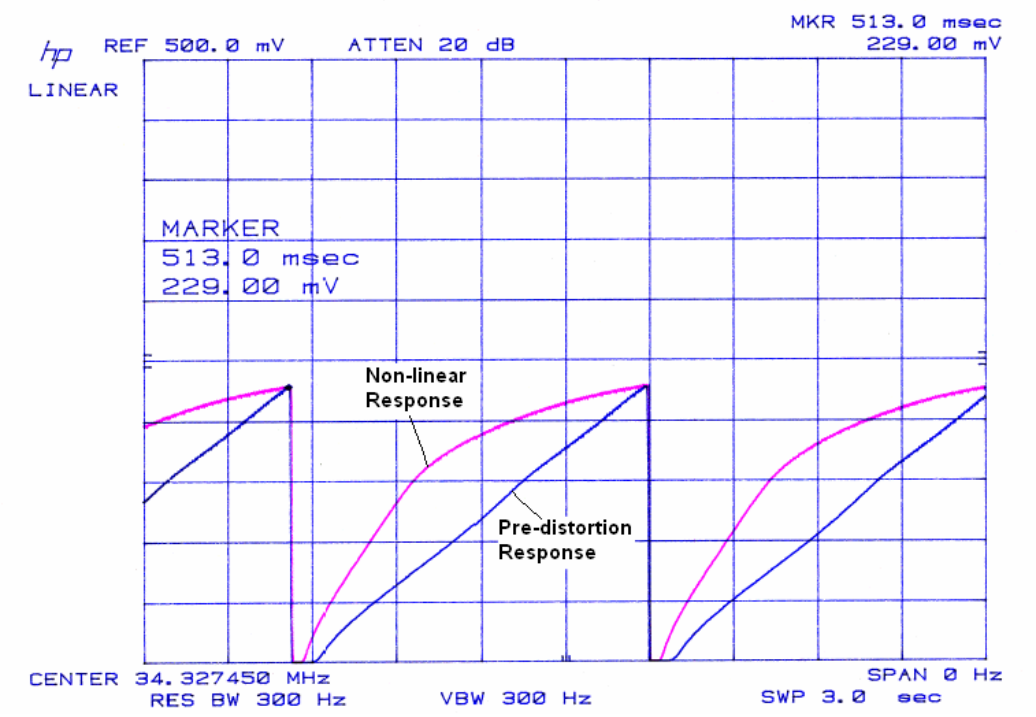

Figure 2.16 Amplifier Input/Output Characteristic

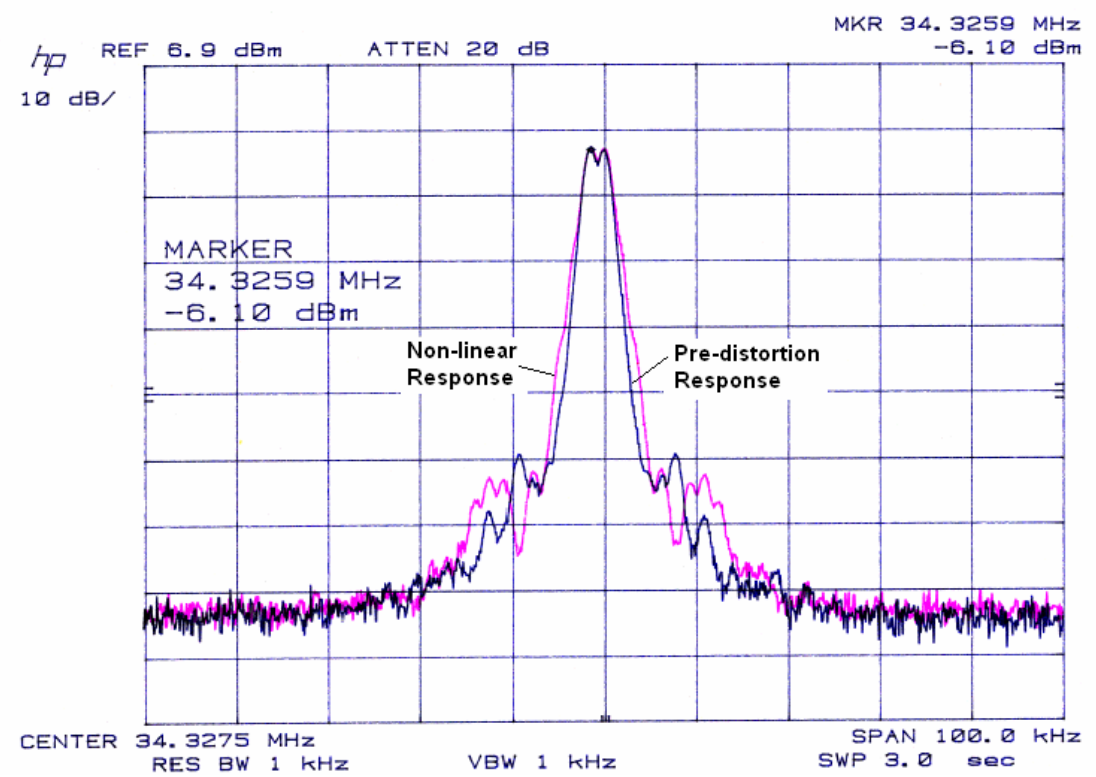

Figure 2.17 **5 Segment Piece-wise Fit – 21 Volt Supply**

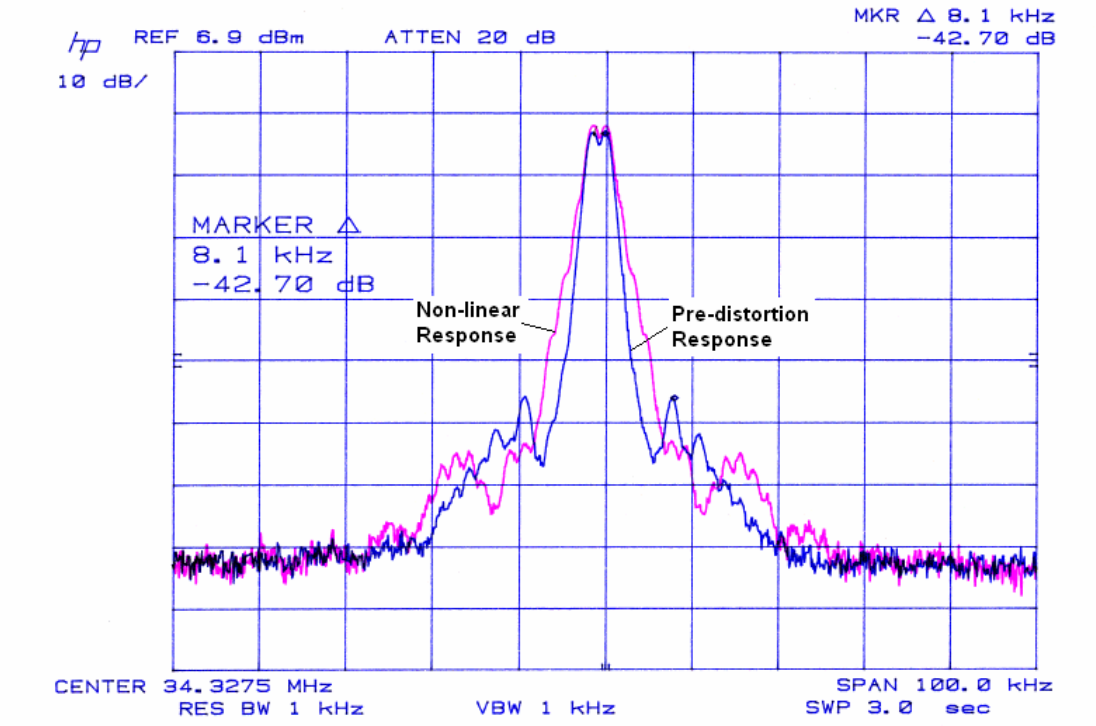

Figure 2.18 **3rd Order Polynomial Fit – 21 Volt Supply**

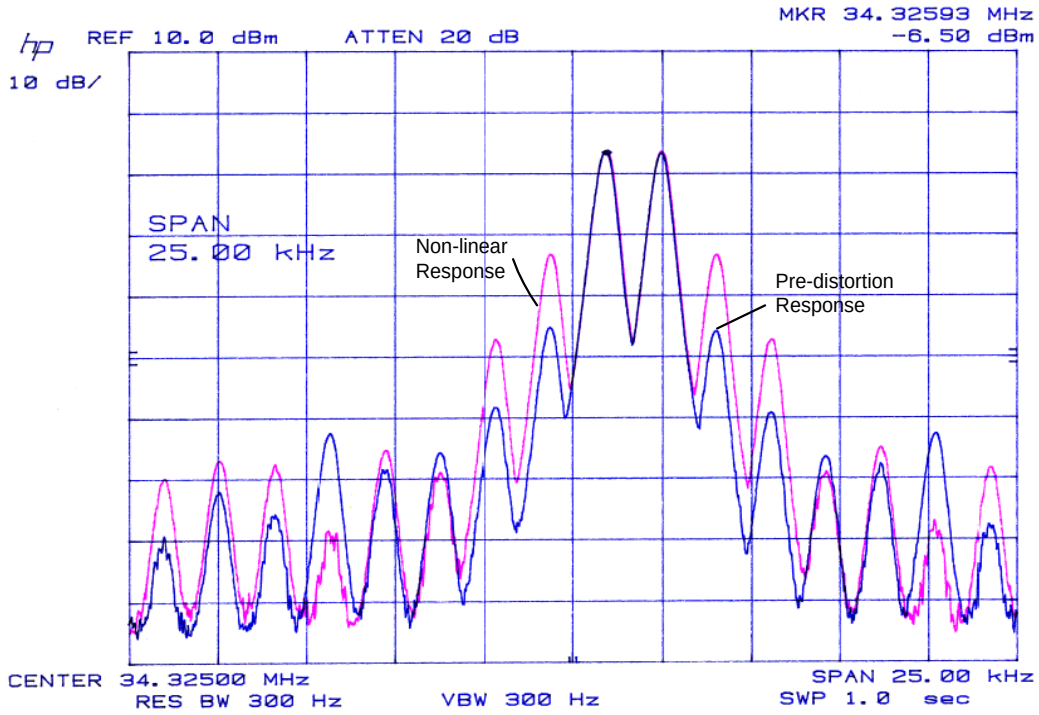

Figure 2.19 **3rd Order Polynomial Fit – 21 Volt Supply**

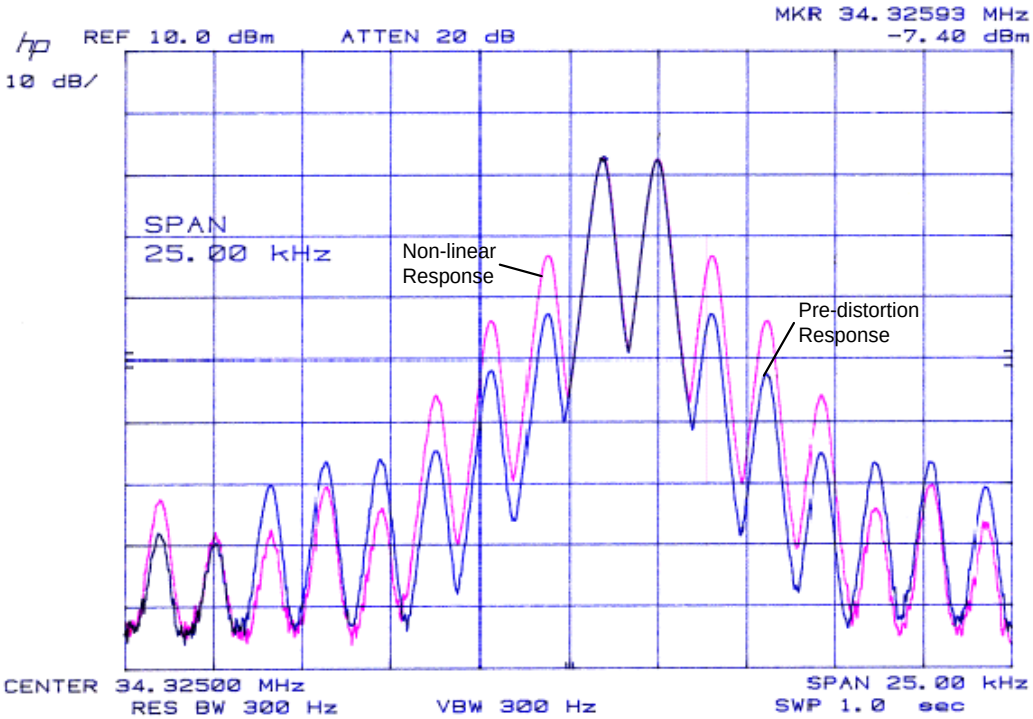

Figure 2.20 **3rd Order Polynomial Fit – 18 Volt Supply**

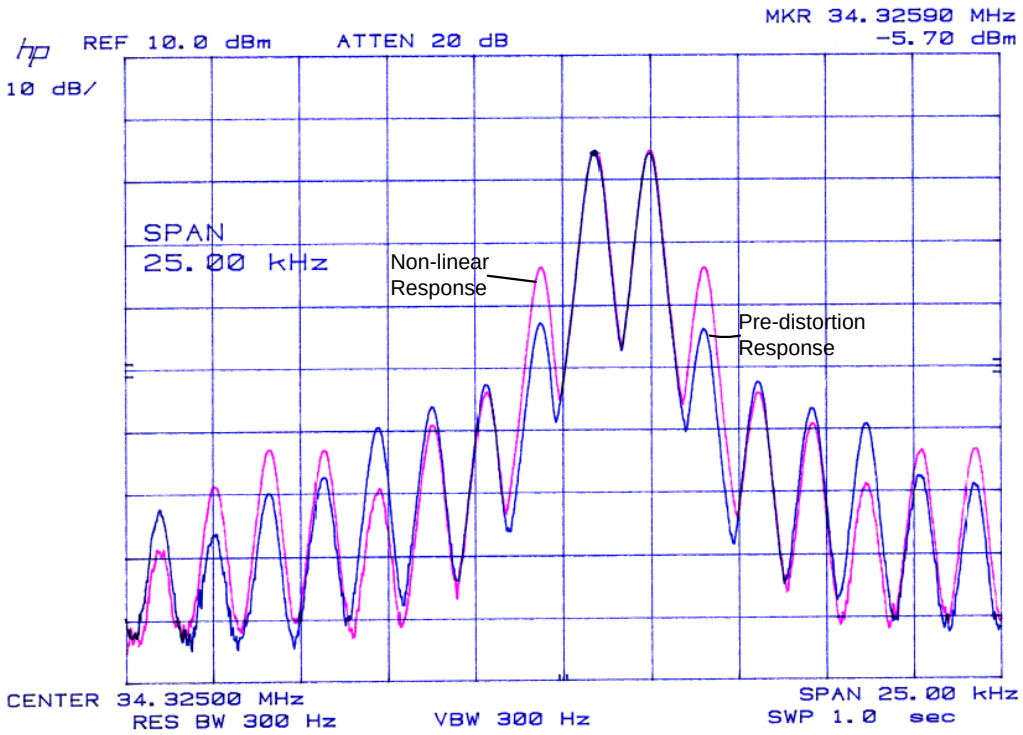

Figure 2.21 **3rd Order Polynomial Fit – 24 Volt Supply**

2.6 Summary

This chapter presented a survey on amplifier models, amplifier output characteristics linearisation methods and a practical investigation of the pre-distortion method of linearisation.

It was found that amplifier models can be used to predict the performance of communication systems. Models exist for amplifiers that have a memory effect (e.g. frequency dependency) as well as those that are memoryless (e.g. frequency independent). Memoryless amplifiers are an approximate representation of the real device over a narrow bandwidth where the frequency dependency is not significant. In cases where the frequency bandwidth is significant, the models with memory should be used.

The amplifier output characteristics (e.g. IMD, ACPR, NPR, EVM etc.) may be used to evaluate and compare the performance of communications systems. It fact, systems usually specify these parameters bearing in mind the requirement that users within the systems may not to interfere with other users within the system or with other systems in adjacent frequency bands.

The Feedforward, Feedback, Pre-distortion, LINC and Envelope Elimination and Restoration methods of linearization can be used to make better use of the available power in a satellite downlink [12]. Additionally, non-linear equalization can also be used at the receiver to improve the system performance [34]. It is possible to employ both linearization and equalization methods in a manner that leads to a simpler implementation of each method within the system [33]. Kang [40] developed a reconfigurable/retunable pre-distorter for an NLA used in a CDMA system that demonstrated a 14 dB improvement in adjacent channel power leakage ratio (ACPR) with an amplifier back-off of 4 dB.

A practical experiment showed that the pre-distortion method may be employed to suppress the IMD products present in the sidebands for systems that make use of a non-linear amplifier. A 12 dB improvement in IMD products was observed. It was shown that the pre-distorter was sensitive to power supply voltage changes. In battery powered applications adequate power supply regulation may be required and/or the pre-distorter needs to be dynamically modified in response to the power supply voltage changes.

It was found that the pre-distorter produced an 8% improvement in RF conversion efficiency and improved the DC power consumption by 29% for an output power of 4.4 watts.

3 Effect of Non-linear Amplifiers on CDMA Systems

3.1 Introduction

In order to achieve power efficiency, an amplifier must be operated near saturation. A non-constant envelope signal presented to such an amplifier produces significant IMD products that result in in-band and out-of-band interference.

Due to their non-constant signal envelopes QAM schemes are susceptible to significant distortion from amplifiers operated near saturation. The performance of such systems improves if the amplifier is operated in the linear region far enough away from the saturation. In remote site applications it is often impractical to operate the amplifier in this way because of the low efficiency. (Recall that an amplifier's efficiency is usually defined as the ratio of the RF power output to the total power supplied by the battery). It is evident that there is a tradeoff between efficiency and linearity requirements. Chang [30] explored the concept of total degradation and suggested that it can be used to determine a suitable output back-off level given a target BER.

Prior to the research presented by Conti [1], simulation and hardware tests provided the only means of evaluating the in-band distortion effects of non-linear amplifiers on CDMA systems. Conti [1] has shown that the bit error rate (BER) and total degradation (TD) of these systems can be analytically evaluated for the cases of synchronous and asynchronous CDMA, provided that there are a large number of users and that each user transmits with the same power. The analysis makes provision for the commonly used chip waveforms.

The relationship between signal-to-noise ratio and bit error rate has been reported in the literature for various types of modulation [15]. Table 3.1 presents a summary of well known BER equations as a function of the energy per bit E_b, one-side power spectral density N_o, the number of bits per symbol P and the order of the modulation M.

These equations do not apply if there is significant signal distortion as a result of the high power amplifier non-linearity or channel fading effects. Conti [1] has formulated an analytical expression for the BER of a CDMA system in the presence of amplifier non-linearity. Prior to this paper, simulation was the only method used to determine the performance of a CDMA system with an NLA at the transmitter.

Modulation Scheme	**BER**	
BPSK, QPSK, MSK	$\frac{1}{2}erfc\sqrt{\frac{E_b}{N_o}}$	3.1
MPSK	$erfc\sqrt{\frac{PE_b}{N_o}\sin^2\left(\frac{\pi}{M}\right)}$	3.2
16 QAM	$2erfc\sqrt{\frac{0.4E_b}{N_o}}$	3.3
Orthogonal MFSK	$\frac{M-1}{2}erfc\sqrt{\frac{NE_b}{2N_o}}$	3.4

Table 3.1 BER for Various Modulation Schemes

This chapter presents a literature survey on the effect of non-linear amplifiers used in CDMA, Multi-code CDMA, MC-CDMA and OFDM systems. Conti's [1] model for a CDMA downlink with an SSPA NLA is then presented. Using a systematic approach a complete set of results is generated. The Matlab code for the CDMA system is included in Appendix B. Additional analytical and simulation results are generated to prove the accuracy of the analytical model. Simulation results for the CDMA uplink with an SSPA type NLA are also presented.

3.2 Survey of CDMA, Multi-Code CDMA and MC-CDMA

Since this survey includes discussions on CDMA, Multi-code CDMA and MC-CDMA, a brief a discussion of each system is first undertaken before the broader survey is presented.

3.2.1 Code Division Multiple Access System (CDMA)

CDMA refers to a channel access method that allows multiple users to share the same channel. A simplified block diagram of a CDMA system is shown in Figure 3.1.

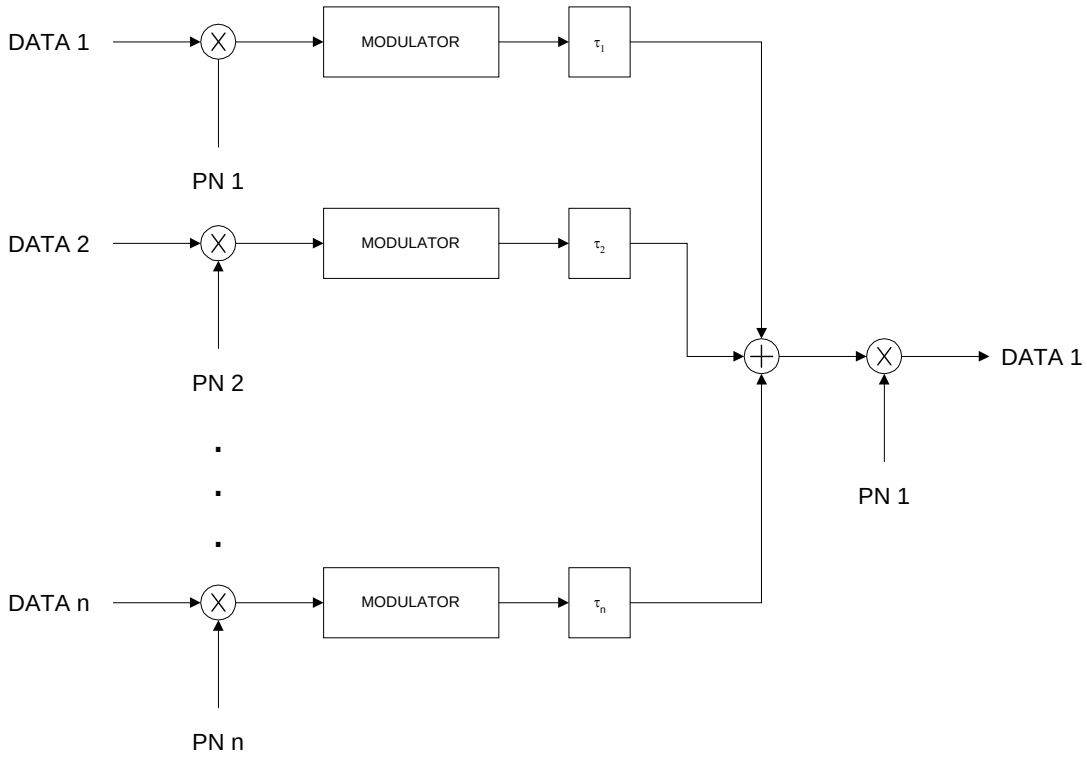

Figure 3.1 CDMA Uplink System

The user data bits are each spread by a sequence that exhibits pseudo-random or orthogonal properties. This spreads the signal over a wider bandwidth that depends on the spreading factor of the sequence. The spread sequences are modulated and transmitted through the channel. At the receiver any 1 of the n data streams may be recovered using the corresponding spreading sequence. CDMA is used in the IS95 standard.

3.2.2 Multiple Carrier CDMA (MC-CDMA)

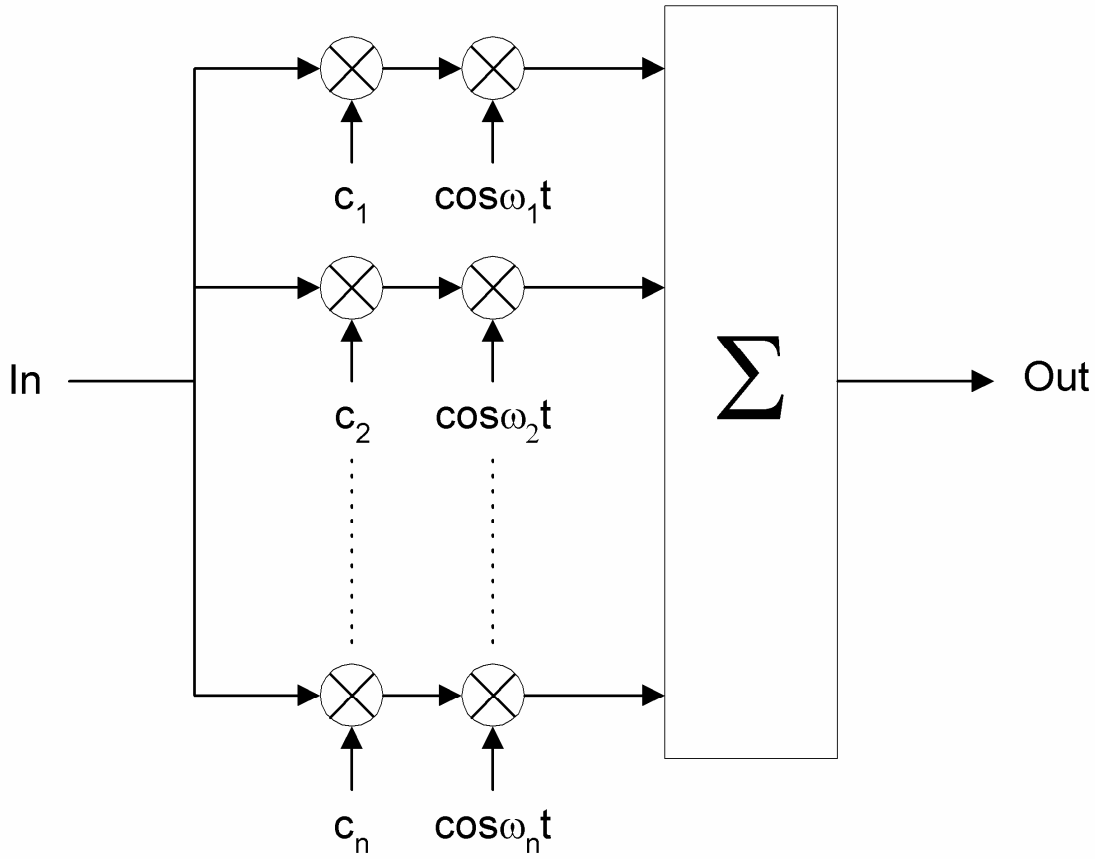

Figure 3.2 MC-CDMA Transmitter

MC-CDMA uses several sub-carriers that carry the same data. Each sub-carrier signal is spread by a different spreading sequence. This scheme offers improved immunity to frequency selective fading [44]. MC-CDMA is used in the CDMA2000 standard.

3.2.3 Orthogonal Frequency Division Multiplexing (OFDM)

In the OFDM system of Figure 3.3 the serial data stream is converted into a parallel format. Depending on the order of modulation, bits may be grouped and modulated (e.g. BPSK, QPSK, QAM, etc). The complex modulated signals are inverse Fourier transformed to yield time-domain signals. Analog-to-digital conversion is applied to the real and complex components, respectively before up-conversion. At the receiver, the incoming signal is down-converted, filtered and converted to a digital representation of real and complex components. A Fourier transform operation is performed on the time-domain data to produce a frequency representation. Symbol detection and recovery of the original bit stream then occur.

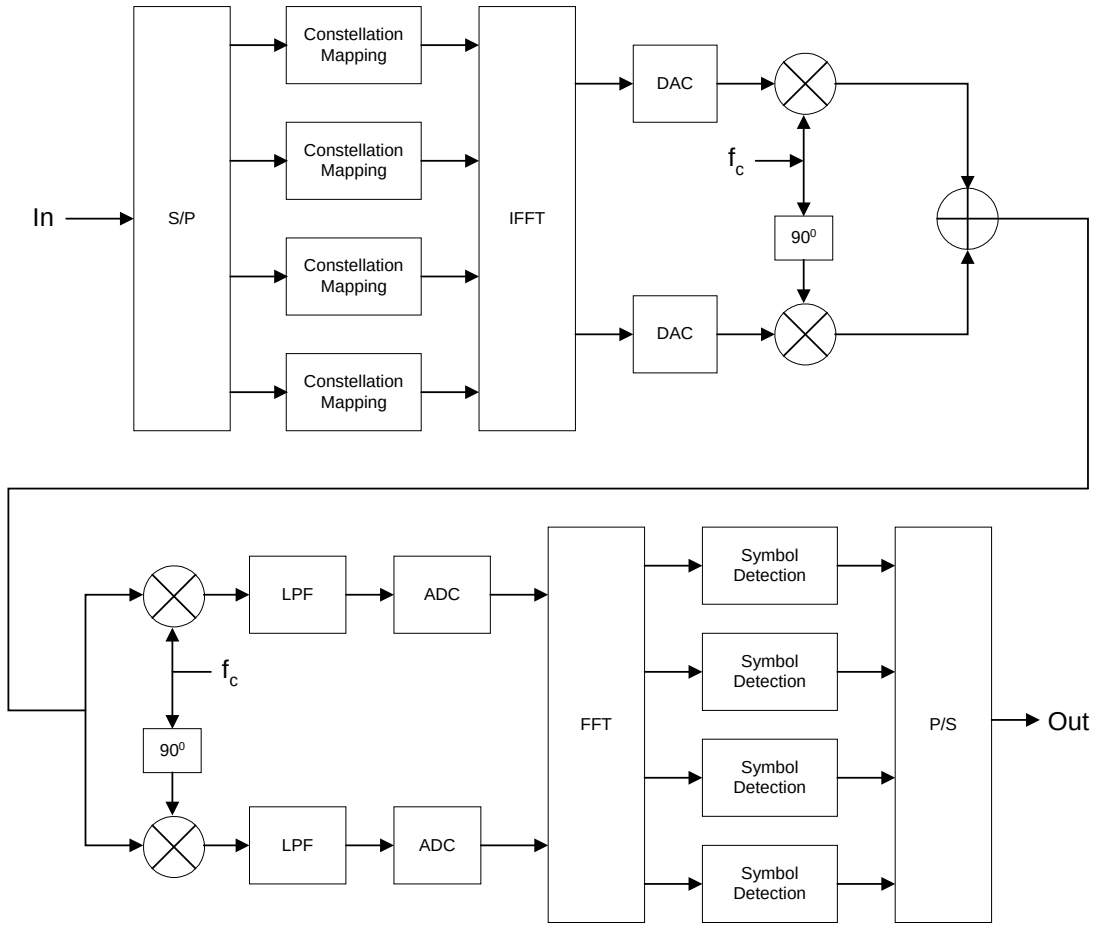

Figure 3.3 OFDM System

The main advantage of OFDM systems over single carrier schemes is its resistance to narrowband interference and frequency selective fading due to multipath effects without the need for equalization filters [43].

The output spectrum and BER performance of OFDM systems in non-linear AWGN channels can be analytically evaluated for a sufficiently large number of sub-carriers [39], [3]. Conti [1] extended that research to a CDMA downlink system. It was shown that, under certain circumstances, this distortion can be regarded as Additive White Gaussian Noise (AWGN) and its effects can therefore be evaluated in a manner similar to that of AWGN [1]. In applications like satellite communications, where the downlink signal may consist of many synchronous or asynchronous components that form a multi-channel signal with a large peak to average ratio, a non-linear amplifier can have a significant effect on the signal vector error, spectral efficiency and interference levels [20]. OFDM is used in the 802.11 protocol, WiMAX (802.16 protocol), E-UTRA (Enhanced UMTS Terrestrial Radio Access and ADSL.

3.2.4 Influence of NLAs on Multi-code CDMA Systems

Guo considered the performance of the uplink multi-code CDMA system with an NLA as shown in Figure 3.4 for the general multi-code DS/CDMA case and Figure 3.5 for the modified multi-code DS/CDMA case. It has been suggested that using a modified scheme with maximum likelihood detection and an appropriately selected Q_i leads to a constant envelope signal and an associated improvement in performance [42]. This result is of particular significance for linear modulation schemes like QAM.

In Figure 3.4, the user symbol $a_m^{(k)}$ is mapped using a codeword Q_i, where $0 \le i \le M$ and $M = 2^m$. The number of bits in the symbol $a_m^{(k)}$ is m. Q_i is pulsed shaped with a rectangular chip waveform

$$c_j(t) = \sum_{j=-\infty}^{\infty} \sum_{n}^{N} c_{j,n} g(t - jT - (n-1)T_c , \qquad 3.5$$

where $c_{j,n}$ is the n^{th} chip of spreading sequence c_j, T_c is the chip duration, T is the symbol period and g(.) is the chip waveform.

The code word Q_i is defined as a either constant weight code (CWC) or bipolar CWC (BCWC) with a weight w; e.g. if $\delta > 0$ then the code (0..0δ0…0δ0…0) is a CWC with w = 2 and the code (0..0$\pm\delta$0…0$\pm\delta$0…0$\pm\delta$0) is a BCWC with w = 3.

The spreading sequence c_j may be generated by super-imposing a Walsh sequence W_j onto a random sequence.

After spreading and up-conversion, to the carrier frequency, the signal is amplified and transmitted through the channel. The signal at the receive experiences a time delay τ relative to the transmitted signal as well as AWGN and multiple access interference (MAI) from other users. The received signal is then down-converted and applied to a coherent maximum-likelihood detector to recover the data symbol $a_m^{(k)'}$.

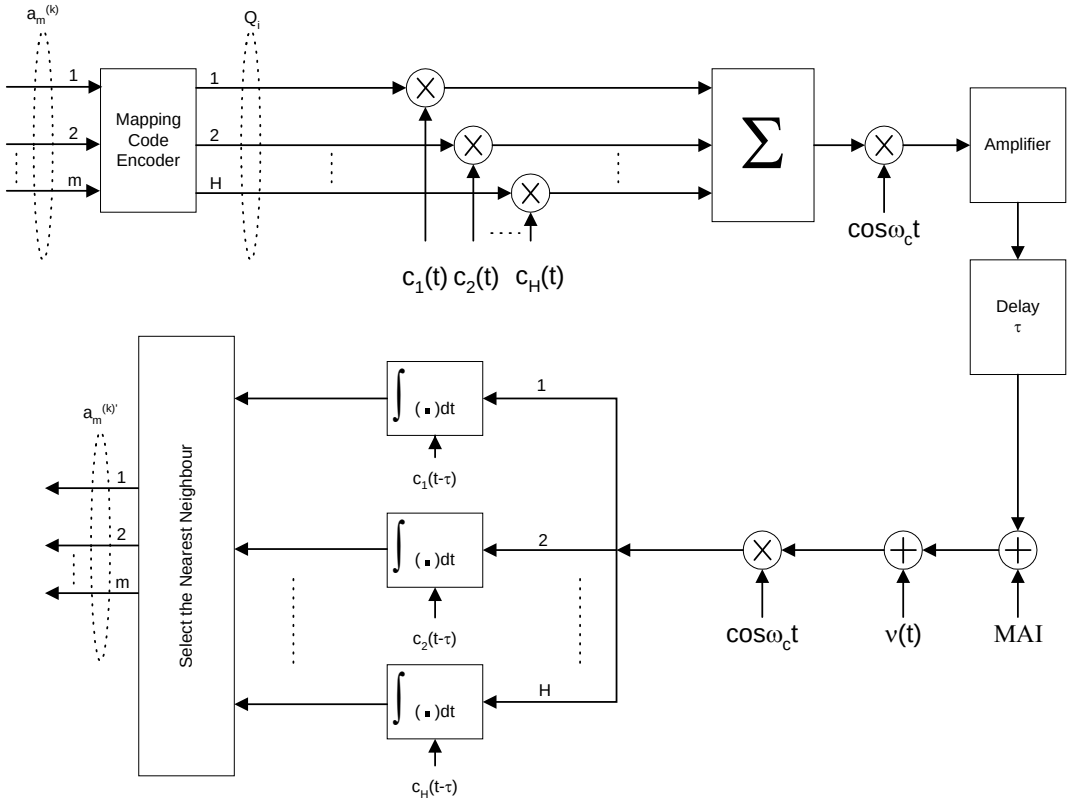

Figure 3.4 General Multi-code DS/CDMA System

In the modified multi-code system of Figure 3.5 two sequences are transmitted in parallel using a pair of quadrature carriers and the code words Q_i are designed such that the w = 2. The receiver also has two branches for the recovery of the data symbols.

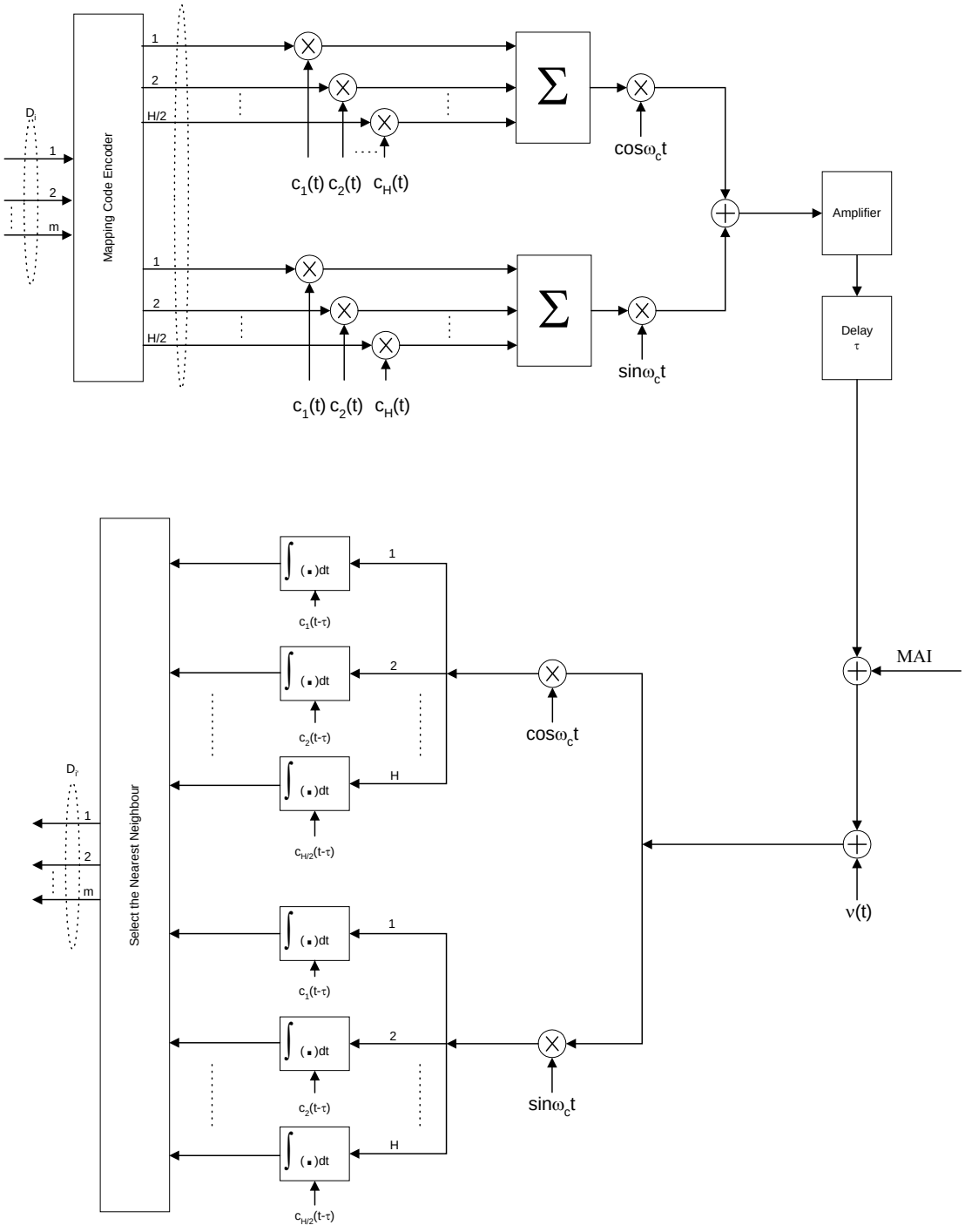

Figure 3.5 Modified Multi-code System with Constant Envelope

Now, in order to compare the two schemes the parameters m, w and H were selected as shown in Table 3.2. The results are illustrated in Figures 3.6 to 3.9.

SYSTEM	M	w	H	NOTES
System 1	4	4	4	all-code parallel
System 1a	4	2	4	partial-code-parallel
System 1b	4	2	4	modified system
System 1c	4	1	8	bi-orthogonal
System2	8	8	8	all-code parallel
System 3	15	15	15	all-code parallel
System 3a	15	2	129	partial-code-parallel
System 3b	15	2	182	modified system
System 3c	15	3	31	partial-code-parallel

Table 3.2 Multi-code System Parameters

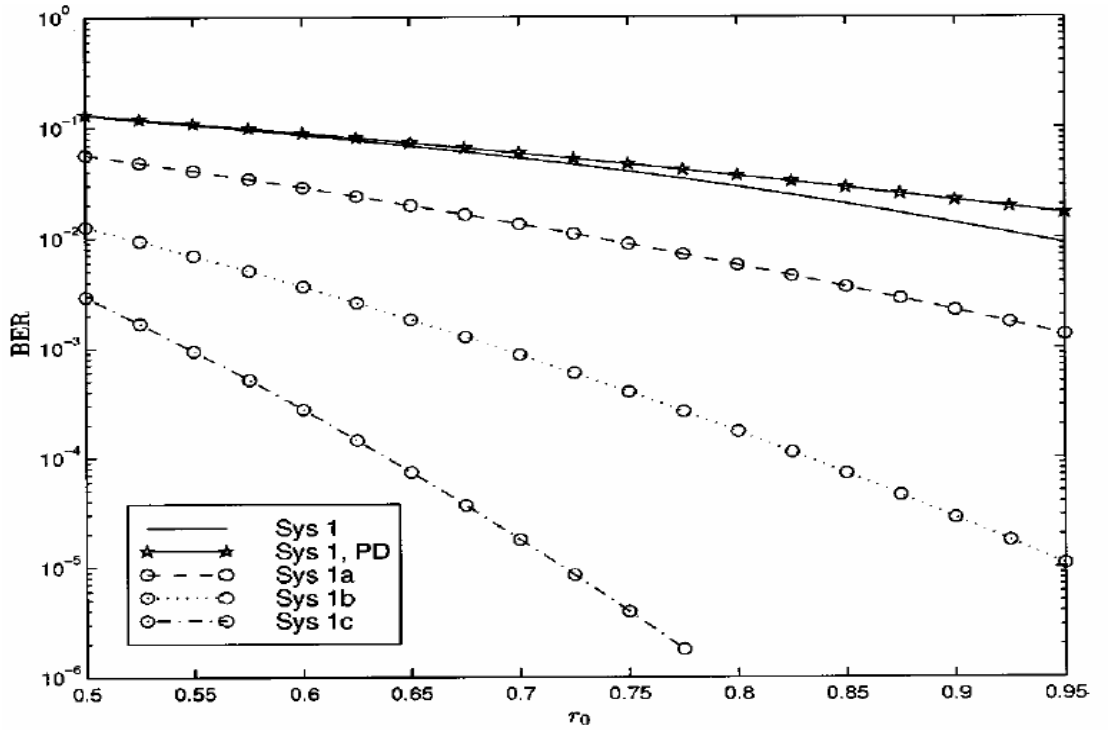

Figure 3.6 Multi-code System - N = 256, K = 1, E_b/N_o = 10 dB, m = 4

(reprinted from [42])

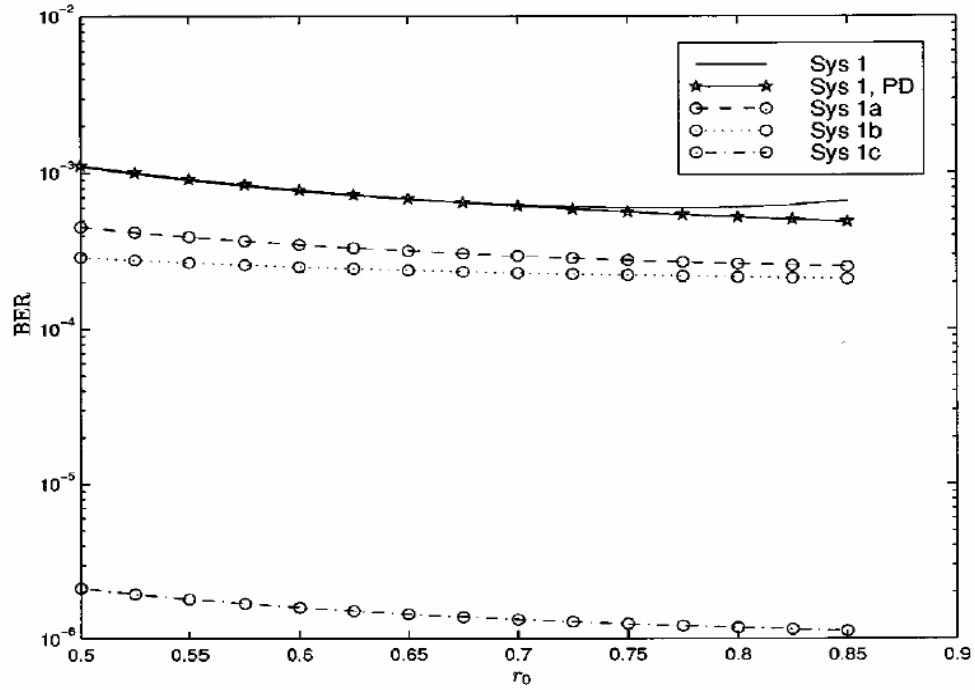

Figure 3.7 Multi-code System N = 256, K = 16 , E_b/N_o = 25 dB, m = 4 (reprinted from [42])

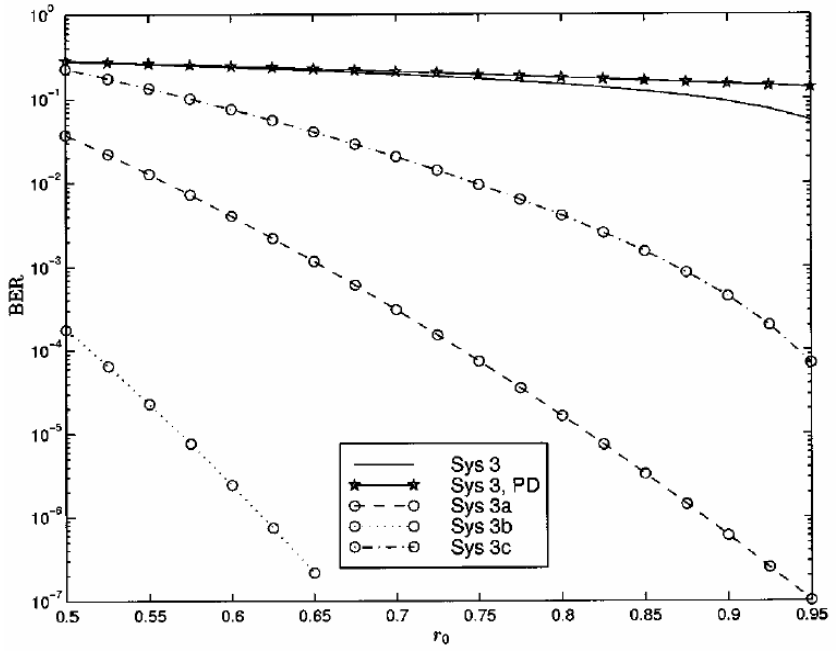

Figure 3.8 Multi-code System - N = 256, K = 1, E_b/N_o = 10 dB, m = 15 (reprinted from [42])

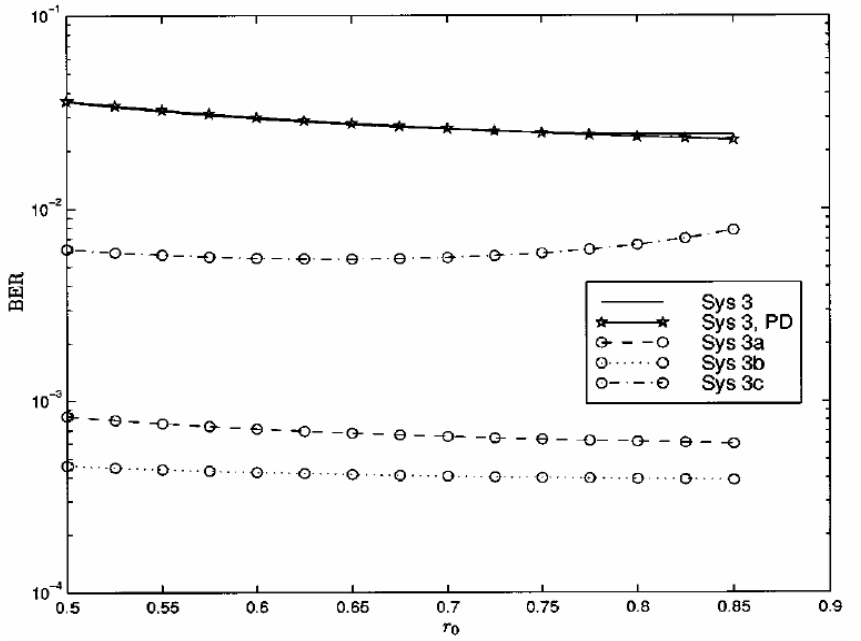

Figure 3.9 Multi-code System - N = 256, K = 12, E_b/N_o = 25 dB, m = 15 (reprinted from [42])

Figure 3.6 indicates that System 1c (i.e. m = 4, w = 1 and H = 8) exhibits the best performance while System 1 with pre-distortion exhibits the worst performance for the single user case (i.e. K = 1). This result is due to the smaller envelope variations of the biorthogonal signal of System 1c compared to the hypercube constellation produced by System 1 [42].

Figure 3.7 shows that for a large number of users (e.g. K = 16) the performance of the systems is not greatly affect by the r_0 term[5], due the dominance of the MAI term. It is also worth noting that the constant envelope signal produced by the modified system for m = 4, w = 2 and H = 4 leads to an improved performance compared to the general multi-code systems of System 1 and System 1a.

Figure 3.8 shows the effect of increasing the number of bits per symbol m to 15. It can be seen that the modified System 3b (i.e. m = 15, w = 2 and H = 182) exhibits the best performance due to the constant envelope while System 3 with pre-distortion exhibits the worst performance for the single user case (i.e. K = 1).

Figure 3.9 shows that for a large number of users (e.g. K = 12) and a large number of bits per symbol (m = 15) the performance of the systems is again not greatly affect by the r_0 term, due

[5] The r_0 term is related to the amplifier saturation level.

the dominance of the MAI term.

The above discussion suggests that multi-code systems can be used to mitigate the effects of amplifier non-linearity. Pre-distortion tends to degrade the system performance for the single user case when w = H while an improvement is observed for the multi-user case when w = H.

3.2.5 Influence of NLAs on MC-CDMA Systems

Fazel [49] studied the effect of a NLA on the performance of a BPSK MC-CDMA system as illustrated in Figure 3.10. The figure illustrates how the signals from K users are combined and modulated using OFDM. The NLA amplifies the signal which is transmitted through an AWGN channel. At the receiver the signal is demodulated and despread to recover the data of User i.

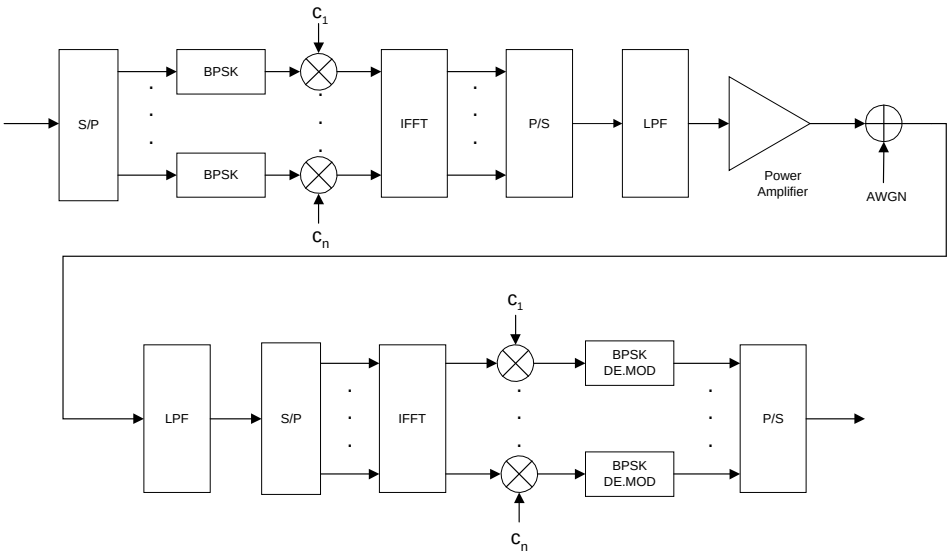

Figure 3.10 MC-CDMA Transmitter

Figure 3.11 presents the system performance in terms of the Total Degradation (TD) vs Output Back-off (OBO) for the uplink and downlink. The TD increases as the number of users increases for a specified BER and OBO. The TD also depends on the OBO.

Figure 3.12 illustrates a typical MC-CDMA system using QPSK. The input bit stream is serial-to-parallel converted. Pairs of bits are then QPSK modulated. The symbol in each branch or sub-channel is spread, modulated, amplified and transmitted through the channel. At the receiver the reverse process occurs and the user information is recovered.

It has been suggested [41] that this scheme has better performance over OFDM with non-linear amplifiers by making use of spreading code assignments based on the following two scenarios viz.

a) 1 x code word for each user in all sub-channels (System I)

b) 1 x code word for each user in each sub-channel; i.e. the codes words for the same users in different channels are different. (System II)

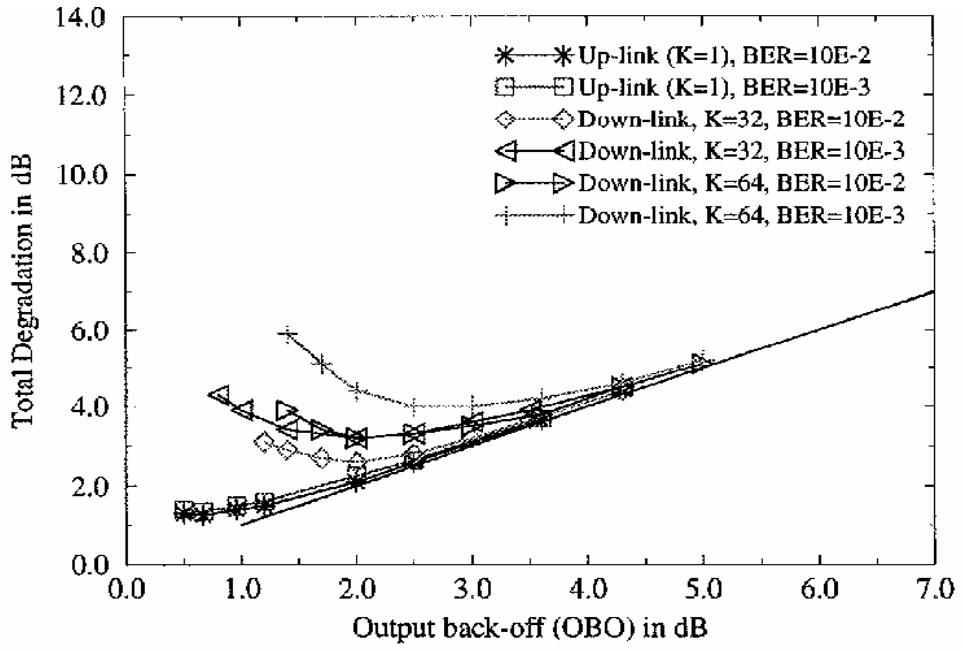

Figure 3.11 MC-CDMA – SSPA (reprinted from [41])

Figure 3.13 plots the performance of the OFDM system in terms of the Total Degradation (TD) and amplifier OBO for a BER of $1x10^{-4}$ and $1x10^{-3}$. Both linear and non-linear amplifiers are considered. The trade-off between the TD and OBO is readily seen and an optimum OBO exists that produces a minimum BER. The TD for the NLA case is 8 dB and 7.5 dB worse for the NLA (compared to the linearised amplifier) for a BER = $1x10^{-4}$ and 7.5 dB $1x10^{-3}$, respectively [41].

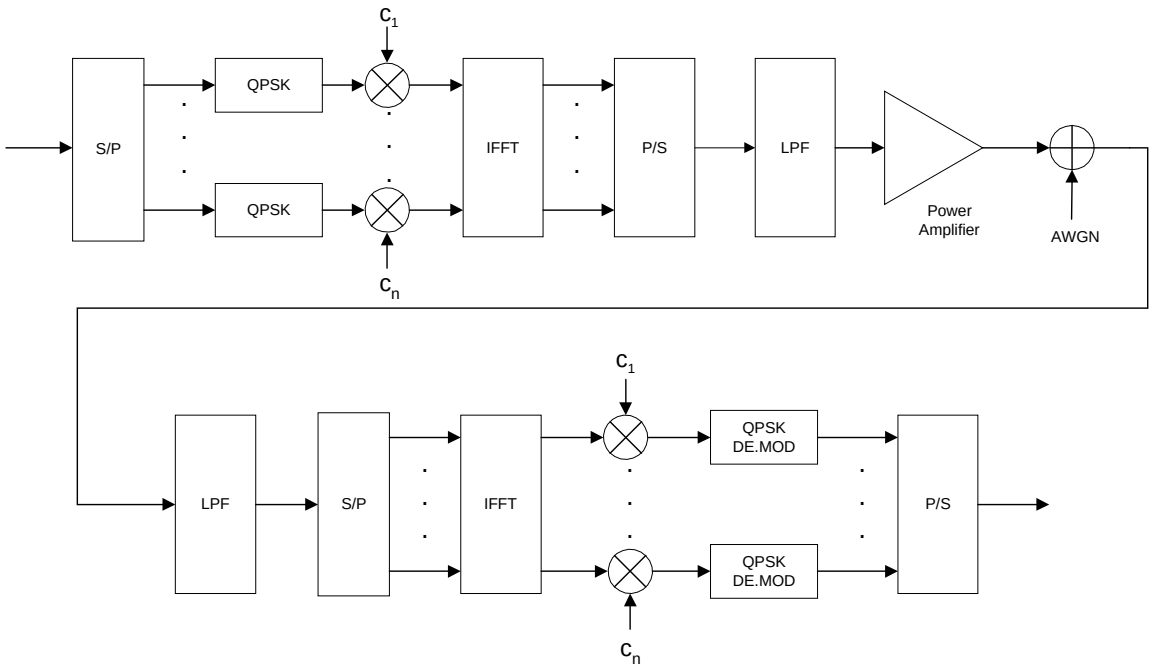

Figure 3.12 OFDM-CDMA System

Figure 3.14 compares the performance of System I and II in terms of the Total Degradation (TD) as a function of the OBO. The NLA and linearised amplifier are considered. It is noted that the System I performance is almost the same as for the OFDM case of Figure 3.13. This is due to all the chips of the OFDM symbol being distorted by the NLA in the same way since the same code is used in all the sub-channels of a user. System I is therefore not a viable option.

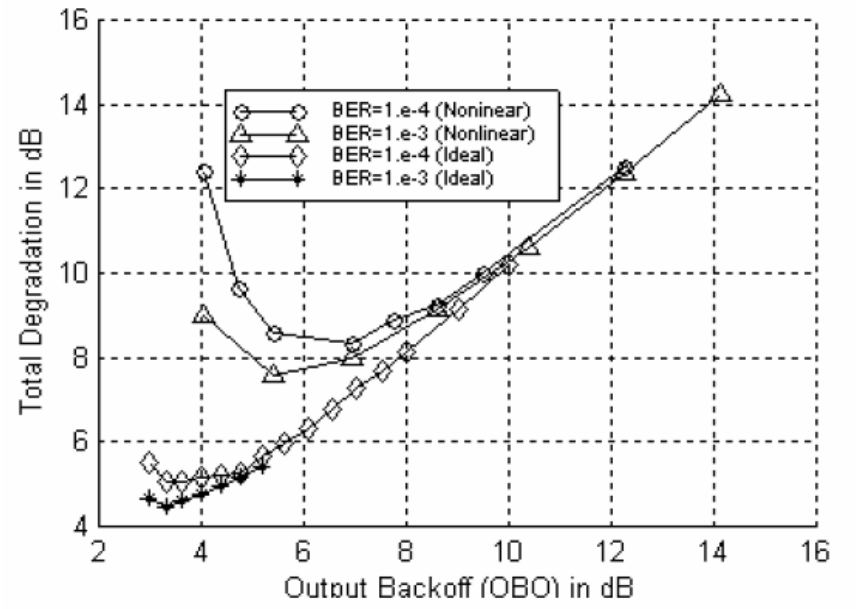

Figure 3.13 OFDM with NLA (reprinted from [41])

In contrast, System II performs better than System I by about 1 dB (single user) because the different codes words used for each sub-channel of a user results in a signal with varying amplitudes within the duration of 1 symbol. Each chip of the OFDM symbols is affected differently by the NLA. Since the receiver uses all the chips of a symbol to determine the symbol, diversity gain is obtained leading to an improved performance.

Figure 3.15 plots the system performance for 10 users. It was found that System II performed better than System I by 0.8 to 1.0 dB when a non-linear amplifier was used. The results of an ideally linearised amplifier system are shown in Figure 3.16. An improvement (relative to the NLA without linearization) of about 3 dB is observed at an OBO level of 5 dB [41].

In summary, MC-CDMA offers better performance over OFDM when different code words are used for each sub-channel of each user.

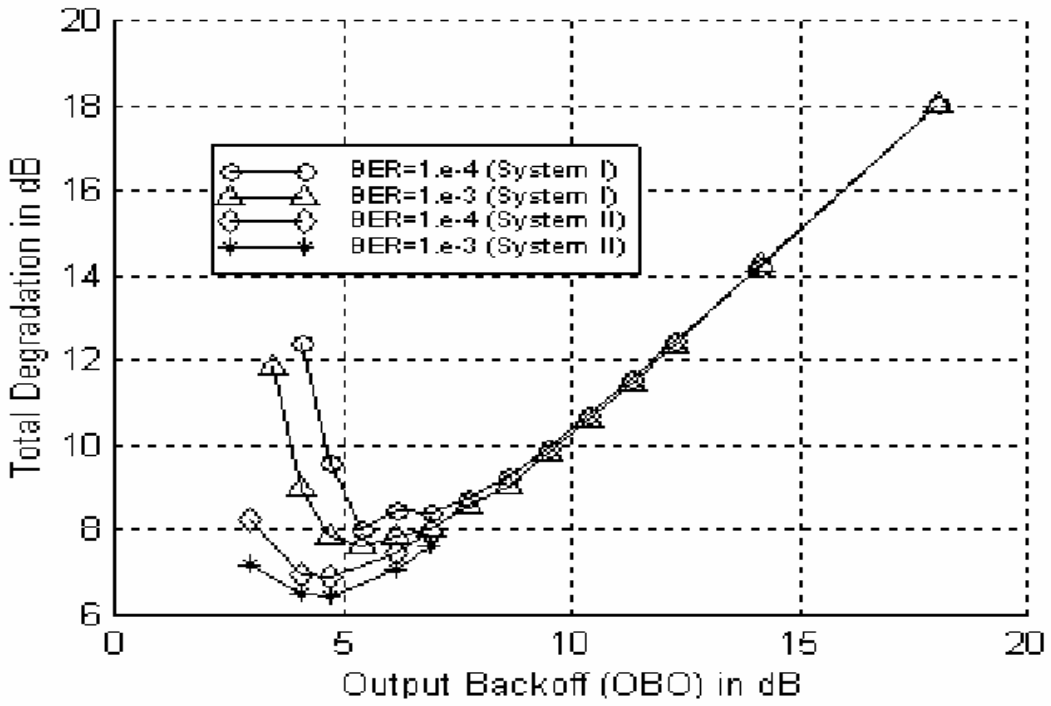

Figure 3.14 OFDM-CDMA NLA – Single User (reprinted from [41])

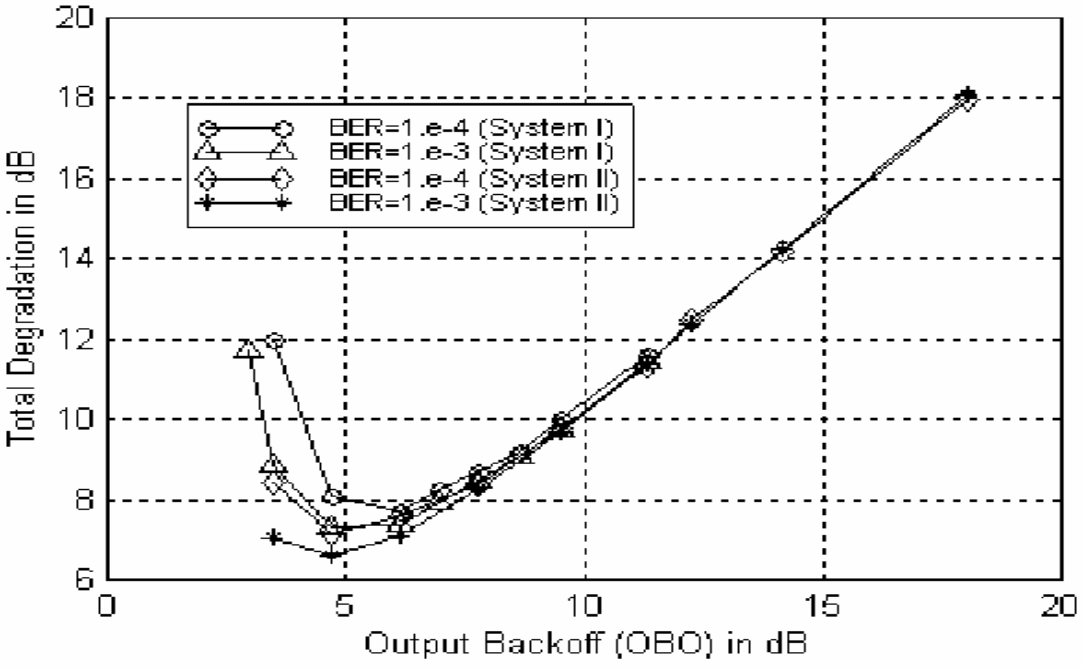

Figure 3.15 OFDM-CDMA NLA – 10 Users (reprinted from [41])

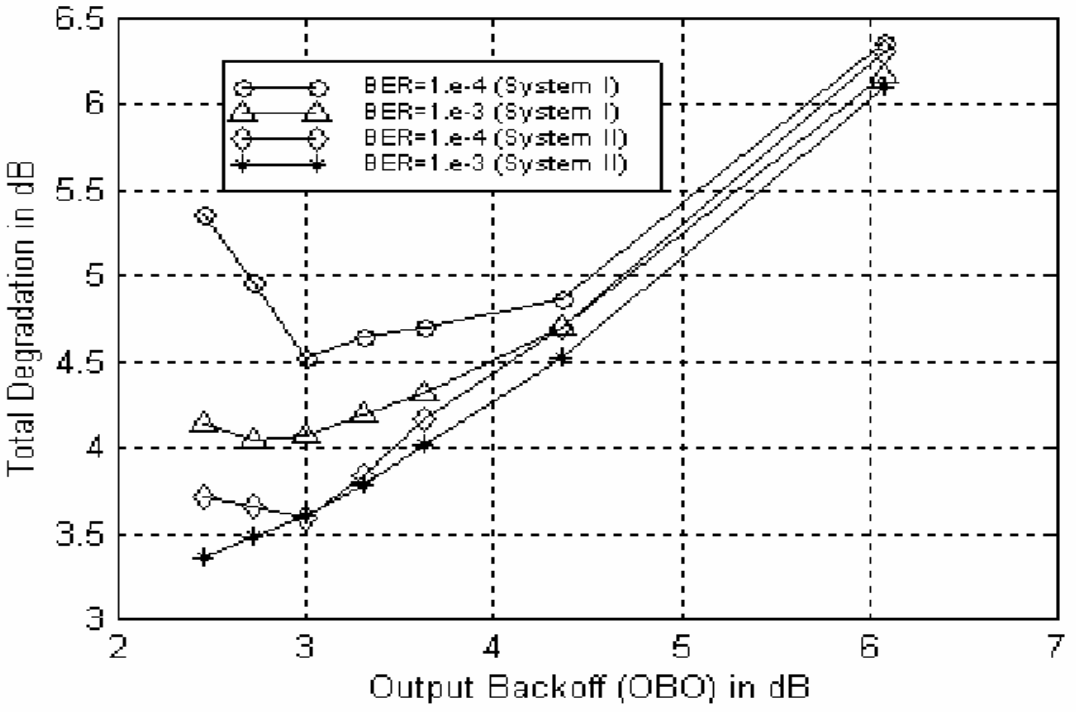

Figure 3.16 OFDM-CDMA Linearised Amplifier – 10 Users (reprinted from [41])

3.3 CDMA Downlink

The purpose of this section is to consider the effect of an NLA on the BER performance of a downlink communication system. An analytical model is reviewed and verified against simulation results.

3.3.1 System Model

Consider the equivalent block diagram of a CDMA system for the general case of asynchronous users, as depicted in Figure 3.17.

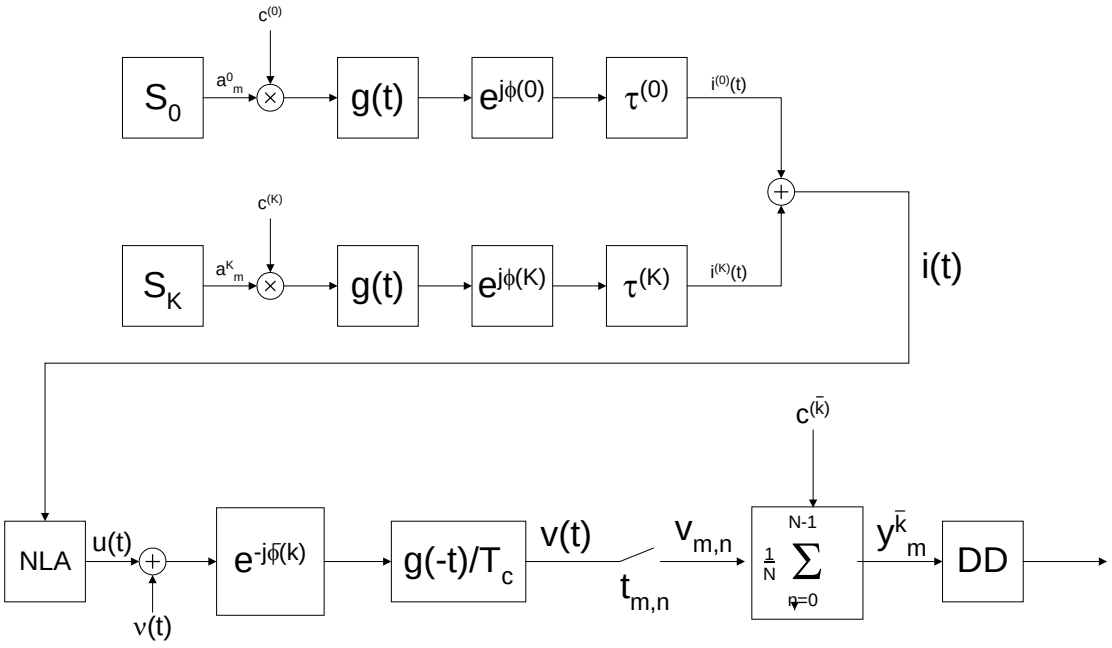

Figure 3.17 Equivalent Block Diagram of CDMA System

The k^{th} user[6] produces symbols $a_m^{(k)}$ that are multiplied by the spreading code c^k with spreading factor N. The resulting data is pulse shaped by the chip waveform g(t) and may be subjected to a phase change $e^{j\phi^{(k)}}$ and delay $\tau^{(k)}$. The signals $i^{(k)}(t)$ of K users are summed and applied to the input of a non-linear amplifier (NLA). The NLA output signal u(t) propagates through the channel. The Additive White Gaussian Noise (AWGN) ν(t) that is added to the signal represents the combined effect of the channel noise as well as the noise contributions of the transmitter and receiver. At the receiver, the signal undergoes phase

[6] $k \geq 1$.

recovery $e^{-j\phi^{(\bar{k})}}$ and coherent demodulation by the matched filter $\frac{1}{T_c}g(-t)$ before being sampled and de-spread. The resulting signal $y_m^{(\bar{k})}$ is presented to the decision device for bit recovery [1]

3.3.2 Analytical Evaluation of CDMA System Performance

According to Conti [1], the BER of the CDMA downlink of Figure 3.17 is given by

$$P_b = \frac{1}{2}\operatorname{erfc}\sqrt{\frac{1}{\frac{N_0}{E_0}(1+\eta)+\frac{\theta PK}{N}+P\mu\frac{K-1}{N}}} \quad 3.6$$

.

$\frac{E_0}{N_0}$ is the signal-to-noise ratio which may be expressed as

$$\frac{E_0}{N_0} = \frac{P_0 T}{KN_0 \log_2 M} \quad 3.7$$

.

P_0 is the signal power at the output of the amplifier, T is the symbol time. η and θ are the signal-to-non-linear-distortion-noise ratios before and after the receive filter $\frac{1}{T_c}g(-t)$, respectively. These ratios are expressed as,

$$\eta = \frac{P_d}{|K_0|^2 P_i} \quad 3.8$$

and

$$\theta = \frac{N\sigma_D^2}{2|K_0|^2 P_i} \quad 3.9$$

.

The non-linear distortion power P_d is calculated from

$$P_d = P_0 - |K_0|^2 P_i \quad 3.10$$

.

The non-linear distortion variance is given by

$$\sigma_D^2 = \frac{2P_d}{N} \quad 3.11$$

.

P_i, the signal power at the input of the amplifier, is given by

$$P_i = \frac{\sigma_0^2}{2}, \qquad 3.12$$

where σ_0^2 is the variance of the input signal. The output power P_0 is determined from

$$P_0 = \frac{1}{2}\int_0^\infty \frac{2\rho}{\sigma_0^2} e^{-\frac{\rho^2}{\sigma_0^2}} |S(\rho)|^2 d\rho \qquad 3.13$$

.

P = 1 for BPSK and P = 2 for QPSK systems, respectively. N is the spreading factor and μ is defined according to Table 3.3 [1]. Finally, the factor describing the non-linear amplifier S(ρ) is

$$K_0 = \frac{1}{2}\int_0^\infty \frac{2\rho}{\sigma_0^2} e^{-\frac{\rho^2}{\sigma_0^2}} [S'(\rho) + \frac{S(\rho)}{\rho}] d\rho \qquad 3.14$$

The above equations are valid if the input signal variance is constant. This occurs under the following conditions that are applicable to a large number of CDMA applications.

a) CDMA systems with a rectangular waveform

b) Synchronous CDMA systems with orthogonal codes

c) Asynchronous CDMA systems.

Synchronism	**Chip Waveform**	**M**
Asynchronous	Rectangular	$\mu = \frac{2}{3}$
Chip-Synchronous or Synchronous	Rectangular	$\mu = 1$
Asynchronous	Root Raised Cosine	$\mu = 1 - \frac{\beta}{4}$
Chip-Synchronous or Synchronous	Root Raised Cosine	$\mu = 1$

Table 3.3 Chip Factor

The preceding paragraphs presented formulae required to calculate the BER of CDMA

systems that use non-linear amplifiers. Using the method below, analytical results were generated to evaluate the dependence of the BER and Total Degradation on the level of additive white Gaussian noise and amplifier operating point.

Method to Calculate BER of CDMA System

a) Conduct measurements of the AM/AM and AM/PM characteristics.

b) Calculate the output power.

c) Calculate the output back-off.

d) Calculate the complex scale factor.

e) Calculate the non-linear distortion power.

f) Calculate the variance of the non-linear distortion noise.

g) Calculate the signal-to-non-linear distortion noise ratios before and after the amplifier.

h) Calculate the bit error rate.

The complex scale factor K_o cannot be evaluated analytically for all transfer functions. A solution for the SSPA as presented by [4] is

$$K_0 = \sqrt{\pi}\beta e^{\beta}\operatorname{erfc}(\beta) + \beta - \sqrt{\beta}e^{\beta}\left\{\sqrt{\pi} - \Gamma\left[\frac{1}{2}, 0, \beta\right]\right\}\left(\beta + \frac{1}{2}\right), \quad 3.15$$

where

$$\Gamma[z, a, b] = \int_a^b x^{z-1}e^{-x}dx \quad 3.16$$

is the generalized Gamma function and

$$\beta = \frac{A_0^2}{2P_i}. \quad 3.17$$

Alternatively, a computer program like Mathcad, by Mathsoft Inc. may be used to calculate K_o using numerical techniques.

Since the magnitude and phase representation of the TWTA transfer function does not produce a tractable solution to the K_o integral, the real and imaginary representation

$$S(\rho) = F_A(\rho)\cos(F_P(\rho)) + jF_A(\rho)\sin(F_P(\rho)), \qquad 3.18$$

may be used. K_o is evaluated and plotted as a function of the output back-off in Figure 3.18.

Rather than solving the formidable integral K_o, it may be more convenient to fit a curve to the data points and use the resulting describing equation to evaluate K_o.

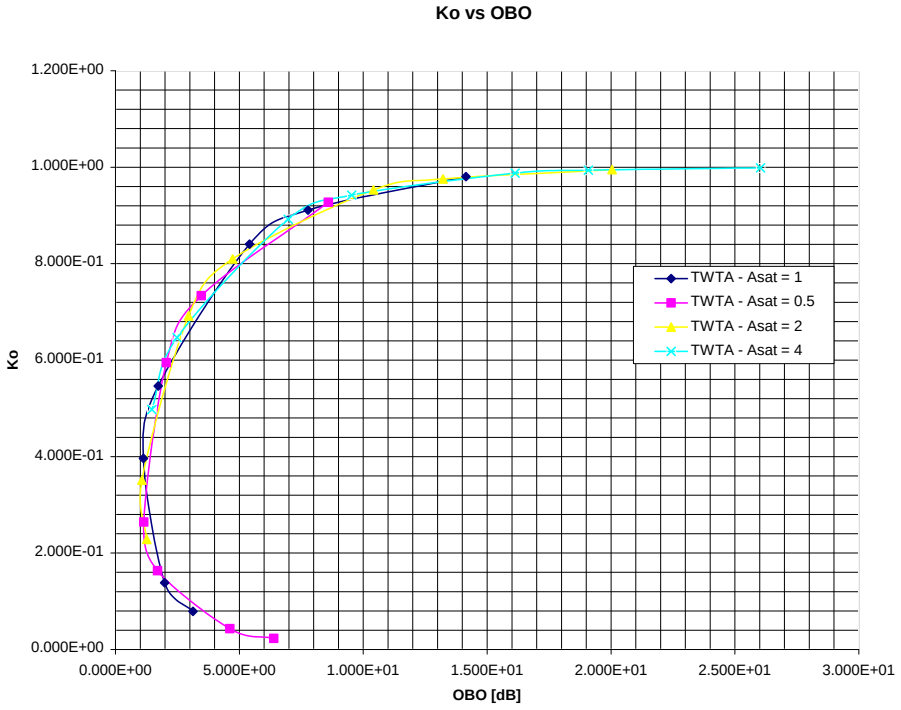

Figure 3.18 Complex Scale Factor vs OBO - TWTA

Using the techniques of Elliptical Curve Fitting [24], it is possible to fit a curve that passes through the four points chosen, as illustrated in Figure 3.19. Refer to Appendix A for the details of the calculation that leads to the elliptic curve fit to the data given by,

$$9636K_0^2 + 49x^2 - 6085K_0 - 650x - 301xK_0 + 1705 = 0, \qquad 3.19$$

where x is the OBO in dB.

Example

Calculate the scale factor K_o that corresponds to an OBO of 8.595 dB.

Substituting x = 8.595 into 3.19 and simplifying yields

$$9636K_0^{\,2} - 8672.095K_0 - 261.923 = 0 \quad . \qquad 3.20$$

Solving for K_o using,

$$K_0 = \frac{-b \pm \sqrt{b^2 - 4ac}}{2a} \quad , \qquad 3.21$$

with a = 9636, b = -8672.095 and c = -261.923 yields K_o = 0.929 or -0.029.

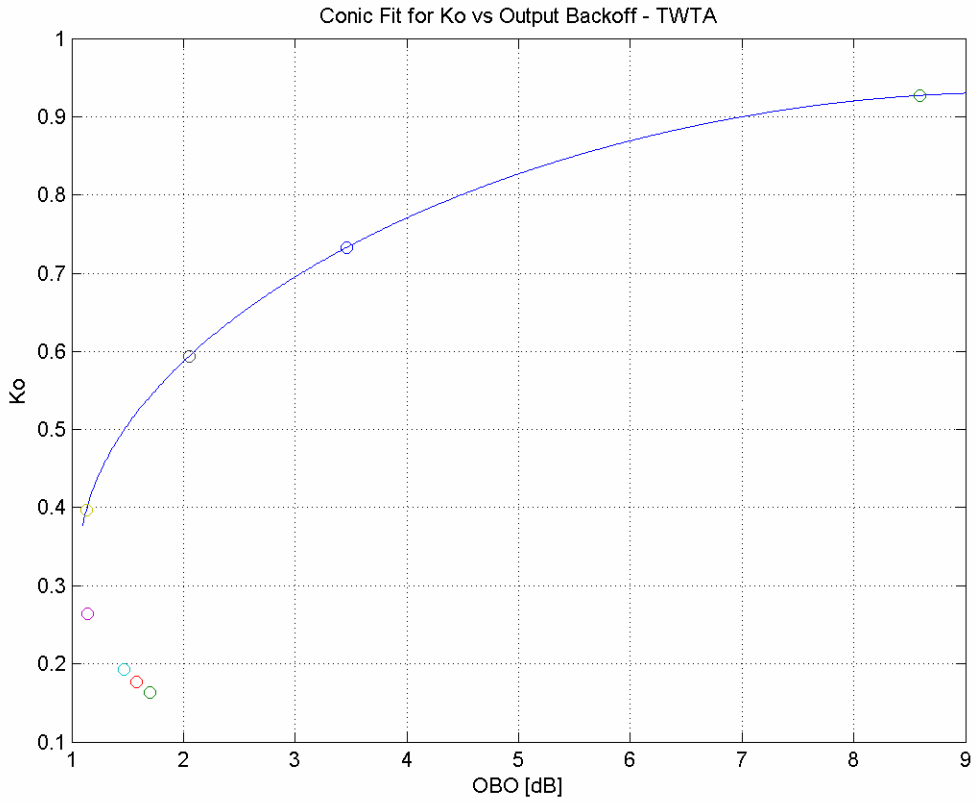

Figure 3.19 Conic Fit – Complex Scale Factor vs OBO – TWTA

Since K_o represents a magnitude, the negative result is discarded. Comparing this result with K_o = 0.9273 obtained from equation 3.14 for an OBO of 8.595, indicates that the error produced by the Elliptic Fit formula is only 0.18%.

The BER are easily calculated from 3.6 using the preceding results and plotted in Figure 3.20 and Figure 3.21 for a power-limited system. The relationship between the BER ($P_{b)}$ and SNR for BPSK and QPSK modulated CDMA systems are shown as well as the effect of different numbers of users, K. To obtain Figure 3.20 and Figure 3.21, W_{max}, and K were selected. OBO

was then varied by changing the amplifier saturation voltage. The BER P_b was then plotted as a function of E_b/N_o.

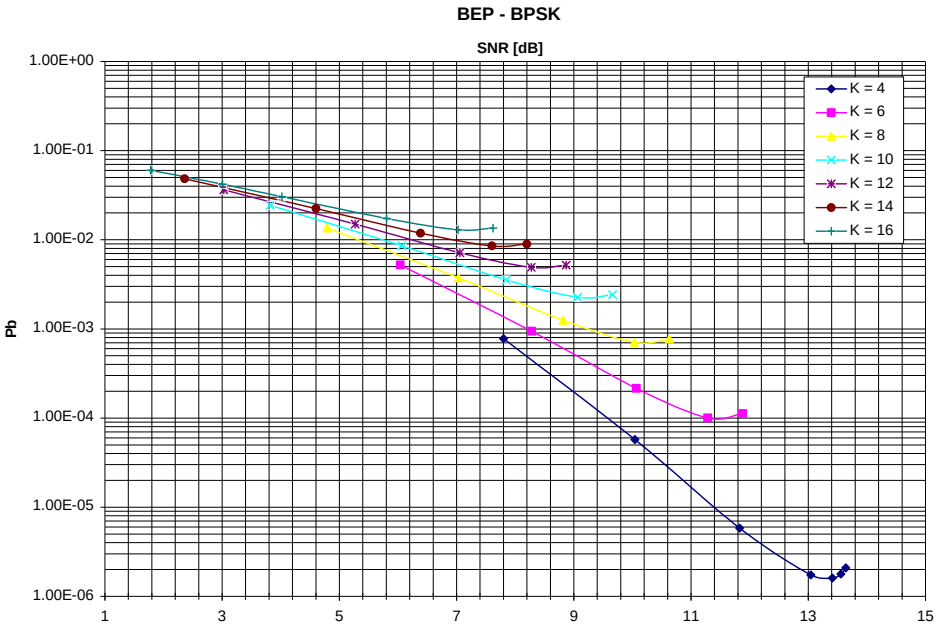

Figure 3.20 BER vs SNR - BPSK

It is evident from Figure 3.20 and Figure 3.21 that, for any given SNR, the BER increases for increasing K. For each K, there is also a turning-point that identifies an optimum SNR that yields the minimum BER. These minima may be explained by considering the power-limiting constraint,

$$W_{max} = K(OBO)\frac{E_b}{N_0}. \qquad 3.22$$

For a fixed W_{max} and K, decreasing the OBO leads to an increasing signal-to-noise ratio, $E_b/N_{o,}$ until a point is reached where the amplifier starts to saturate. Any further attempt to increase the output power leads to severe BER degradation.

The turning-points in Figure 3.22 are the minimum BER values, Pb_Min that correspond to the lowest BER. These values are plotted against the number of users, K for the BPSK and QPSK modulation formats. The dependence of the optimum operating point on the number of users is evident. Note the correspondence of the results that were obtained using Mathcad with those obtained by Conti [1], for the QPSK modulation scheme.

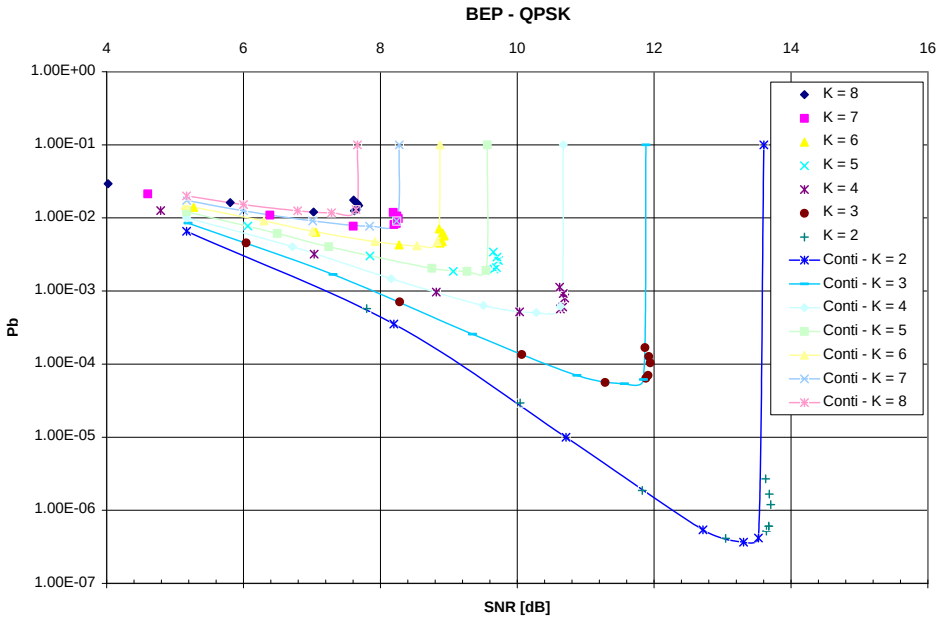

Figure 3.21 BER vs SNR – QPSK

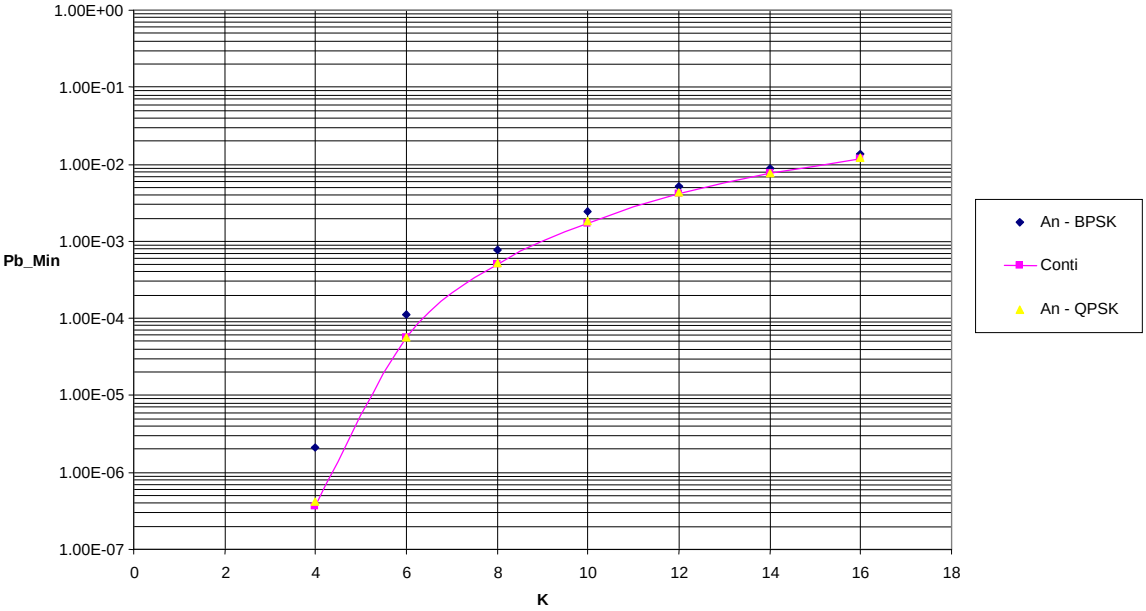

Figure 3.22 BER vs Number of Users, K – Wmax = 120

3.3.3 Simulator

The Matlab code for the downlink CDMA system is shown in Program Listings C1 and C2 (refer to Appendix B). The extract from "test.m" sets the test parameters before calling the model in "model.m." The BER is determined for various test conditions and saved to a file. The results are plotted in the next section.

3.3.4 Simulation Results

Figure 3.23 presents the simulation results of the CDMA downlink for 1 user. The simulation and analytical results are compared for BPSK modulation and the excellent agreement between them proves that the validity of the analytic model[b].

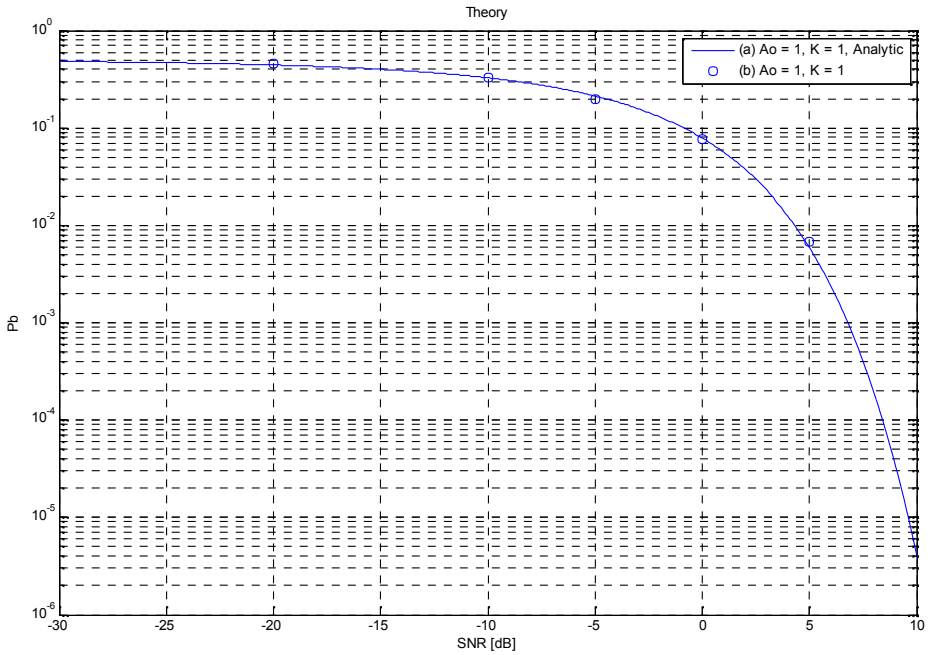

Figure 3.23 Downlink CDMA BER Performance – 1 User

Simulation results for the CDMA downlink for 20 users are presented in Figure 3.24 for an SSPA with $A_o = 1$. The parameters used are tabulated in Table 3.4. The results show good agreement between the theory and simulation.

Parameter	**K = 20**
A_o	1
σ_o^2	20
K_o	1.91×10^{-1}
P_o	4.35×10^{-1}
μ	$\frac{2}{3}$
η	1.93×10^{-1}
θ	1.29×10^{-1}

Table 3.4 Parameters – Downlink

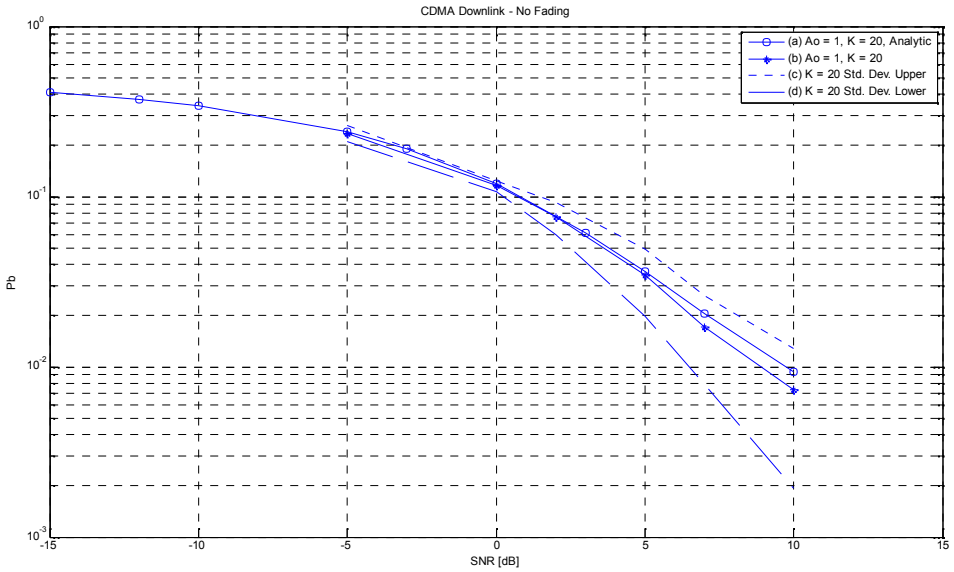

Figure 3.24 Downlink CDMA BER Performance – 20 Users

3.4 CDMA Uplink

The purpose of this section is to consider the effect of a NLA on the BER performance of an uplink communication system. The system is investigated by simulation only.

3.4.1 System Model

Each terrestrial user independently transmits information via an uplink. The BER for a particular user as received at the remote site is studied.

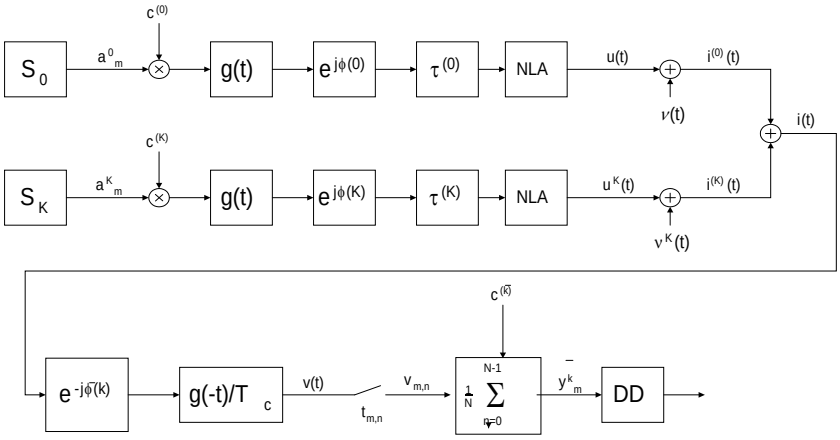

Figure 3.25 Equivalent Block Diagram of CDMA System

3.4.2 Simulator

The Matlab code for the uplink CDMA system is shown in Program Listings C3 and C4 (refer to Appendix B). The extract from "test.m" sets the test parameters before calling the model in "model_uplink.m." The BER is determined for various test conditions and saved to a file. The results are plotted in the next section.

3.4.3 Simulation Results

Figure 3.26 presents the simulation results for the CDMA uplink for the cases of 1, 10

and 20 users. An SSPA was used with $A_o = 1$.

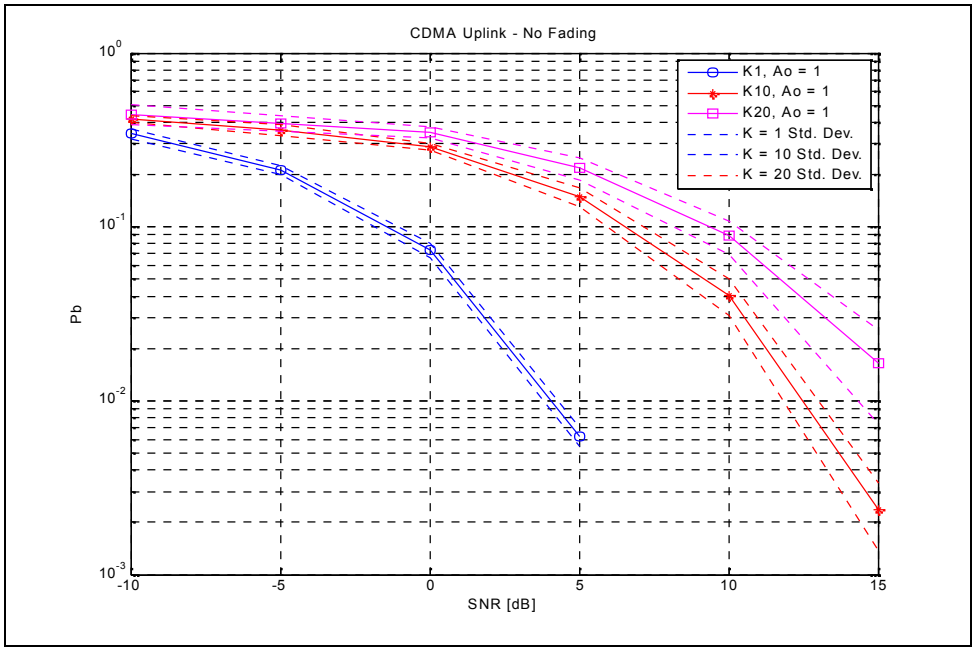

Figure 3.26 Uplink CDMA System (Ao = 1) without Fading – SSPA

The plot clearly shows the degradation of BER performance as the number of users increases. The standard deviation for each data set is also plotted to give an indication of the degree of uncertainty associated with the simulation. The uncertainty may be improved by increasing the number of bits transmitted during the simulation. The simulation run time will increase in proportion.

Figures 3.27, 3.28 and 3.29 demonstrate the independence of the amplifier operating point on the uplink BER performance for varying number of users in a non-fading environment. This was due to the smaller signal level of the single user presented to the amplifier as well as the smaller level of the envelope variations[7].

[7] In the downlink the signals from many channels combine to yield a signal with large envelope variations. This large signal is distorted more by the NLA than a signal of a smaller amplitude.

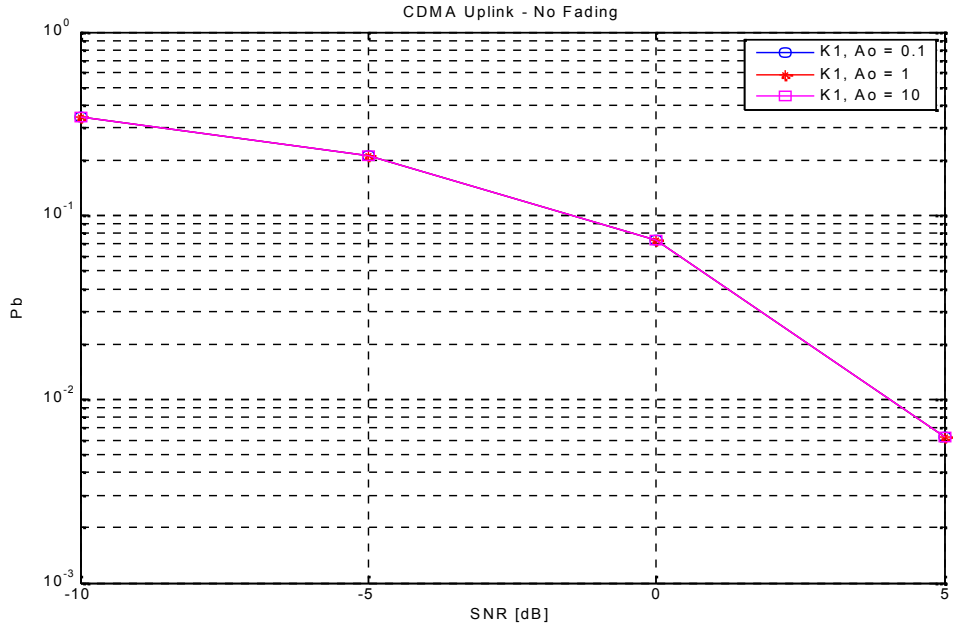

Figure 3.27 Uplink CDMA System (K = 1) without Fading – SSPA

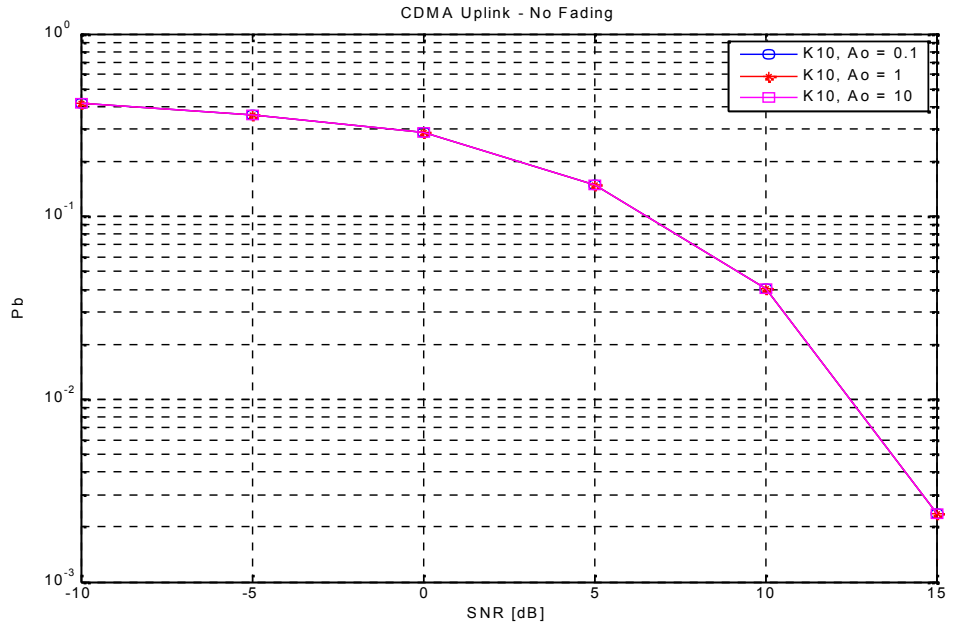

Figure 3.28 Uplink CDMA System (K = 10) without Fading – SSPA

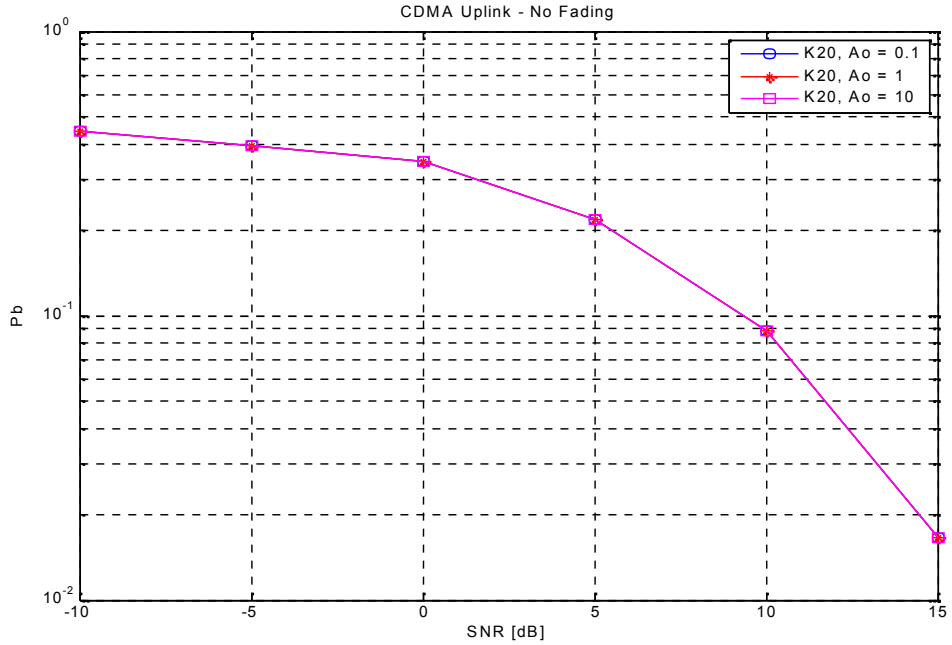

Figure 3.29 Uplink CDMA System (K = 20) without Fading – SSPA

3.5 Summary

A survey of CDMA, Multi-code CDMA and MC-CDMA was conducted. It was noted that coding techniques can be used to improve the performance of the CDMA system and that MC-CDMA systems performed better than CDMA systems in the downlink. CDMA performed better than MC-CDMA in the uplink. It was also noted that MC-CDMA offered better performance over OFDM when different code words are used for each sub-channel of each user.

Multi-code systems may be used to mitigate the effects of amplifier non-linearity. These systems use codes to reduce the amplitude of the RF signal envelope with a resulting improvement in performance. It was found that for a large number of users the system performance was not greatly affect by the amplifier OBO, due the dominance of the MAI term.

Non-linear amplifiers affect the performance of a BPSK MC-CDMA system. The TD increases as the number of users increases for a specified BER and OBO. An optimum OBO exists that produces a minimum BER. MC-CDMA performs better than OFDM in the presence of non-linearity due to the use of spreading code assignments and the observation that each chip of the OFDM (part of the MC-CDMA scheme) symbol is affected differently

by the NLA. Since the receiver uses all the chips of a symbol to determine the symbol, diversity gain is obtained leading to an improved performance.

Analytical results for the BER performance of the CDMA downlink with an NLA were generated and verified by simulation. The CDMA uplink was investigated by means of simulation for various numbers of users and NLA operating points.

The downlink and uplink performance was affected by the number of users. The BER performance became worse as the number of users increased. This was due to the signals of other users increasing the noise floor after being spread by the spreading code of the user that was being despread.

The downlink showed a dependence on the amplifier OBO. This was due to the varying envelope of the RF signal being subjected to the AM/AM characteristic of the SSPA amplifier.

The uplink performance did not show a dependence on the NLA OBO. This was due to the smaller signal level of the single user presented to the amplifier as well as the smaller level of the envelope variations.

The downlink power-limited system was investigated and the optimum OBO that produced the lowest BER was identified for a particular number of users. The optimum OBO changed as a function of the number of users.

4 CDMA with Non-linear Amplifier and Rayleigh Fading

4.1 Introduction

The effect of non-linear amplifiers is extended to apply to a downlink satellite communication system where fading effects are observed. This scenario may typically appear in cases where the receiver is located within a densely built up area.

The effect of fading on the system performance was adequately treated by Proakis [45] for the case of BPSK and no NLA. Additionally, there is no reference to an analytical method of evaluating the combined effect of both fading and NLAs in such systems. It is for this reason that the sections that follow develop, prove and verify an analytical model for evaluating the BER of a CDMA system in the presence of both non-linear amplifiers and channel fading.

The performance of the system discussed in chapter 3 will now be influenced by the nature of the fading. Two models for fading may be used to characterize this effect as applicable to the scenario under investigation i.e.

a) Rayleigh Fading

b) Rician Fading

Rayleigh fading is applicable in cases where there is no dominant signal path between the transmitter and receiver, while Rician fading is applicable when there is a dominant signal path.

The purpose of this chapter is to consider the effect of fading on the BER performance of a downlink and uplink CDMA communication system with a non-linear amplifier at the transmitter and fading effects present in the channel. The channel model will be developed for the Rayleigh fading case only. The idea may be easily extended to apply to a Rician channel as well. The system and analytical models are developed and verified against simulation results.

4.2 CDMA Downlink

4.2.1 System Model

The system model for the CDMA downlink is depicted in Figure 4.1 for a Rayleigh channel. The channel parameter r(t) is introduced after the NLA to impart a random modulation of the signal envelope.

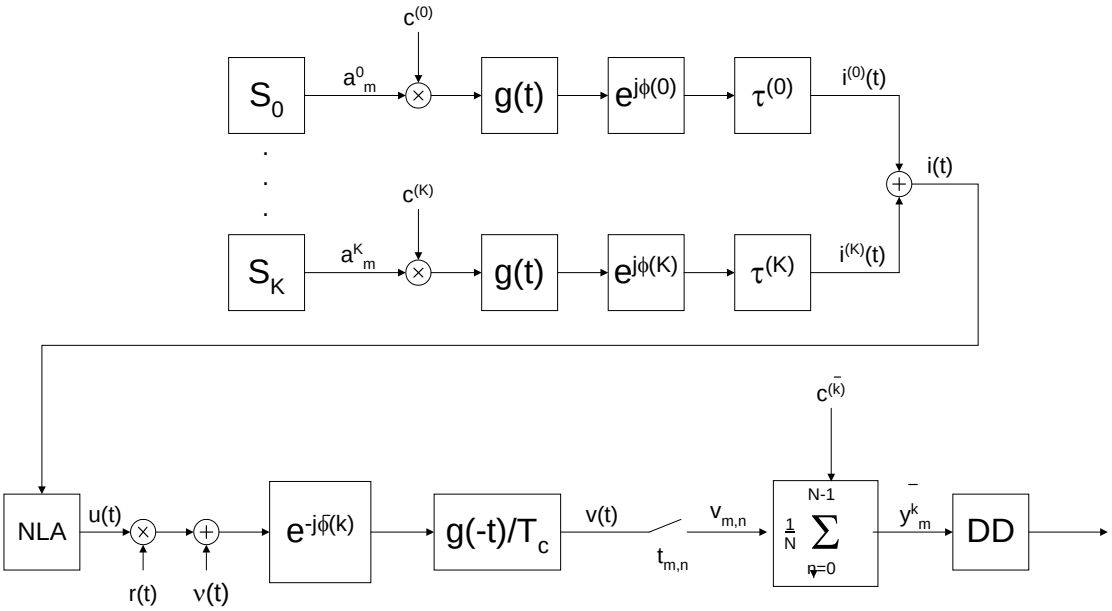

Figure 4.1 Downlink CDMA System with Fading

4.2.2 Analytical Model

The signal of the k[th] user may be written as

$$i^k(t) = V_o \sum_{l=-\infty}^{\infty} a_l^{(k)} c^k\left(t - lT - \tau^{(k)}\right) e^{j\phi(k)} \quad , \tag{4.1}$$

where the spreading waveform is

$$c^{(k)}(t) = \sum_{j=0}^{N-1} c_j^{(k)} g\left(t - jT_c\right), \tag{4.2}$$

Substituting 4.2 into 4.1 yields

$$i^k(t) = V_o \sum_{l=-\infty}^{\infty} \sum_{j=0}^{N-1} a_l^{(k)} c_j^{(k)} e^{j\phi(k)} g\left(t - jT_c - lT - \tau^{(k)}\right), \tag{4.3}$$

where

$$T = NT_c . \tag{4.4}$$

The signal at the input of the NLA may be written as

$$i(t) = V_o \sum_{k=0}^{K-1} \sum_{l=-\infty}^{\infty} \sum_{j=0}^{N-1} a_l^{(k)} c_j^{(k)} e^{j\phi(k)} g\left(t - jT_c - lT - \tau^{(k)}\right). \tag{4.5}$$

Now substitute $t_{m,n}^{(\bar{k})} = nT_c + mT + \tau^{(\bar{k})}$ into 4.2 to yield[8]

$$c_n^{(\bar{k})} = c^{(\bar{k})}(t_{m,n}^{(\bar{k})}) = \sum_{j=0}^{N-1} c_j^{(k)} g\left((n-j)T_c + mT + \tau^{(\bar{k})}\right), \tag{4.6}$$

i(t) now becomes

$$i(t_{m,n}^{(\bar{k})}) = V_o \sum_{k=0}^{K-1} \sum_{l=-\infty}^{\infty} \sum_{j=0}^{N-1} a_l^{(k)} c_j^{(k)} e^{j\phi(k)} g\left((n-j)T_c + (m-l)T + \tau^{(\bar{k})} - \tau^{(k)}\right). \tag{4.7}$$

Now, since the output of the NLA is

$$u(t) = K_o(t) i(t) + d(t) \tag{4.8}$$

and

$$K_o(t) = K_o\left(1 + \alpha(t)\right) \tag{4.9}$$

where

$$\alpha(t) = \sum_{i=-\infty}^{\infty} \alpha_i e^{j2\pi i t / T} \tag{4.10}$$

is the Fourier transform of α(t) and

$$\alpha_i(t) = \frac{1}{T} \int_{-T/2}^{T/2} \alpha(t) e^{-j2\pi i t / T} dt , \tag{4.11}$$

the amplifier output now becomes

$$u(t) = K_o i(t) + K_o \sum_{i=-\infty}^{\infty} \alpha_i i(t) e^{j2\pi i t / T} + d(t) . \tag{4.12}$$

[8] $t_{m,n}^{(\bar{k})}$ is the sample time of chip n of symbol m of user $\bar{k}$.

Defining the receiver responses to $i(t)e^{j2\pi t/T}$, $d(t)$ and $g(t)$, respectively as

$$i_{ri}(t) = i(t)e^{j2\pi t/T}, \tag{4.13}$$

$$d_r(t) = d(t) \tag{4.14}$$

and

$$g_r(t) = g(t) \tag{4.15}$$

and noting that the decision variable for the m[th] symbol of the $\bar{k}$ [th] user is

$$y_m^{(\bar{k})} = \frac{1}{N}\sum_{n=0}^{N-1} v_{m,n}^{(\bar{k})} c_n^{(\bar{k})}, \tag{4.16}$$

where

$$v_{m,n}^{(\bar{k})} = z_{m,n}^{(\bar{k})} + w_{m,n}^{(\bar{k})}. \tag{4.17}$$

allows $z_{\underline{m},n}^{(\bar{k})}(t)$ to be expressed as

$$z_{\underline{m},n}^{(\bar{k})}(t) = r(t_{\underline{m},n})u(t_{\underline{m},n}^{(\bar{k})})e^{j\phi^{(\bar{k})}} * \left(\frac{1}{T_c}\right) g(-t). \tag{4.18}$$

Manipulation and substituting leads to

$$z_{\underline{m},n}^{(\bar{k})}(t) = r(t_{\underline{m},n})u_{\underline{m},n}^{(\bar{k})}(t)e^{j\phi^{(\bar{k})}} g_r\left((n-j)T_c + (\overline{m}-l)T + \tau^{(\bar{k})} - \tau^{(k)}\right) \tag{4.19}$$

Or

$$\begin{aligned} z_{\underline{m},n}^{(\bar{k})}(t) &= K_o V_o \sum_{k=0}^{K-1}\sum_{l=-\infty}^{\infty}\sum_{j=0}^{N-1} r(t_{\underline{m},n}) a_l^{(k)} c_j^{(k)} e^{j(\phi(k)-\phi(\bar{k}))} g_r\left((n-j)T_c + (\overline{m}-l)T + \tau^{(\bar{k})} - \tau^{(k)}\right) \\ &+ K_o \sum_{i=-\infty}^{\infty} r(t_{\underline{m},n})\alpha_i i_{r,i}\left(t_{\underline{m},n}^{(\bar{k})}\right)e^{-j\phi^{(\bar{k})}} + d_r\left(t_{\underline{m},n}^{(\bar{k})}\right) \end{aligned} \tag{4.20}$$

Substituting the above into 4.16 leads to

$$\begin{aligned} y_{\underline{m}}^{(\bar{k})} &= K_o V_o \frac{1}{N}\sum_{k=0}^{K-1}\sum_{l=-\infty}^{\infty}\sum_{n=0}^{N-1} r(t_{\underline{m},n}) a_l^{(k)} c_n^{(k)} c_n^{(\bar{k})*} e^{j(\phi(k)-\phi(\bar{k}))} g_r\left((n-j)T_c + (\overline{m}-l)T + \tau^{(\bar{k})} - \tau^{(k)}\right) \\ &+ K_o \frac{1}{N}\sum_{i=-\infty}^{\infty}\sum_{n=0}^{N-1} r(t_{\underline{m},n})\alpha_i i_{r,i}\left(t_{\underline{m},n}^{(\bar{k})}\right)c_n^{(\bar{k})*} e^{-j\phi^{(\bar{k})}} + \frac{1}{N}\sum_{n=0}^{N-1} r(t_{\underline{m},n}) d_r\left(t_{\underline{m},n}^{(\bar{k})}\right)c_n^{(\bar{k})*} + \frac{1}{N}\sum_{n=0}^{N-1} w_{m,n}^{(\bar{k})} c_n^{(\bar{k})*}. \end{aligned} \tag{4.21}$$

If the input power is kept constant and the m[th] symbol of the $\bar{k}$ th user is separated then

$$y_{\underline{m}}^{(\bar{k})} = K_o r(t_{\underline{m,n}})\left(V_o a_m^{\bar{k}} \frac{1}{N}\sum_{n=0}^{N-1} c_n^{(k)} c_n^{(\bar{k})*} + MAI_o \right) + \frac{1}{N}\sum_{n=0}^{N-1} r(t_{\underline{m,n}}) d_r\left(t_{\underline{m,n}}^{(\bar{k})}\right) c_n^{(\bar{k})*} + \frac{1}{N}\sum_{n=0}^{N-1} w_{m,n}^{(\bar{k})} c_n^{(\bar{k})*} \quad 4.22$$

Now defining the generic modulation symbol as

$$A = a_m^{\bar{k}}, \quad 4.23$$

and substituting the distortion term with

$$D_{\underline{m}}^{(\bar{k})} = \frac{1}{N}\sum_{n=0}^{N-1} d_r\left(t_{\underline{m,n}}^{(\bar{k})}\right) c_n^{(\bar{k})*}, \quad 4.24$$

and the noise term with

$$W_{\underline{m}}^{(\bar{k})} = \frac{1}{N}\sum_{n=0}^{N-1} w_{m,n}^{(\bar{k})} c_n^{(\bar{k})*} \quad 4.25$$

results in

$$y_{\underline{m}}^{(\bar{k})} = K_o r(t_{\underline{m,n}})\left(AV_o + MAI_o\right) + r(t_{\underline{m,n}}) D_{\underline{m}}^{(\bar{k})} + W_{\underline{m}}^{(\bar{k})}. \quad 4.26$$

For a given value of $r(t_{\underline{m,n}})$ = r, the conditional bit error rate for the system may be written as

$$P_b\big|_r = \frac{1}{2} erfc \sqrt{\frac{\left|K_0\right|^2 r^2 V_0^2}{\sigma_w^2 + r^2\sigma_D^2 + r^2\left|K_0\right|^2 \sigma_{MAI_0}^2}}. \quad 4.27$$

For practical purposes it is usually more convenient to refer to signal-to-noise rather than signal variance; hence the conditional probability will be expressed in terms of E_b/N_o.

Since

$$\frac{E_b}{N_o} = \frac{2P_o}{\sigma_w^2 K}, \quad 4.28$$

implies that the noise variance is

$$\sigma_w^2 = \frac{N_o}{E_b}\frac{2P_o}{K}, \quad 4.29$$

and the multiple access interference from users other than user k is

$$\sigma_{MAI}^2 = \frac{2P_i(K-1)\mu}{KN} \quad . \qquad 4.30$$

respectively. N_0 is the one-sided power spectral density, N is the spreading factor and P_d is the non-linear distortion power given by

$$P_d = P_0 - |K_0|^2 P_i \quad . \qquad 4.31$$

P_i is the signal power at the input of the amplifier given by

$$P_i = \frac{\sigma_0^2}{2} \quad . \qquad 4.32$$

μ is a factor that depends on the characteristics of the chip waveform and on the form of synchronism as described in Table 3.3.

Now substituting 4.29, 4.30 and $P_o = V_0^2/2$ into 4.7 yields,

$$P_b|_r = \frac{1}{2} erfc \sqrt{\frac{|K_0|^2 r^2 2P_o}{\frac{N_o}{E_b}\frac{2P_o}{K} + r^2\sigma_D^2 + r^2|K_0|^2 \frac{2P_i(K-1)\mu}{KN}}} \quad . \qquad 4.33$$

Substitution P_o from,

$$P_d = P_0 - |K_0|^2 P_i \qquad 4.34$$

leads to,

$$P_b|_r = \frac{1}{2} erfc \sqrt{\frac{|K_0|^2 r^2 2P_o}{\frac{N_o}{E_b}\frac{2}{K}\left(|K_0|^2 P_i + P_d\right) + r^2\frac{2P_d}{N} + r^2|K_0|^2 \frac{2P_i(K-1)\mu}{KN}}} \quad . \qquad 4.35$$

Re-arranging the above equation leads to,

$$P_b|_r = \frac{1}{2} erfc \sqrt{\frac{1}{\frac{N_o}{E_b}\frac{2|K_0|^2 P_i}{K|K_0|^2 r^2 2P_o}\left(1+\frac{P_d}{|K_0|^2 P_i}\right) + \frac{r^2\sigma_D^2}{|K_0|^2 r^2 2P_o} + \frac{r^2|K_0|^2}{|K_0|^2 r^2 2P_o}\frac{2P_i(K-1)\mu}{KN}}} \quad . \qquad 4.36$$

Simplifying gives

$$P_b\big|_r = \frac{1}{2} erfc \sqrt{\frac{1}{\frac{N_o}{r^2 E_b}\frac{P_i}{KP_o}\left(1+\frac{P_d}{|K_0|^2 P_i}\right)+\frac{\sigma_D^2}{2|K_0|^2 P_o}+\frac{1}{P_o}\frac{P_i(K-1)\mu}{KN}}} \quad 4.37$$

Substituting

$$\eta = \frac{P_d}{|K_o|^2 P_i} \quad 4.38$$

and

$$\theta = \frac{N\sigma_D^2}{2|K_o|^2 P_i}, \quad 4.39$$

as previously defined in chapter 3 results in

$$P_b\big|_r = \frac{1}{2} erfc \sqrt{\frac{1}{\frac{N_o}{r^2 E_b}\frac{P_i}{KP_o}(1+\eta)+\theta\frac{P_i}{NP_o}+\frac{1}{P_o}\frac{P_i(K-1)\mu}{KN}}} \quad 4.40$$

Next, define

$$P = \frac{P_i}{KP_o}. \quad 4.41$$

Hence the conditional probability may be written as

$$P_b\big|_r = \frac{1}{2} erfc \sqrt{\frac{1}{\frac{N_o}{r^2 E_b}P(1+\eta)+\theta\frac{PK}{N}+P\mu\frac{P_i(K-1)}{N}}} \quad 4.42$$

Note that the above probability is a conditional probability which means that the equation gives the BER for a particular value of r. In order to derive the equation for the unconditional error probability the conditional probability has to be averaged over the Rayleigh probability density function $f_R(r)$ [45], [47] i.e.,

$$P_b = \int_0^\infty P_b\big|_r f_R(r) dr \quad 4.43$$

where $f_R(r)$ is the probability density function for Rayleigh fading given by

$$f_R(r) = \frac{r}{\alpha^2} e^{-r^2/2\alpha^2}, \quad 4.44$$

and, α is a constant that describes the shape of the distribution [15]. Applying the relevant substitutions yields

$$P_b = \int_0^{\infty} \left(\frac{1}{2} erfc \sqrt{\frac{1}{\frac{N_0}{r^2 E_b} P(1+\eta) + \frac{\theta PK}{N} + P\mu \frac{(K-1)}{N}}} \right) \frac{r}{\alpha^2} e^{-r^2/2\alpha^2} dr \qquad 4.45$$

.

This equation can be conveniently solved by a computer program like Mathcad, using similar methods to those presented in chapter 3. The analytical results from 4.45 are tabulated below for selected values of $N_o./E_{b,}$, number of users and NLA operating point. These results are compared with the simulation results in the next section.

Parameter	**K = 20**	**K = 20**	**K = 10**	**K = 10**
A_o	1	100	1	100
σ_o^2	2	2	1	1
K_o	1.91×10^{-1}	9.98×10^{-1}	2.62×10^{-1}	9.99×10^{-1}
P_o	4.35×10^{-1}	9.96	4.00×10^{-1}	4.99
μ	$\frac{2}{3}$	$\frac{2}{3}$	$\frac{2}{3}$	$\frac{2}{3}$
η	1.93×10^{-1}	1.97×10^{-6}	1.61×10^{-1}	4.97×10^{-7}
θ	1.29×10^{-1}	1.32×10^{-6}	1.08×10^{-1}	3.31×10^{-7}

Table 4.1 Parameters – Downlink with Fading

4.2.3 Simulator

The Matlab code for the downlink CDMA system with Rayleigh fading is shown in

Program Listing C5 (refer to Appendix B). The extract from "test.m" sets the test parameters before calling the model in "model.m" (refer to Program Listing C2).

The model uses a vector of Rayleigh parameters that are computed from a pair of Gaussian Random Variables (GRV) X_1 and X_2 of equal variance $\sigma_1^2 = \sigma_2^2$ and mean $\mu_1 = \mu_2 = 0$ according to the equation

$$r_i = \sqrt{X_{1i}^2 + X_{2i}^2}, \qquad 4.46$$

where r_i is the i[th] Rayleigh distributed sample generated from the Gaussian distributed samples X_{1i} and X_{2i} [46].

In order not to change the power of the signal, the mean of the Rayleigh disturbance was set to 1. This was done by first noting [46] that since the GRV

$$\mu_1 = \sigma_1 \sqrt{\frac{\pi}{2}}, \qquad 4.47$$

then

$$\sigma_1^2 = \frac{\pi}{2}. \qquad 4.48$$

Similarly

$$\sigma_2^2 = \frac{\pi}{2}. \qquad 4.49$$

The variance of the Rayleigh variables now becomes

$$\sigma_r^2 = \left(\frac{4-\pi}{2}\right)\frac{2}{\pi}. \qquad 4.50$$

Once the model parameters were determined the simulator was run. The BER was determined for various test conditions and saved to a file. The results are plotted in the next section.

4.2.4 Simulation Results

A simulator was developed to verify the analytical model. Preliminary tests were first conducted using a 1 user BPSK signal in a Rayleigh fading channel.

The test results are plotted as points (a) in Figure 4.2 together with analytical results [45] (curve (b)). The simulation results are consistent with the theory[a] i.e.

$$P_b = \frac{1}{2}\left(1 - \sqrt{\frac{\bar{\gamma}_b}{1+\bar{\gamma}_b}}\right), \qquad 4.51$$

where the signal-to-noise ratio $\bar{\gamma}_b$ is

$$\bar{\gamma}_b = \frac{E_b}{N_0} E\left(\alpha^2\right) \quad 4.52$$

.

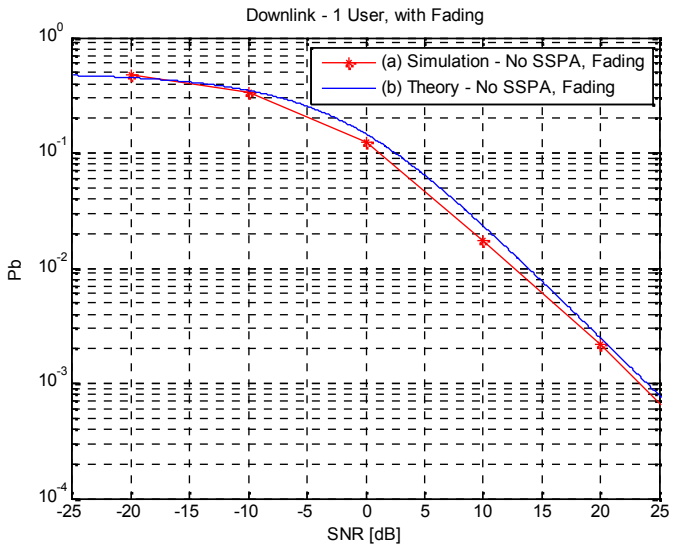

Figure 4.2 Simulator Test - Downlink CDMA System with Fading

The simulator was configured to generate results for 20 users in a CDMA system with an NLA in the downlink and Rayleigh fading present in the channel. The results are plotted in Figures 4.3 to 4.6. The results show a close match between the simulation and analytical model of equation 4.45[b].

Figure 4.3 plots the BER for K = 20 and K = 10 users respectively under 2 different operating conditions ($A_o = 1$ and $A_o = 100$). The $A_o = 1$ case was chosen so as to observe the effect of the non-linearity on the BER (the amplifier was operating in the non-linear region). The $A_o = 100$ case was chosen so as to observe the effect of an amplifier operating in the linear region.

The plot illustrates how the BER performance in a Rayleigh fading environment degrades as the number of users increase. It is also evident that the amplifier non-linearity also leads to BER degradation.

Figure 4.4 plots the analytical and simulated BER for K = 20 users in a Rayleigh fading environment. The plot shows the close match between the simulation and analytical model of equation 4.45[b].

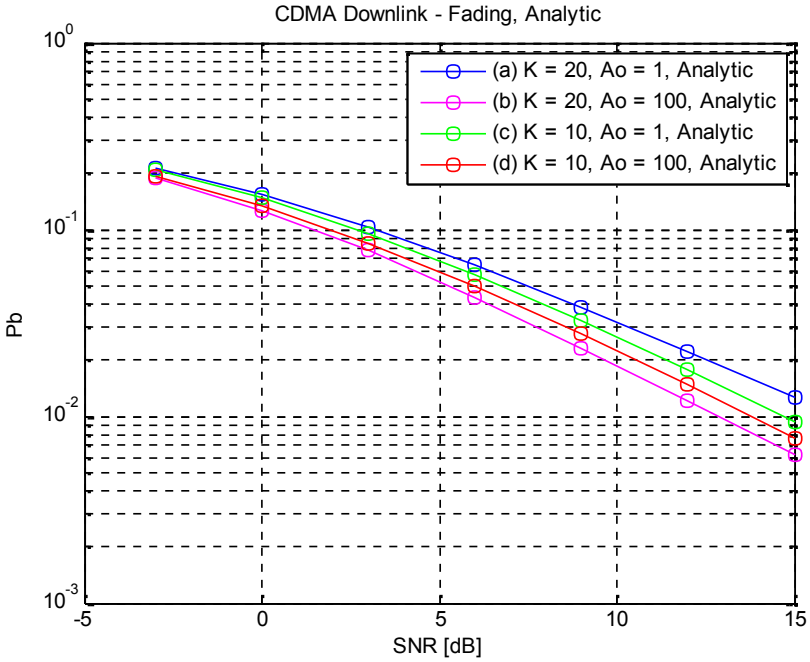

Figure 4.3 Downlink CDMA System with Fading – Analytic

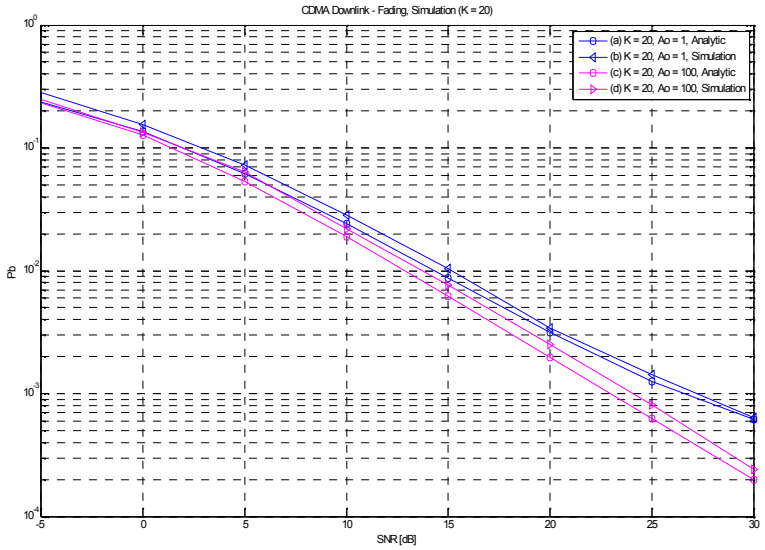

Figure 4.4 Downlink CDMA System with Fading – 20 Users

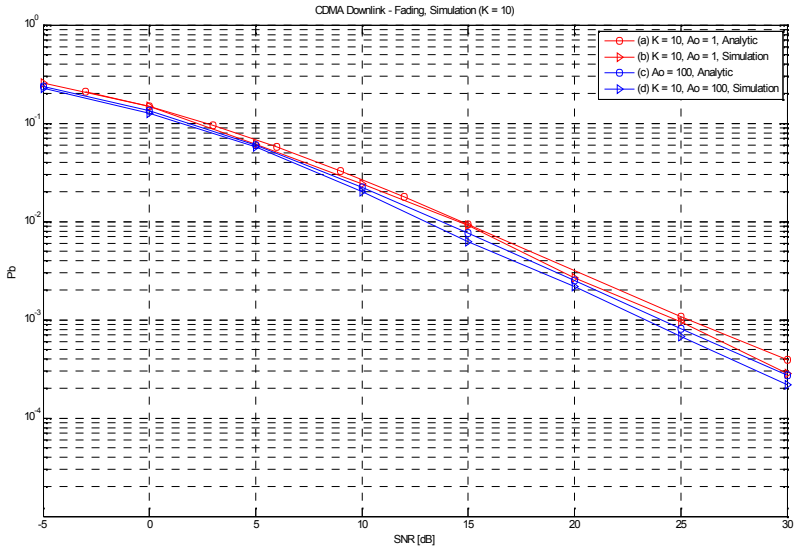

Figure 4.5 Downlink CDMA System with Fading – 10 Users

Figure 4.5 plots the analytical and simulated BER for K = 10 users in a Rayleigh fading environment. The plot shows the close match between the simulation and analytical model of equation 4.45[b].

Figure 4.6 analytically compares the effect of fading on the system performance to the non-fading case for K = 10 and P = 1. The degradation in the BER floor is clearly evident for large values of signal-to-noise ratio.

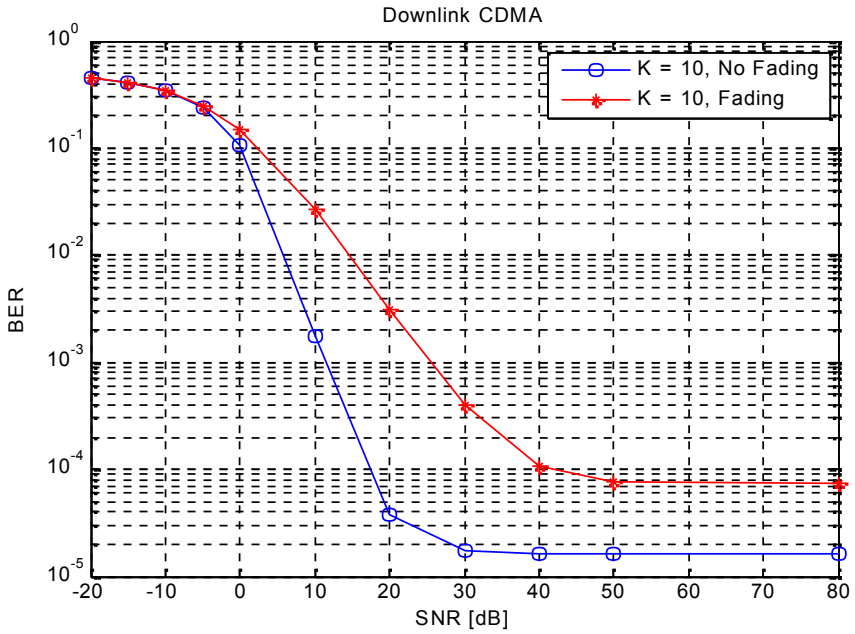

Figure 4.6 Downlink CDMA BER Performance – 10 Users

Figure 4.7 compares the effect of fading on the performance of a power limited CDMA system with $W_{max} = 120$. The signal-to-noise ratio E_b/N_o was computed from

$$W_{max} = K(OBO)\frac{E_b}{N_0}, \qquad 4.53$$

as discussed in chapter 3, for various levels of amplifier output back-off. (In contrast, no limitation was placed on W_{max} for the power-unlimited case considered in Figure 4.6). The results suggest that fading significantly affects the performance of power-limited systems.

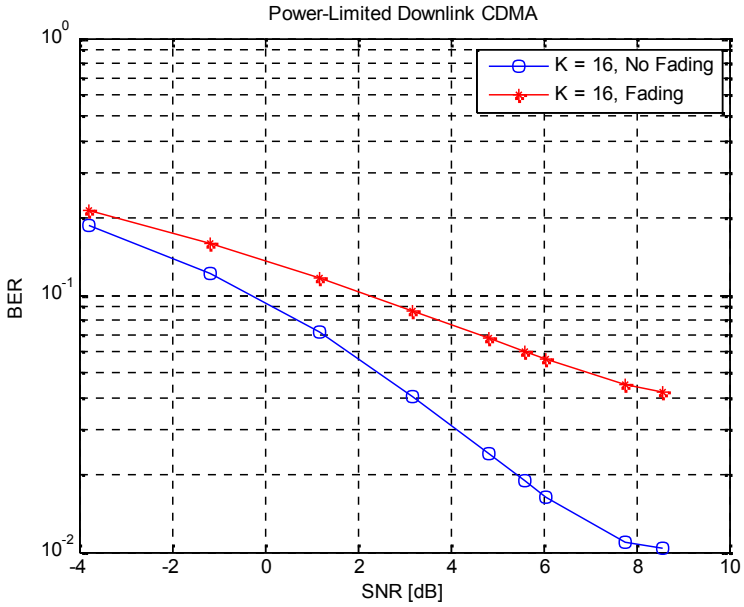

Figure 4.7 Power Limited BER Performance – 16 Users

4.3 CDMA Uplink

The purpose of this section is to consider the effect of fading on the BER performance of an uplink communication system with non-linear amplifiers at the transmitter and fading effects present in the channels. The system will be simulated for the Rayleigh fading channel only.

4.3.1 System Model

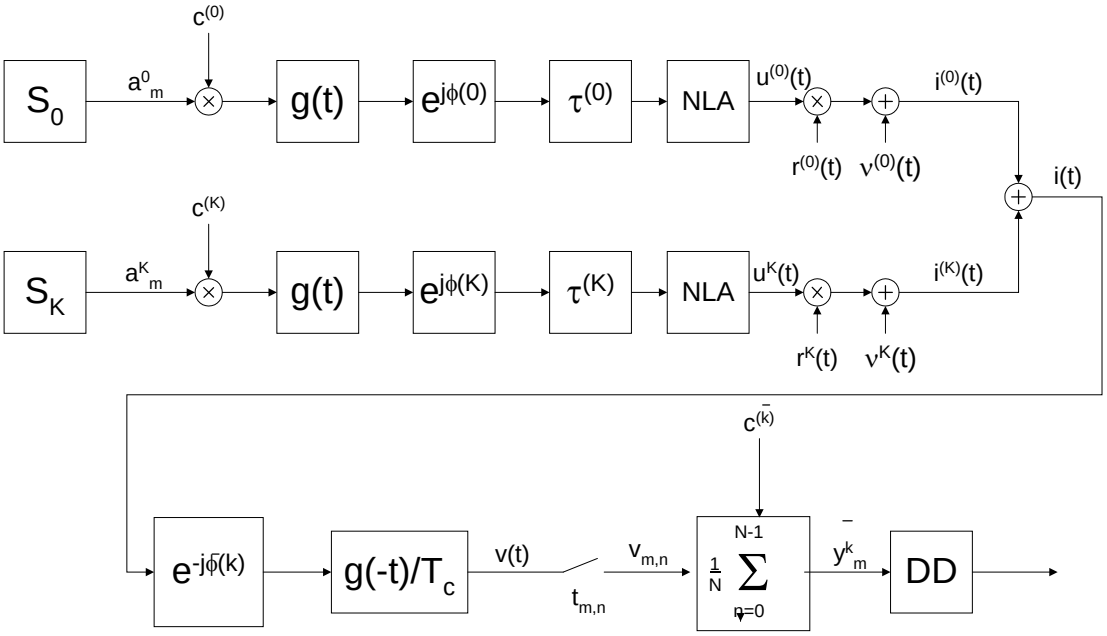

Figure 4.8 Equivalent Block Diagram of an Uplink CDMA System

Figure 4.8 illustrates a typical CDMA uplink system with K users. The bit stream of each user is spread by c(t) and pulsed shaped by g(t) before being amplified by an NLA. Each user experiences a random phase change φ^k and delay τ^k. The resulting distorted signal experiences fading according to a set of parameters $\alpha(t)$. The parameters belong to a set of Rayleigh distributed random variables. Since slow fading is being considered each Rayleigh sample will be held constant over the bit duration T.

The receiver is presented with the sum of the signals of each user as well as noise. Demodulation and phase recovery are performed. The signal is then sampled and integrated over the symbol period to yield a decision variable y_m. The decision device decodes a logic "1" if $y_m \geq 1$ and "0" if $y_m \leq 1$.

4.3.2 Simulator

The Matlab code for the uplink CDMA system with Rayleigh fading is shown in Program Listing C5. The extract from "test.m" sets the test parameters before calling the model in "model_uplink.m" (refer to Program Listing C4). The BER is determined for various test conditions and saved to a file. The results are plotted in the next section.

4.3.3 Simulation Results

A simulator was designed and implemented to measure the BER of the uplink CDMA system incorporating NLAs at the transmitters and a slow Rayleigh fading channel. The Solid Sate Amplifier (SSPA) model was used as described in chapter 2 with $A_o = 1$.

Figure 4.9 compares the simulation and analytical results for the case of a single user in the uplink with a Rayleigh fading channel. It is evident that there is good agreement between the analytical results of plot (b) and the simulation results of plot (a).

Figure 4.10 presents the simulation results for the cases of 1, 10 and 20 users in the uplink CDMA system with Rayleigh fading channels. An SSPA was used with $A_o = 1$. The broken lines (f to i), represent the standard deviation of the data sets. The plot clearly shows the degradation in BER performance as the number of users was increased from 1 to 20.

Figures 4.11, 4.12 and 4.13 demonstrate the independence of the amplifier output back-off on the uplink BER performance for varying number of users in a fading environment.

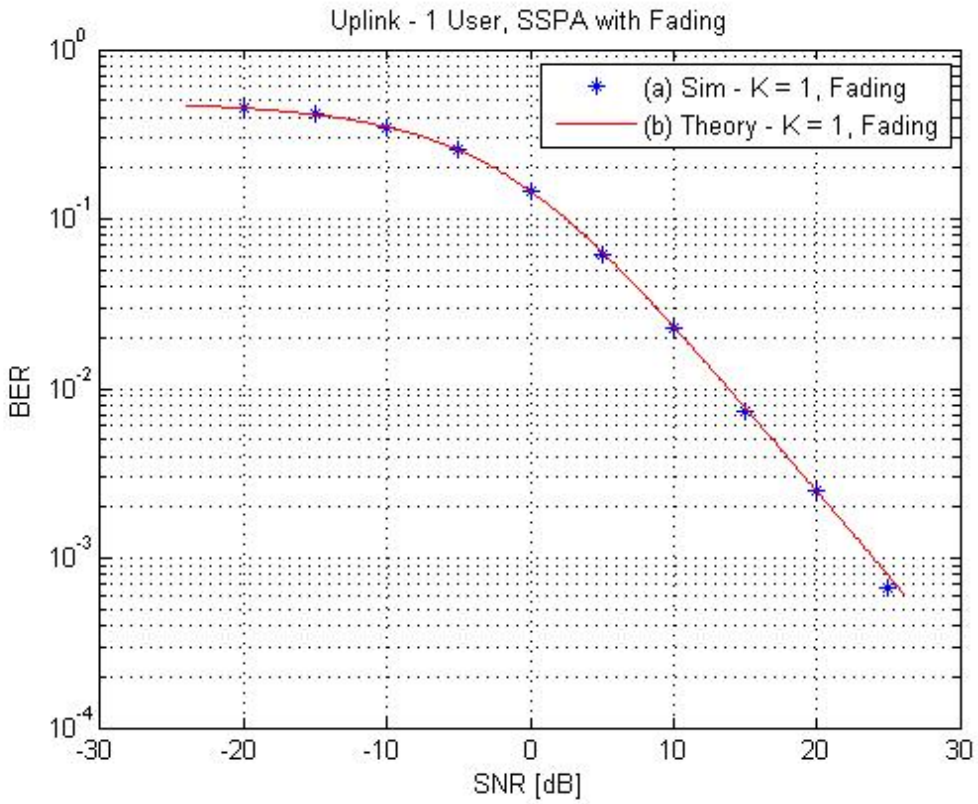

Figure 4.9 Uplink CDMA System with Fading – 1 User, SSPA

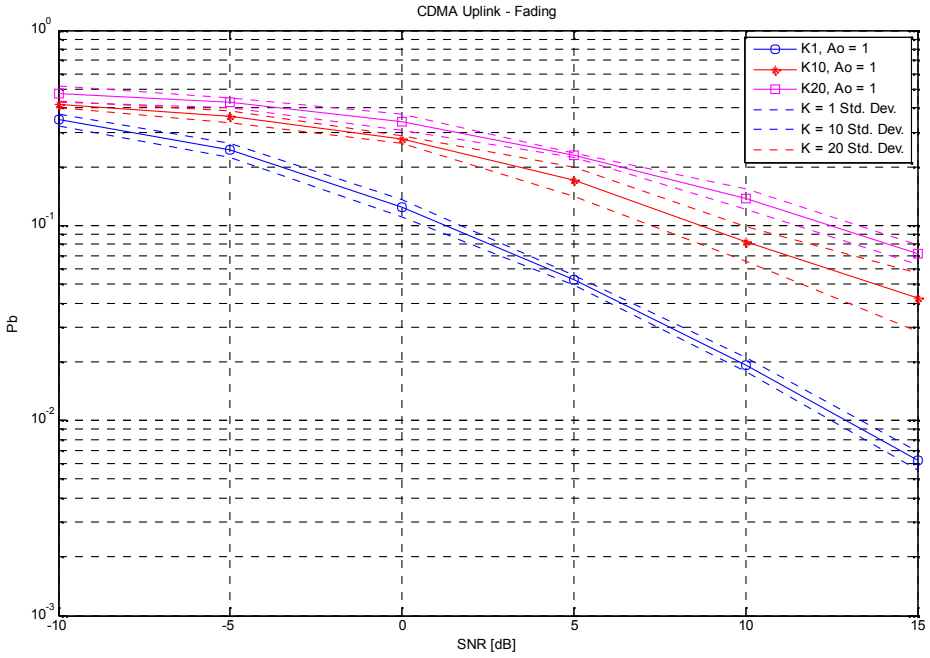

Figure 4.10 Uplink CDMA System (A_o = 1) with Fading – SSPA

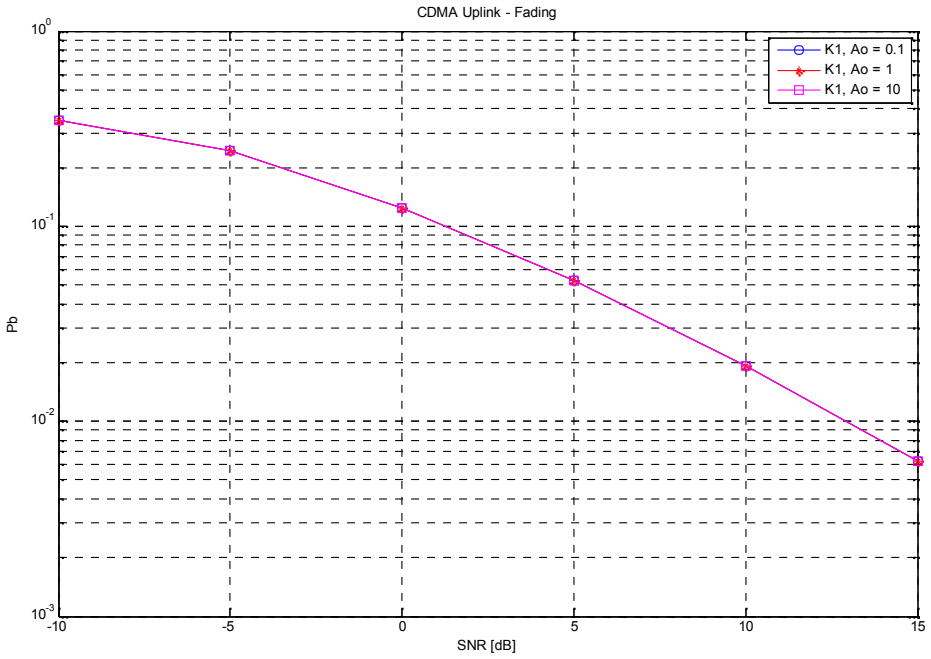

Figure 4.11 **Uplink CDMA System (K = 1) with Fading – SSPA**

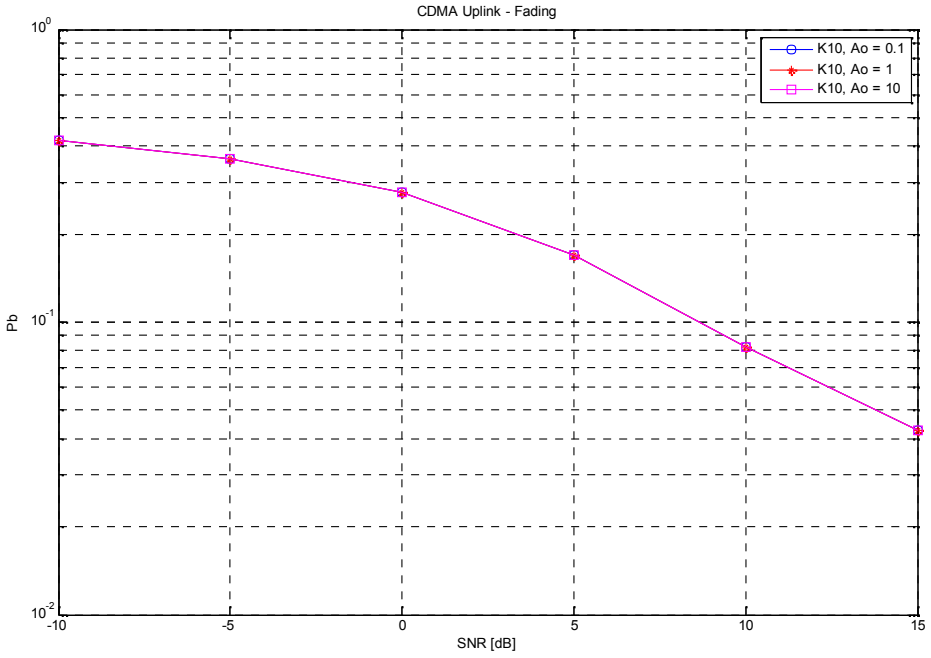

Figure 4.12 **Uplink CDMA System (K = 10) with Fading – SSPA**

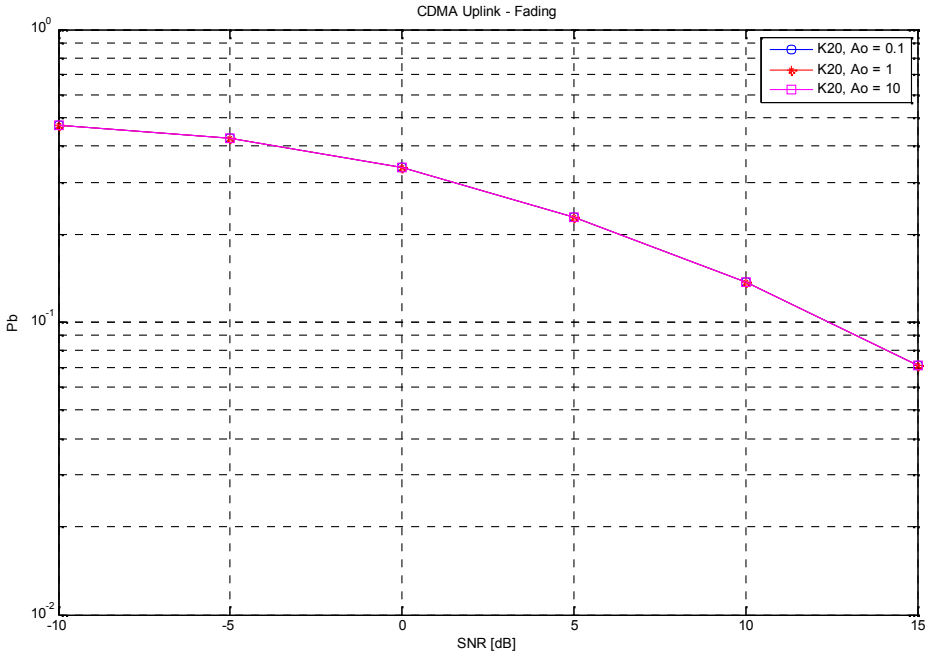

Figure 4.13 Uplink CDMA System (K = 20) with Fading – SSPA

4.4 Summary

An analytical model for the CDMA downlink system with NLA and Rayleigh fading was developed and proved. Simulation results were produced to verify the validity of the model. The downlink performance was affected by the number of users and the amplifier output back-off.

Simulation results for the CDMA uplink system with NLAs and Rayleigh fading were presented. The uplink performance in a fading environment was affected by the number of users and did not show a dependence on the NLA output back-off.

The downlink power-limited and unlimited systems with Rayleigh fading was investigated and compared to the corresponding non-fading cases. The non-fading scenarios performed better than the fading cases. A larger BER floor was observed when a Rayleigh fading channel was used.

5 Conclusion

The effect of amplifier non-linearity on the performance of a CDMA system with non-linear amplifiers was studied. A systematic methodology was introduced to calculate the BER for the downlink. Simulation results were presented and successfully compared with theoretical predictions. It was also found that coding techniques and linearization methods may be employed to improve the performance of CDMA systems with non-linear amplifiers in a non-fading environment.

Amplifier models can be used to assess the performance of communication systems. Models may be classified as either having a memory effect or being memoryless. Memoryless models are an approximate representation of the real device over a narrow bandwidth where the frequency dependency is not significant. In cases where the frequency bandwidth is significant, the models with memory should be used.

The dissertation shows how RF performance parameters like power spectral density, output power, intermodulation distortion, adjacent channel power rejection, noise power ratio, carrier-to-noise ratio, peak-to-average ratio, multi-tone intermodulation ratio, error vector magnitude, efficiency and output-backoff may be used to compare the performance of systems and components within a system.

The Feedforward, Feedback, Pre-distortion, LINC and Envelope Elimination and Restoration techniques may be used to linearise amplifiers. Practical results were presented on the method of pre-distortion linearisation and it was shown that this method leads to a reduction in the IMD products and an improvement in the power amplifier efficiency.

Non-linear amplifiers affect the performance of a BPSK MC-CDMA system. The TD increases as the number of users increases for a specified BER and OBO. An optimum OBO exists that produces a minimum BER. MC-CDMA performs better than OFDM in the presence of non-linearity due to the diversity gain introduced by the code word assignments.

MC-CDMA systems performed better than CDMA systems in the downlink. CDMA performed better than MC-CDMA in the uplink. It was also noted that MC-CDMA offers better performance over OFDM when different code words are used for each sub-channel of each user.

Multi-code systems may be used to mitigate the effects of amplifier non-linearity by using codes to reduce the amplitude of the RF signal envelope. It was found that for a large number of users the system performance was not greatly affected by the amplifier OBO, due the dominance of the MAI term. Pre-distortion used with these systems degrades the system performance when the number of users is small and improves the performance for a large number of users.

Analytical results for the BER performance of the CDMA downlink with an NLA and no fading were generated and verified by simulation. The CDMA uplink was investigated by means of simulation for various numbers of users and NLA OBO levels.

An analytical model describing the BER performance of a downlink communication system with a non-linear amplifier at the satellite and a Rayleigh fading channel was developed, proved and successfully verified against simulation results.

Simulation results on the effect of non-linear amplifiers on the uplink CDMA system in non-fading and Rayleigh fading channels were presented. It was shown that, for a unity gain Rayleigh fading vector, the SSPA output back-off had no influence on the system performance. The downlink and uplink BER performance became worse as the number of users increased. The downlink showed a dependence on the amplifier output back-off while the uplink did not show such dependence. The downlink power-limited and unlimited systems with Rayleigh fading were investigated and compared to the corresponding non-fading cases. The non-fading scenarios performed better than the fading cases. A larger BER floor was observed when a Rayleigh fading channel was used.

Future Research

a) Development of an analytical model for the CDMA downlink with a non-linear amplifier and Rician fading.

b) Inclusion of coding effects in the analytical models.

c) Simulation results for the CDMA uplink with a non-linear amplifier in a Rician fading environment.

d) Development of analytical models for the CDMA uplink with fading.

6 Bibliography

[1] Andrea Conti, Davide Dardari and Velio Tralli, “An Analytical Framework for CDMA Systems with a Nonlinear Amplifier and AWGN,” IEEE Transactions on Communications, Vol. 50, No. 7, July 2002.

[2] Seng-Woon Chen, William Panton and Robert Gilmore, “Effects of Nonlinear Distortion on CDMA Communication Systems,” IEEE Transactions of Microwave Theory and Techniques, Vol. 44, No. 12, December 1996.

[3] Davide Dardari, Velio Tralli and Alessandro Vaccari, “A Theoretical Characterization of Nonlinear Effects in OFDM Systems,” IEEE Transactions on Communications, Vol.48, No.10, October 2000.

[4] Davide Dardari and Velio Tralli, “Analytical Evaluation of Total Degradation in OFDM Systems with TWTA or SSPA,” IEICE Transactions on Communications, Vol. E85-B, No. 4, April 2002.

[5] Aldo N. D’Andrea, Vincenzo Lottici and Ruggero Reggiannini, “Nonlinear Predistortion of OFDM Signals over Frequency-Selective Fading Channels,” IEEE Transactions on Communications, Vol.49, No.5, May 2001.

[6] Elena Costa, Michele Midrio and Silvano Pupolin, “Impact of Amplifier Nonlinearities on OFDM Transmission System Performance,” IEEE Transactions on Communications, Vol.3, No.2, February 1999.

[7] Elena Costa and Silvano Pupolin, “M-QAM-OFDM System Performance in the Presence of a Nonlinear Amplifier and Phase Noise,” IEEE Transactions on Communications, Vol.50, No. 3, March 2002.

[8] Ahmad R.S. Bahai, Manoneet Singh, Andrea J. Goldsmith and Burton R. Saltzberg, “A New Approach for Evaluating Clipping Distortion in Muliticarrier Systems,” IEEE Journal on Selected Areas in Communications, Vol. 20, No. 5, May 2002.

[9] A. Springer, T. Frauscher, B. Adler, D. Pimingsdorfer and R. Weigel, “Impact of Nonlinear Amplifiers on the UMTS System,” IEEE 6th International Symposium on

Spread Spectrum Techniques and Applications, NJIT, New Jersey, USA, Sept. 6-8, 2000.

[10] N. Y. Ermolova, "Spectral Analysis of Nonlinear Amplifier Based in the Complex Gain Taylor Series Expansion," IEEE Communications Letters, Vol. 5, No.12, December 2001.

[11] Je-hong Jong and Wayne E. Stark, "Performance Analysis of Coded Multicarrier Spread-Spectrum Systems in the Presence of Multipath Fading and Nonlinearities," IEEE Transactions on Communications, Vol. 49, No. 1, January 2001.

[12] Georges Karam and Hikmet Sari, "Analysis of Predistortion, Equalization and ISI Cancellation Techniques in Digital Radio Systems with Nonlinear Transmit Amplifiers," IEEE Transactions on Communications, Vol. 37, No. 12, December 1989.

[13] Adel A.M. Saleh, "Frequency-Independent and Frequency-Dependent Nonlinear Models of TWT Amplifiers," IEEE Transactions on Communications, Vol. Com-29, No. 11, November 1981.

[14] "Measuring Bit Error Rate Using the ESG-D Series RF Signal Generators, Option UN7," Agilent Product Note 5966-4098E, Agilent Technologies, USA, 2000.

[15] Herbert Taub and Donald L. Schilling, "Principles of Communications Systems," 2nd Edition, McGraw-Hill Inc., New York, 1991.

[16] Bernard Sklar, "Digital Communications: Fundamentals and Applications," 2nd Edition, Prentice Hall, 2001.

[17] G. Santella and F. Mazzenga, "A Hybrid Analytical-Simulation Procedure for Performance Evaluation in M-QAM-OFDM Schemes in the Presence of Nonlinear Distortions," IEEE Transactions on Vehicular Technology, Vol.47, February 1998.

[18] Simon Haykin, "Digital Communications," John Wiley & Sons Inc., New York, 1988.

[19] Leonard J. Cimini, "Analysis and Simulation of a Digital Mobile Channel Using Orthogonal Frequency Division Multiplexing," IEEE Transactions on

Communications, Vol. 33, No.7, July 1985.

[20] Peter B. Kenington, "High-linearity RF Amplifier Design," Artech House Inc., Norwood, MA, 2000.

[21] ETSI TS125 101 V4.3.0, "Universal Mobile Telecommunications System (UMTS); UE Radio T UE Radio Transmission and Reception (FDD)," ETSI 3rd Generation Partnership Project (3GPP), 2001.

[22] TS125 213 V4.2.0, "Universal Mobile Telecommunications System (UMTS); Spreading and Modulation (FDD)," ETSI 3rd Generation Partnership Project (3GPP), 2001.

[23] 3GPP2 C.S0002-D Version 2.0, "Physical Layer Standard for CDMA2000 Spread Spectrum Systems, Revision D," 3rd Generation Partnership Project 2 (3GPP2), 2005.

[24] George B. Thomas Jr. and Ross L. Finney, "Calculus and Analytical Geometry," Addison-Wesley Publishing Company, California, 1988.

[25] "Digital Modulation in Communication Systems – An Introduction," Application Note 1298, Agilent Technologies, USA.

[26] "WinIQSim 4.20 Help File," Agilent Technologies, USA.

[27] C. Langton, "Link Budgets, Intuitive Guide to Principles of Communications," Web site: "www.complextoreal.com/Chapters/linkbud.pdf," 2002.

[28] Murray R. Spiegel and John Liu, "Mathematical Handbook of Formulas", Second Edition, Mcgraw-Hill, California, 1999.

[29] K. Kashyap, T. Wada, M. Katayama, T. Yamazato and A. Ogawa, "The Performance of CDMA System using π/4-shift QPSK and π/2-shift BPSK with the nonlinearity of HPA," Department of Information Electronics, Nagoya University, Japan.

[30] L. Chang and J.V. Krogmeier, "Analysis of the Effects of Linearity and Efficiency of Amplifiers in QAM Systems," School of Electrical and Computer Engineering, Purdue University, USA.

[31] S.P. Stapleton, “Amplifier Linearization Using Adaptive Digital Predistortion,” Applied Microwave & Wireless, February 2001.

[32] S.P. Stapleton, “Amplifier Linearization Using Adaptive RF Predistortion,” Applied Microwave & Wireless.

[33] L. Giugno, M. Luise and V. Lottici, “Adaptive Pre- and Post-Compensation of Nonlinear Distortions for High-Level Data Modulations,” IEEE Transactions on Wireless Communications, Vol. 3, No. 5, September 2004.

[34] S. Benedetto and E. Biglieri, “Nonlinear Equalization of Digital Satellite Channels,” IEEE Journal on Selected Areas in Communications, Vol. 1, January 1983.

[35] S. van Fleteren, “Traveling Wave Tube vs Solid State Amplifiers,” Communications and Power Industries, 2000.

[36] I. Santamaria, J. Ibanez, M. Lazaro, C, Pantaleon and L. Vielva, “Modeling Nonlinear Power Amplifier in OFDM Systems from Subsampled Data: A Comparative Study Using Real Measurements, EURASIP Journal on Applied Signal Processing, February 2003.

[37] F.H. Gregorio and T.I. Laakso, “The Performance of OFDM-SDMA Systems with Power Amplifier Non-linearities,” Proceedings of the 2005 Finnish Signal Processing Symposium, Finland – FINSIG’05, August 2005.

[38] G. T. Zhou, “Predicting Spectral Regrowth of Nonlinear Power Amplifiers,” IEEE Transactions on Communications,” Vol. 50, No. 5, May 2002.

[39] P. Banelli and S. Cacopardi, “Theoretical Analysis and Performance of OFDM Signals in Nonlinear AWGN Channels,” IEEE Transactions on Communications, Vol. 48, No. 3, March 2000.

[40] H. Kang, “RF Reconfigurable Predistorter for Power Amplifiers,” IEICE Transactions on Electronics, Vol. E90-C, No.9, 2007.

[41] J. Li and M. Kavehrad, “OFDM-CDMA Systems with Non-linear Power Amplifier,”

Proc. IEEE WCNC, September 1999.

[42] N. Guo and L. B. Milstein, “Uplink Performance Evaluation of Multi-code DS/CDMA Systems in the Presence of Nonlinear Distortions,” IEEE Journal on Selected Areas in Communications,” Vol. 18, No. 8, August 2000.

[43] “Orthogonal Frequency Division Multiplexing” Web site: “http://en.wikipedia.org/wiki/OFDM”

[44] A.H.M. Ross, “CDMA Cellular Radio Systems Research,” Web site: “http://www.cdg.org/technology/cdma%5Ftechnology/a%5Fross/cdmarevolution.asp,” 1999.

[45] J. G. Proakis, “Digital Communications,” 2nd Edition, McGraw Hill, 1989

[46] “Rayleigh Distribution,” Web site: “http://en.wikipedia.org/wiki/Rayleigh_distribution”

[47] A. Papoulis, “Probability, Random Variables and Stochastic Processes,” McGraw Hill, 1965.

[48] P. B. Kenington, “Linearized Transmitters: An Enabling Technology for Software Defined Radio,” IEEE Communications Magazine, February 2002.

[49] K. Fazel and S. Kaiser, “Analysis of non-linear distortions on MC-CDMA,” Proc. IEEE ICC, June 1998.

[50] “Using Error Vector Magnitude Measurements to Analyze and Troubleshoot Vector-Modulated Signals,” Product Note PN 89400-14, Agilent Technologies, USA.

[51] G.G.G. Gonzales, “Measurements for Modeling of Wideband Nonlinear Power Amplifiers for Wireless Communications,” Department of Electrical and Communications Engineering, Helsinki University of Technology.

[52] E. Arabi and A. Ali, “Behavioral Modeling of RF Front End Devices in Simulink,” Signal Processing Group, Department of Signals and Systems, Chalmers University of Technology.

[53] J. Zyren and A. Petric, “Tutorial on Basic Link Budget Analysis,” Application Note AN9804.1, June 1998.

[54] A. Ghrayeb, W.E. Ryan, N-H. Yeh, “Performance of Random Access Memory Equalizers in Magnetic Recording,” IEEE Transactions Magazine, Vol. 36, No. 6, November 2000.

[55] Z. Wu, J.M. Cioffi, “Turbo Decision Aided Equalization for Magnetic Recording Channels,” Proc. GLOBECOM, 1999.

[56] C. E. Burnet, S.A. Barbulescu, W.G. Cowley, “Turbo Equalization of the Nonlinear Satellite Channel” Institute for Telecommunications Research, University of South Australia

[57] G.F. Herrmann, “Performance of Maximum-Likelihood Receiver in The Nonlinear Channel,” IEEE Transactions on Communications, Vol. Com-26, No. 3, March 1978.

[58] G.F. Herrmann, “Power Series Characterization of the Discrete Nonlinear Channel Satellite Channel,” IEEE Transactions on Communications, Vol. Com-26, No. 11, November 1978.

[59] C.C. Bantin, R.G. Lyons, “The Evaluation of Satellite Link Availability,” IEEE Transactions on Communications, Vol. Com-26, No. 6, June 1978.

[60] A. Weinberg, “The Impact of Pulsed RFI on the Coded BER Performance of the Nonlinear Satellite Communication Channel,” IEEE Transactions on Communications, Vol. Com-29, No. 5, May 1981.

[61] T. Huang, W.C. Lindsey, “PN Spread-Spectrum Signalling Through a Nonlinear Satellite Channel Disturbed by Interference and Noise,” IEEE Transactions on Communications, Vol. Com-30, No. 5, May 1982.

[62] R. De Gaudenzi, A. Guillen, A. Martinez, “Performance Analysis of Turbo-Coded APSK Modulations over Nonlinear Satellite Channels,” IEEE Transactions on Wireless Communications, Vol. 5, Issue 9, September 2006.

Appendix A

K0_Conic_Fit.m

```
%TWTA
%Ko

%Order of polynomial
N = 2;
M = 2;

%Asat = 0.5
x1 = [1, 0.9, 0.8, 0.5, 0.25, 0.1, 0.05 0.01];
x2 = x1;
x3 = x1;
x4 = x1;
y1 = [1.636e-1 1.768e-1 1.924e-1 2.644e-1 3.963e-1 5.948e-1 7.334e-1
9.273e-1];
Po_1 = [2.113e-2, 2.170e-2, 2.230e-2, 2.402e-2, 2.409e-2, 1.948e-2,
1.408e-2, 4.319e-3];

%Asat = 1
y2 = [3.963e-1 4.184e-1 4.436e-1 5.463e-1 6.915e-1 8.403e-1 9.112e-1
9.805e-1];
Po_2 = [9.635e-2, 9.523e-2, 9.364e-2, 8.399e-2, 6.346e-2, 3.598e-2,
2.089e-2, 4.809e-3];

%Asat = 2
y3 = [6.915e-1 7.117e-1 7.333e-1 8.099e-1 8.920e-1 9.529e-1 9.758e-1
9.95e-1];
Po_3 = [2.538e-1, 2.403e-1, 2.253e-1, 1.683e-1, 1.004e-1, 4.55e-2,
2.382e-2, 4.951e-3];

%Asat = 4
y4 = [8.92e-1 9.015e-1 9.112e-1 9.42e-1 9.699e-1 9.877e-1 9.938e-1
9.988e-1];
Po_4 = [4.016e-1, 3.686e-1, 3.343e-1, 2.225e-1, 1.177e-1, 4.878e-2,
2.469e-2, 4.988e-3];

OBO_1_dB = 10*log10(((0.5/2)^2)./(2.*Po_1));
OBO_2_dB = 10*log10(((1/2)^2)./(2.*Po_2));
OBO_3_dB = 10*log10(((2/2)^2)./(2.*Po_3));
OBO_4_dB = 10*log10(((4/2)^2)./(2.*Po_4));

figure(3);
Ko_1_OBO = [3.129 1.982 1.131 1.727 5.408 7.770 1.415e1];
Ko_2_OBO = [6.39 4.622 1.700 1.143 2.053 3.462 8.595];
Ko_1 = [7.902e-2 1.383e-1 3.963e-1 5.463e-1 8.403e-1 9.112e-1 9.805e-
1];
Ko_2 = [2.289e-2 4.321e-2 1.636e-1 2.644e-1 5.948e-1 7.334e-1 9.273e-
1];
plot(OBO_1_dB,y1,OBO_2_dB,y2,OBO_3_dB,y3,OBO_4_dB,y4,Ko_1_OBO,Ko_1,'o
',Ko_2_OBO,Ko_2,'*');
title('Ko vs Output Back-off - TWTA');
xlabel('OBO [dB]');
ylabel('Ko');
legend('Ao = 0.5','Ao = 1','Ao = 2','Ao = 4');
grid;
```

```
%conicfit Ko vs OBO
pt1 = [OBO_1_dB(1,4) y1(1,4)];
pt2 = [OBO_1_dB(1,5) y1(1,5)];
pt3 = [OBO_1_dB(1,6) y1(1,6)];
pt4 = [OBO_1_dB(1,7) y1(1,7)];
pt5 = [OBO_1_dB(1,8) y1(1,8)];
pp = sym('[x^2 x*y y^2 x y 1]');
p(1,:) = pp;
p(2,:) = [pt1(1,1).^2 pt1(1,1)*pt1(1,2) pt1(1,2).^2 pt1(1,1) pt1(1,2)
1];
p(3,:) = [pt2(1,1).^2 pt2(1,1)*pt2(1,2) pt2(1,2).^2 pt2(1,1) pt2(1,2)
1];
p(4,:) = [pt3(1,1).^2 pt3(1,1)*pt3(1,2) pt3(1,2).^2 pt3(1,1) pt3(1,2)
1];
p(5,:) = [pt4(1,1).^2 pt4(1,1)*pt4(1,2) pt4(1,2).^2 pt4(1,1) pt4(1,2)
1];
p(6,:) = [pt5(1,1).^2 pt5(1,1)*pt5(1,2) pt5(1,2).^2 pt5(1,1) pt5(1,2)
1];
B = vpa(det(p))
yyy_ = solve(B,'y')
x=1.1:0.01:9;
yyy = subs(yyy_(1,:));
figure(4);
plot(x,yyy,OBO_1_dB(1,1),y1(1,1),'o',OBO_1_dB(1,2),y1(1,2),'o',OBO_1_
dB(1,3),y1(1,3),'o',OBO_1_dB(1,4),y1(1,4),'o',OBO_1_dB(1,5),y1(1,5),'
o',OBO_1_dB(1,6),y1(1,6),'o',OBO_1_dB(1,7),y1(1,7),'o',OBO_1_dB(1,8),
y1(1,8),'o');
title('Conic Fit for Ko vs Output Back-off - TWTA');
xlabel('OBO [dB]');
ylabel('Ko');
grid;
```

Appendix B

```
%test.m Extract
%DOWNLINK
SNR_20_a = [-5 0 2 5 7 10];
if 0
    K = 20;
    NL = 1;
    Gain = 1;
    Ao = 1;
    phi = 2*pi*(rand(1,K));
    phi(1) = 0;
    nErrors_1_b = 0;
    nBits_1_b = 0;
    POut_K20_a = 0;
    for k = 1:length(SNR_20_a)
        k
        SNR = SNR_20_a(k);
        nErrors = 0;
        nBits = 0;
        for h = 1:10000
            model;
            if nErrors == 100
                break;
            end
            POut_K20_a = POut_K20_a + POut;
        end
        nErrors_20_a(1,k) = nErrors
        nBits_20_a(1,k) = nBits
        BER_20_a = nErrors_20_a./nBits_20_a
    end
    POut_K20_a = POut_K20_a/(sum(nBits_20_a));
    'Waiting for key press before saving data...'
    beep;
    pause
    save Results_K20_1_a_5 nErrors_20_a nBits_20_a BER_20_a
         POut_K20_a;
end
```

Program Listing C1 Downlink CDMA – 20 Users

```
%model.m Generate random data for user 1
clear In1;
In1 = randsrc(K,1);

% Perform spreading
load gold_codes gold g1;
In1_ = repmat(In1,1,63).*gold(1:K,:);

% Sum signals of all users
if K > 1
    In = sum(In1_.*repmat(complex(cos(phi),sin(phi))',1,63),1);
else
    In = In1_;
end

% Amplify
Ang = angle(In);
Rho = abs(In);
PIn = 0.5*sum(abs(Rho).^2)/length(Rho);

if NL == 1
    Amp_Out = Rho./(sqrt(1+(Rho/Ao).^2));
else
    Amp_Out = Rho;
end
POut = 0.5*sum(abs(Amp_Out).^2)/length(Amp_Out);

% Signal transmitted through channel
if Fading == 1
    Alpha=sqrt(((sqrt(2/pi).*repmat(randn,1,63)).^2)
    +(sqrt(2/pi).*repmat(randn,1,63)).^2));
end
DistSig = complex(Amp_Out.*cos(Ang),(Amp_Out.*sin(Ang)));
if Fading == 1
    DistSig = Alpha.*DistSig;
end

% Add noise
No = POut*63./(K*(10.^(SNR/10)));
noise_r = sqrt(No)*randn(1,63);
DistSigNoise = DistSig + noise_r;

% Despread user 1
DistSigNoise = DistSigNoise.*g1;

% Integrate user 1
RXSig = sign(real(sum(DistSigNoise)));

% Determine BER
if In1(1) ~= RXSig
    nErrors = nErrors + 1;
end
nBits = nBits + 1;
```

Program Listing C2 Downlink CDMA Model

```
%test.m Extract
%UPLINK
%K = 20, No Fading
if 0
    clear;
    for m = 1:5
        m
        SNR_20_UL_b_ = [0 5 10 15 20];
        K = 20;
        NL = 1;
        Gain = 1;
        Ao = 1;
        Fading = 0;
        phi = 2*pi*(rand(1,K));
        phi(1) = 0;
        BitCnt = 10000;
        ErrorCnt = 100;
        for k = 1:length(SNR_20_UL_b_)
            SNR = SNR_20_UL_b_(k);
            nErrors = 0;
            nBits = 0;
            for h = 1:BitCnt
                model_uplink;
                if nErrors == ErrorCnt
                    break;
                end
            end
            nErrors_20_UL_b(m,k) = nErrors
            nBits_20_UL_b(m,k) = nBits
            BER_20_UL_b = nErrors_20_UL_b./nBits_20_UL_b
        end
        POut_K20_UL_b = POut;
        'Waiting for key press before saving data...'
        beep;
        pause
        save Results_K20_UL_b nErrors_20_UL_b nBits_20_UL_b
             BER_20_UL_b POut_K20_UL_b;
    end
end
```

Program Listing C3 Uplink CDMA – 20 Users

```
%model_uplink.m Extract
%Generate random data for user 1
clear In1;
In1 = randsrc(K,1);

% Perform spreading
load gold_codes gold g1;
In1_ = Gain*repmat(In1,1,63).*gold(1:K,:);

% Amplify
Ang = angle(In1_);
Rho = abs(In1_);
if NL == 1
    Amp_Out = Rho./(sqrt(1+(Rho/Ao).^2));
else
    Amp_Out = Rho;
end
DistSig = complex(Amp_Out.*cos(Ang),(Amp_Out.*sin(Ang)));
POut = 0.5*sum(abs(Amp_Out).^2,2)/length(Amp_Out);

% Signal transmitted through channel
if Fading == 1
    Alpha = sqrt(((sqrt(2/pi).*repmat(randn(K,1),1,63)).^2) +
    ((sqrt(2/pi).*repmat(randn(K,1),1,63)).^2));
    DistSig = Alpha.*DistSig;
end

% Add noise
No = POut*63./(1*(10.^(SNR/10)));
noise_r = repmat(sqrt(No),1,63).*randn(K,63);
DistSigNoise = DistSig + noise_r;

% Sum signals of all users
Signal_Total =
sum(DistSigNoise.*repmat(complex(cos(phi),sin(phi))',1,63),1);

% Despread user 1
RXSig_1 = Signal_Total.*g1;

% Integrate user 1
RXSig = sign(real(sum(RXSig_1)));

% Determine BER
if In1(1) ~= RXSig
    nErrors = nErrors + 1;
end
nBits = nBits + 1;
```

Program Listing C4 Uplink CDMA Model

```
%test.m Extract
%DOWNLINK with Fading
%K = 20, Fading, Ao = 1
if 0
    clear;
    for m = 1:5
        m
        SNR_20_c = [-10 -5 0 5 10 15];
        K = 20;
        NL = 1;
        Gain = 1;
        Fading = 1;
        Ao = 1;
        BitCnt = [1e4 1e4 1e4 1e4 1e4 1e6];
        ErrorCnt = [1e2 1e2 1e2 1e2 1e2 1e3];
        phi = 2*pi*(rand(1,K));
        phi(1) = 0;
        POut_K20_c = 0;
        for k = 1:length(SNR_20_c)
            k
            SNR = SNR_20_c(k);
            nErrors = 0;
            nBits = 0;
            for h = 1:BitCnt(k)
                model;
                if nErrors == ErrorCnt(k)
                    break;
                end
                POut_K20_c = POut_K20_c + POut;
            end
            nErrors_20_c(m,k) = nErrors
            nBits_20_c(m,k) = nBits
            BER_20_c = nErrors_20_c./nBits_20_c
        end
    end
    Fading = 0;
    POut_K20_c = 5*POut_K20_c/sum((sum(nBits_20_c)));
    'Waiting for key press before saving data...'
     beep;
     pause;
    'Saving...'
    save Results_K20_2 nErrors_20_c nBits_20_c BER_20_c
         POut_K20_c;
```

Program Listing C5 Downlink CDMA with Fading – 20 Users

Appendix C

End Notes

[a] The theoretical and simulation results agree within a SNR range of 1 dB at a BER of 10e-3.